An Investigation of the Heat Transfer by conduction and radiation between Hot Glass and Mould Tooling

A thesis presented

By

Ezzeddin Gheblawi

For the Degree of
Doctor of philosophy

At

Northumbria University

December 2005

ACKNOWLEDGEMENTS

Thanks must go to my supervisor Dr. Roger Penlington, for all his help and support throughout a most demanding project. Thanks go also to Dr. Sean Danaher for his continued efforts in supporting me with any problems I have had, Prof. Fary Ghassemlooy for his direction and encouragement to Dr. Mark leach for his support and help and finally to all of the mechanical technical staff, without whom the practical work would not have been possible.

ABSTRACT

This research work investigates heat transfer through the contact line between a glass mould and plunger in a press forming process. Models are formed and compared with experimental measurements to enable clarification of the glass properties that should be used in the optimisation process and have been suggested in previous research works. Two case of heat transfer are considered in the models firstly the case of both conductive and radiative are present and then the case of radiative (reheat).

The models developed during the study are based on one-dimensional heat transfer. The model is based on the period of the formation process starting from the point at which the molten glass is brought into contact with a mould until the time at which the formed glass is inverted. The models are concerned with the changes in temperature profile during this period at both the centre and the surface of the glass depending on the mode of heat transfer considered, the properties of the glass, and the properties of the tooling. The properties of the glass considered in the models include the absorption coefficient, refractive index, heat transfer coefficient, internal and external emissivity, specific heat and conductivity.

In the radiation case the modelling results show the internal emissivity has a little effect on the surface temperature while the external emissivity has an effect temperature fall.

Modelling of changes in glass thickness and glass absorption coefficient during the reheat stage of the process has been carried out based on white and green glass. Validation of these models has been accomplished by performing experimental work.

TABLE OF CONTENTS

TITLE **Page**

CHAPTER THREE – GLASS PROPERTIES

CHAPTER FOUR – THE COMPARISON BETWEEN FOUR MODELS (RO, DTRM, P-1, DO)

CHAPTER FIVE – MODELLING GLASS PROPERTIES

CHAPTER SIX – HEAT FLUX AND STRESS

CHAPTER SEVEN – EXPERIMENTAL WORK

CHAPTER EIGHT – COMPARISON BETWEEN WHITE AND GREEN GLASS

CHAPTER NINE – CONCLUSION AND FUTURE WORKS

NOMENCLATURE

α	Spectral absorption coefficient (m^{-1})
C_p	Specific heat of semitransparent material (J/kg K)
t	Thickness of plane layer (m)
E_{vb}	Blackbody spectral energy for n = 1 (W-s/m^2)
E	Exponential integral functions
G	The flux quantity (W/m^2)
HTC	Heat transfer coefficient (W/m^2 K)
I_v	Spectral radiative source function (W. s/m^2)
I_I	Spectral radiant intensity (W.s/m^2. sr)
K	Thermal conductivity (W/m. K)
K_r	Radiative thermal conductivity (W/m. K)
n	Refractive index
q_{rv}	Spectral radiative flux (W.s/m^2)
T	Absolute temperature (K)
T_o	Initial temperature (K)
T_s	Temperature of the surroundings (K)
n	Refractive Index
θ_1	Angle of incidence (rad)
θ_2	Angle of refraction (rad)
x	Coordinate in direction across plane layer (m)
ϵ	Spectral emissivity
I_o	Intensity of radiation (W.s/m^2)
θ	Angle measured from the x-direction (rad)
L	Optical thickness (mm)
λ	Wavelength of radiation (μ m)
D	Density of semitransparent material (Kg/m^2)

σ	Stefan-Boltzmann constant ($W/m^2 K^4$)
η	Viscosity (Kg/m.s)
τ	Time (s)
E	Young's modulus (N/m^2)
G	Modulus of rigidity (Shear modulus) (N/m^2)
K	Bulk modulus (N/m^2)
μ	Poisson's ratio
RO	Roseland radiation model
DTRM	Discrete transfer radiation model
P-1	(P-1) radiation model
DO	Discrete ordinates radiation model
TD	Temperature difference (K)
F	Heat flux (W/m^2)

LIST OF FIGURES

LIST OF TABLES

CHAPTER ONE – INTRODUCTION

1.1. INTRODUCTION

To optimise the process involved in the manufacture of glass containers it is important to have an in depth knowledge of the heat transfer and temperature distributions that occur between the glass body and the tools used to form it. Traditional mathematical approaches are based on the effective conductivity of the glass. However this is only truly appropriate for large bodies of glass as it fails to adequately represent surface temperature gradients in thin walled bodies during deformation.

To predict and optimise the commercial forming processes, a comprehensive understanding of the balance of the heat transfer mechanisms during the deformation process is required to accurately predict product properties, e.g. wall thickness or quality defects in commercial ware. In addition, a greater understanding of the transient conditions of the forming processes is required.

Much work over the past 50 years has looked at defining and modelling the different properties of glass during each stage of the glass formation process. However no consensus has been met between researchers regarding the properties, which should be employed during modelling. As such it is difficult for a manufacturer to know how to optimise their production process or indeed which research to base the optimisation on. To obtain high-speed production, it is desirable that the glass entering the mould has minimum heat content so that the heat-extraction phase can be as short as possible. However, the glass must contain sufficient heat to keep it fluid enough to move readily

during the forming process. At the same time, the temperature must not exceed a maximum value if adhesion of the molten glass to the mould is to be prevented.

Although there are many stages in the glass formation process for which it is necessary to model the heat transfer this work is concerned only with the period of time from first contact with the mould until the glass is inverted prior to being applied to the mould, as will be shown later. This work aims to provide clarification of the effects on modelling outcomes of using different properties to describe the glass and hence offers a clearer picture of how to best optimise the process. Four different modelling algorithms are investigated to find which provides the most accurate representation of the actual process.

This research explores the heat transfer and temperature distributions in white soda-lime glass during the manufacture of glass bottles. This exploration will be carried out by modelling the process for a range of glass properties and considering the heat transfer cases of conduction and radiation when the glass has contact with the mould and plunger and then only radiation when the glass is inverted. The ranges of the glass properties will be decided by studying previous works and comparisons of the effects of the different glass properties used will be carried out by performing experiments.

1.2. AIMS AND OBJECTIVES

The main aim of this research work is to investigate heat transfer through glass as it undergoes heat transfer by conduction and internal radiation during its contact with a mould/plunger and by radiation only while it is in air. The work will look at the effects of different material and thermal properties for both the glass and mould/plunger. To accomplish the investigation both modelling and experimental work will be undertaken. The models will be based on one-dimensional heat transfer.

To achieve these aims, the following objectives have been formulated:

- To investigate the quantity of heat transfer by conduction and internal radiation between a hot glass melt and a mould over a specific time and observe their consequences on the temperature profile through the glass. All Chapters.
- To investigate the quantity of heat transfer by radiation during the reheat process (glass in air) over a specific time and observe its consequence on the temperature profile through the glass. All Chapters.
- To investigate the effect of the glass thermal and mechanical properties: absorption coefficient, refractive index, heat transfer coefficient, internal and external emissivity, specific heat and thermal conductivity on the heat transfer by both conduction and radiation. Chapter 3, 5.
- To investigate the results obtained from four different modelling algorithms (Rosseland (RO), Discrete Transfer DTRM, P-1, and Discrete Ordinates (DO)), and compare those results with equivalent experimental results for heat transfer by both conduction and radiation in hot glass. Chapter 4.

- To investigate the relationship between the rate of heat flux, and stress with the temperature distribution through the profile of hot glass as it cools over a given time period when heat transfer is by conduction, conduction and internal radiation and radiation only. Chapter 6
- To perform experimental work on the heating and cooling of different thicknesses of soda-lime glass in order to observe the temperature distribution through the glass and compare results obtained with the simulated results. Chapter 7.
- To investigate by both modelling experimental work the effect of the absorption coefficient on the glass on the rate of heating and cooling of the glass. Chapter 8.

1.3 CONTRIBUTION OF THIS WORK

- By studying the four model cases of heat transfer by conduction and radiation between the glass and the mould, the incorrect behaviour of the Rosseland RO and discrete transfer DTRM models is observed. They do not satisfy the radiative heat transfer requirements, due to a lack of sampling. In the P-1 and Discrete Ordinates DO models, the DO provides better results every where near the surface in comparison to experimental results. Chapter 4.

- Modelling using the DO formulation, the refractive index is seen to have a significant effect on fall of the temperature at the centre of the glass in both the conduction-radiation and radiation only cases of heat transfer. The effect on the surface temperature in the radiation case is more prominent than in the conduction radiation case. Chapter 5.

- Modelling using the DO formulation, the external emissivity is seen to have little effect on the centre temperature of the glass as it cools and heat transfer is by either conduction-radiation or radiation only. However it has a significant effect on the surface temperature of the glass in the radiation only case (during reheat). As the external emissivity increases the surface temperature decrease over the same period of time is greater. Chapter 5.

- In the reheat case the effect of conduction is very small in comparison to radiation i.e. most of the heat is lost from the centre of the glass to the surface by radiation. Chapter 2.

- As the heat transfer inside the glass increases so does the rate of flux and the stress. As cooling time increases the point of maximum flux moves from the surface of the glass. Chapter 6.
- As the absorption coefficient of the glass increases, so does the ability of the glass to lose or gain heat energy. This was confirmed by both modelling and experimental work through the observation of the glass surface temperature as the glass was cycled through the heating and cooling process. Chapter 8.

1.4 CHAPTER OUTLINE

Chapter 2 – Provides a review of literature, investigating previous work carried out regarding heat transfer processes and modelling the temperature distribution, thermal conductivity and glass thickness during the pressing and reheat processes.

Chapter 3- Introduces the study of the properties of glass, to show the effect of properties, such as density, viscosity, refractive index, specific heat and internal and external emissivity, on heat transfer from and the temperature distribution through a glass body.

Chapter 4- Introduces the software used for modelling, the application of radiative heat transfer, a comparison of the four models used, and a description of the results. The advantages afforded by the discreet ordinates formulation are also presented.

Chapter 5- Studies the properties of glass by modelling. The effect of density, viscosity, refractive index, specific heat and internal and external emissivity, on the centre and surface temperature of the glass is observed.

Chapter 6 Investigates the effect of heat flux and thermal gradient across a glass body as it cools in contact with mould tool and the rate of change of the internal stress against temperature.

Chapter 7 Presents the experimental work performed including: equipment used, sample preparations and results. The results are obtained by the cycling of the heating and cooling process on different thicknesses of glass and by observing the temperature at different depths into the glass body.

Chapter 8 Experimental and modelling work carried out in order to compare the effect of the absorption coefficient on the cooling of the surface and centre temperature of a glass body. The work utilises two types of glass, white and green, to provide the variation in absorption coefficient.

Chapter 9 Offers conclusions that can be drawn from this work, together with suggestions for further study in this area.

CHAPTER TWO – LITERATURE REVIEW

2.1 INTRODUCTION

In the manufacture of glass containers and pressed ware, heat is extracted from the glass by bringing it into contact with the surface of the metal mould or plunger, the temperature of which is considerably lower than that of the glass. Many factors determining the rate of heat extraction interact in a complicated way. These factors include: the initial temperature difference between the two surfaces, the thermal resistance of the glass-metal interface, the thermal properties of the glass and the metal, and the radiation absorption and emission properties of the glass. In heat transfer under glass forming conditions both conduction and semi-transparent body radiative heat transfer must be considered if a complete understanding of the process is to be obtained. The relative importance of these two transport mechanisms is not clear from previous work in this subject area. This chapter provides a review and discussion of published results concerning the different effects of each of the properties and mechanisms mentioned above on the temperature drop in the glass during the stages of initial mould contact and reheat/blank-open.

The effect of the glass absorption coefficient on the temperature distribution through the glass during the initial mould contact stage will be investigated in Sections 2.3.1 and 2.3.2. Two types of glass opaque and white will be simulated to provide a varying absorption coefficient. A comparison between the simulations performed and previously published works will be made.

In Section 2.4 the glass surface temperature drop is examined during the reheat stage. Consideration of the initial mould contact stage is first required to provide a relative

temperature drop. The effect of external emissivity is also investigated with the simulations performed based on previously published work. Consideration of not accounting for the conductive heat loss during the reheat stage is also discussed.

Section 2.5 investigates the effect of the glass thickness on the rate of heat loss during the initial mould contact stage. Simulations are carried out for different thicknesses and the results are compared with previously published work.

The effect of the initial mould and plunger temperature on the rate of heat lost from the glass during contact is discussed in Sections 2.6 and 2.7. In each case simulations for different initial temperatures have been performed and comparisons made with previously published works.

Tables of the modelling results attained by different authors are provided in Section 2.8, where the modelling parameters are also included to allow direct comparison of each author's work.

Finally, a further discussion of key points highlighted throughout the chapter is provided in Section 2.9, followed by a chapter summary.

2.2 LITERATURE REVIEW

The findings published in previous works are now discussed, these will be later simulated to provide clarification of their findings and allow a more detailed discussion Jones and Basnett [1] have calculated the temperature distribution through 10 mm thick glass pressings for both opaque and semi-transparent glass, using a glass to mould heat transfer coefficient of 1500 W/m^2 K. The work showed that radiation plays a small but important part in the extraction of heat from the glass.

Gardon [5] studied the heating and cooling of glass sheets; his analysis of radiative heat transfer is so fundamental that it can be applied directly to glass forming problems by changing the boundary conditions these are the initial glass temperature and the initial mould temperature. The work shows that these initial temperatures are very important in terms of the level of heat transfer from the glass to the mould. As the initial mould temperature decreases more heat transfers to the mould because of the larger temperature gradient. McGraw [6] used computer analysis to conclude that the contribution of radiation to the total heat lost from the glass during mould contact is negligible and therefore does not significantly change the temperature distribution within molten glass during cooling (parison). However, Trier [7], who measured the temperature distribution and heat flow through the glass in the mould using a needle insertion method, found that at a high temperature heat is transferred not only by conduction but also by radiation. The radiation of the glass becomes significant at temperatures above 500 ^{o}C, the more the glass is heated the greater the radiation. Gardon [8] attributed this difference to the methods of experimentation.

Work by Jones [9] concurs with similar work by Rawson [11] that when hot glass comes into contact with cooler metal, there is the possibility for the surface layer of the

glass to drop in temperature substantially and for it then to reheat by some tens of degrees. When the mould is moved away from the glass, the centre temperature decreases and the surface temperature increases, this is because heat is transferred from the centre of the glass to the surface, which gives rise to surface reheating for a time of around 2 seconds.

Trier [10] has made a brief theoretical study of reheating but considers it justifiable to ignore the contribution of conduction during the reheat phase.

Rawson [11] showed that when the parison is released from the mould during the reheat process, the rate of rise of surface temperature could be as high as 250 K/s. As he correctly points out, the rate of reheat will be affected by the length of time for which the parison has been in the mould and by the heat transfer conditions that exist during that time. However most of the heat is extracted from the glass by conduction to the cold mould during pressing.

Fellows and Shaw [3] carried out a laboratory experiment to measure the thermal contact between the glass and the mould during pressing, and the effect of the initial mould temperature on the heat transfer and temperature drop. Their results agreed with the work by Gardon [8] that the initial mould temperature affects the rate of heat lost from the glass, with the greater heat being lost for lower initial mould temperatures.

Babcock and McGraw [13] made a detailed study of heat transfer during the pressing process, their experimental work included measurements at different positions in the mould and plunger and of the heat contact of the glass at various stages in the pressing cycle. They found that most of the heat is transferred during the first second after the insertion over the plunger.

Kent [4] measured mould temperature and heat flow during the production of press-ware and containers. Numerical methods for computing surface heat fluxes from measured temperatures in the mould, initially at a uniform temperature, have been developed by Howse, Kent and Rawson [14] as a result of laboratory investigations of the heat transfer during glass pressing and casting. The measured surface heat fluxes were used to calculate the cooling experienced by the glass. However, in many forming operations the mould is not at an initially uniform temperature, and the analysis of mould temperature data to calculate heat fluxes is extremely difficult. The effect of changing the operating temperature of the plunger on the surface temperature and surface flux is the same as that of the mould. For lower initial plunger temperatures greater heat transfer occurs.

2.3 MODELLING PREVIOUS WORK

The following modelling work is divided into 5 main sections; in each section the simulations performed are based on previously published work and aim to provide clarification of the authors' findings. The 5 topics considered are the effect of the absorption coefficient, reheat, glass thickness, initial mould temperature and initial plunger temperature on heat lost from the glass.

Following the work of Jones and Basnett [1], in this example a simulation of the heat transfer between transparent and opaque soda-lime molten glass and a mould-plunger is performed with properties as shown in table 2.1, to see the effect of the absorption coefficient on the heat loss. This work was also discussed by Kruszewski [15]. The simulations are carried out using the properties and initial conditions detailed in Tables 2.1 and 2.2 .Material properties glass and mould-plunger (Conduction-Radiation) press

Table 2.1 Initial glass and mould temperatures and the properties of glass and steel used in the mould and plunger as used by Jones and Basnett [1]

Property	Units	Glass (fluid)	Mould and plunger steel (solid)
Density	Kg/m^3	2500	8000
C_p (Specific heat)	J/Kg K	1350	500
Thermal conductivity	W/m K	1.45	200
Heat transfer coefficient	W/m^2 K	-	1500
Absorption co. white G.	m^{-1}	23, 45, 100	-
Absorption co. opaque G		23, 45, 300	
Refractive index	-	0.5	-
Initial temperature	°C	1050	490
Thickness	mm	10	20
Time	Second	5	5

Table 2.2 Bands of wavelengths and absorption coefficients, as used by Jones and Basnett [1], for white glass

Bands	A C (α) white glass	A C (α) Opaque glass	Wavelength (μ)
Band-1	23 m^{-1}	23 m^{-1}	(0.8--2.25) μ
Band-2	45 m^{-1}	45 m^{-1}	(2.25--2.75) μ
Band-3	100 m^{-1}	300 m^{-1}	(2.75--4.3) μ

2.3.1 Investigating the effect of opaque glass absorption coefficient on the centre and surface temperature

In this section a simulation to show the effect on the centre and surface temperature fall for 10 mm thick opaque glass over a time period from 0.05 to 5 seconds is performed. The initial conditions for the tooling and absorption coefficients for the opaque glass in each of the three radiating bands are given in Table 2.1 and 2.2.

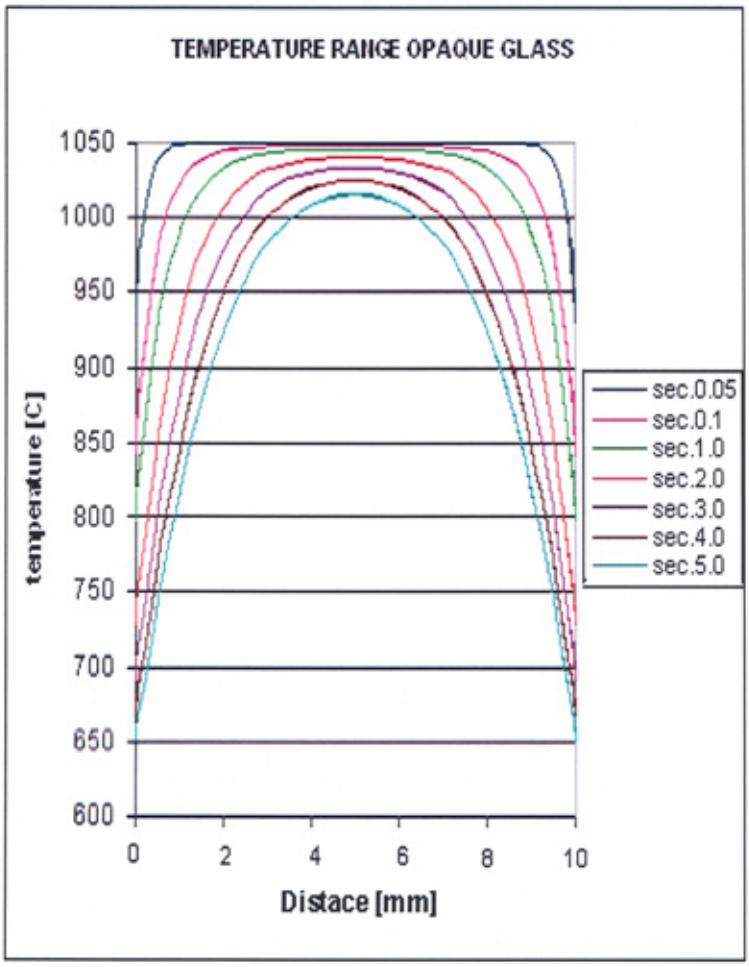

Figure 2.1 Temperature distributions through 10 mm thick opaque glass at times 0.05 to 5.0 sec.

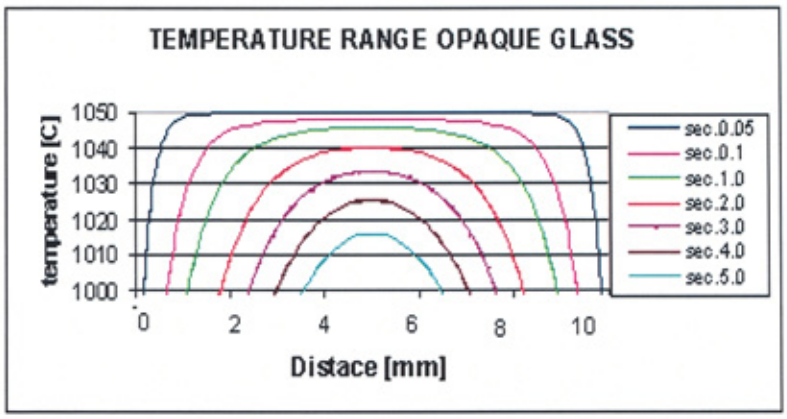

Figure 2.2 Centre temperature drop from 1050-1015 °C opaque glass at times 0.05 To 5.0 sec

Figure 2.1 shows the temperature distribution through 10 mm thick opaque glass at times from 0.05 to 5.0 seconds. The initial glass temperature was 1050 °C and both conduction–radiation heat transfers were considered. Throughout the forming period the surface temperature drops from 1050 °C to 650 °C, and the centre temperature drops from 1050 °C to 1015 °C a 35 K deference is observed. Table 2.3 summarises the results obtained for this opaque glass.

Table 2.3 Results of central and surface temperature drop in the opaque glass

Time (seconds)	0.1	0.5	1.0	2.0	3.0	4.0	5.0
Cen. Temp	1050°C	1048°C	1045°C	1040°C	1034°C	1025°C	1015°C
Surf. Temp.	930°C	860°C	800°C	730°C	690°C	670°C	650°C

2.3.2 Investigating the effect of white glass on the centre and surface temperature

In this section a simulation to show the effect on the centre and surface temperature fall for 10 mm thick white glass over a time period from 0.05 to 5 seconds is performed. The initial conditions for the tooling and absorption coefficients for the opaque glass in each of the three radiating bands are given in Table 2.1 and 2.2.

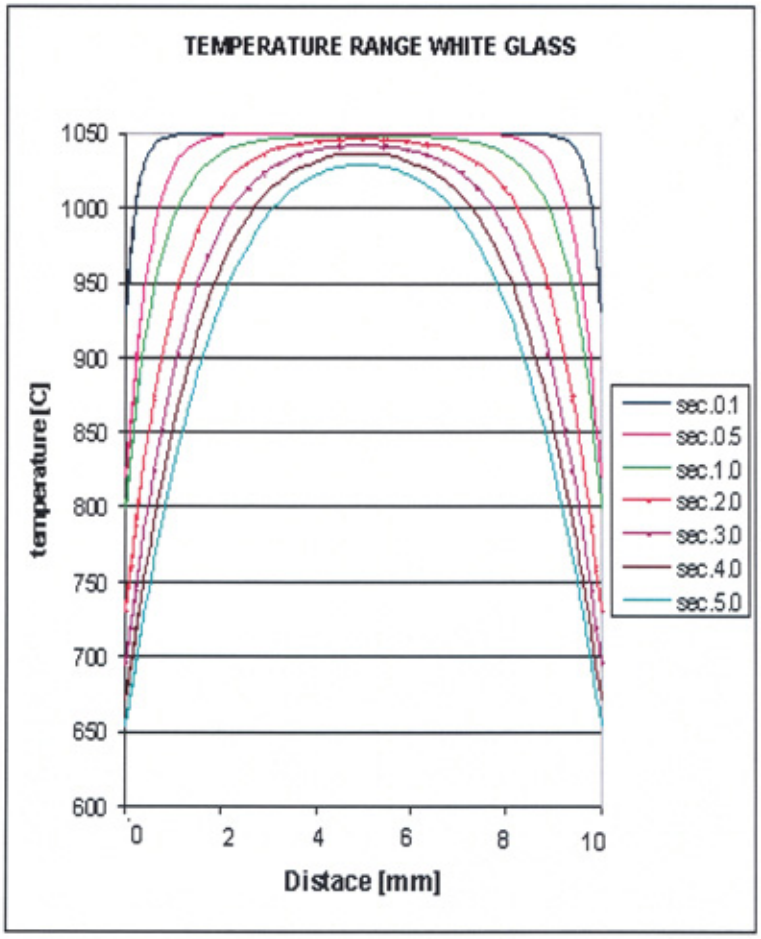

Figure 2.3 Temperature distributions through 10 mm thick white glass at times 0.05 to 5.0 sec

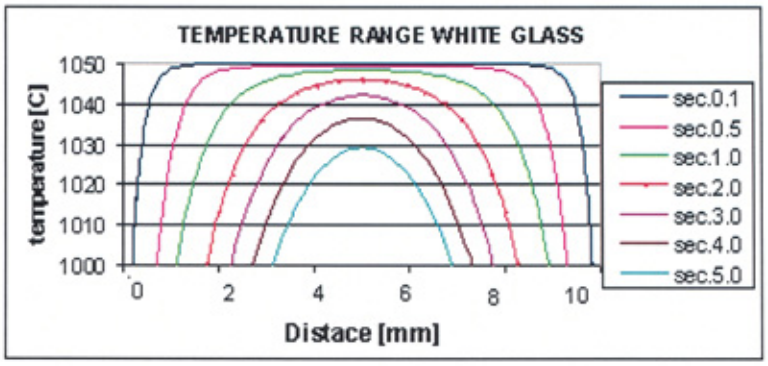

Figure 2.4 Centre temperature drop from 1050-1030 °C white glass at times 0.05 to 5.0 sec.

Figure 2.3 shows the temperature distribution through 10 mm thick white glass at times from 0.05 to 5.0 seconds. The same initial conditions were applied for the simulation however it should be noted from Table 2.2 that the absorption coefficient in the third radiating band is less than that of the opaque glass For the white glass, throughout the contact period the surface temperature drops from 1050 °C to 650 °C, and the centre temperature drops from 1050 °C to 1030 °C a 20 K difference is observed. Table 2.4 summarises the results obtained for white glass.

Table 2.4 Results of central and surface temperature drop in the white glass

Time(seconds)	0.1	0.5	1.0	2.0	3.0	4.0	5.0
Cen. Temp	1050°C	1049°C	1048°C	1046°C	1042°C	1037°C	1030°C
Surf. Temp	930°C	860°C	800°C	730°C	690°C	670°C	650°C

McGraw [6] derived similar results to those observed above for white glass over a 5.0 second period. His results show that the centre temperature and the surface temperature dropped to 1030 °C and 650 °C respectively. See experimental results Chapter 8 for

further discussion of cooling white and green glass. This topic has also been discussed by Kruszewski [15].

For the two types of opaque and white glass, the surface temperatures of the two types are identical throughout the contact period. The temperature at the centre of the glass at the end of the pressing period of 5.0 seconds has dropped to 1015 °C for the opaque glass, and 1030 °C for the white glass. The 20 K difference is a result of the higher absorption coefficient of the opaque glass in the third radiation band. Those results are similar to those published by Jones and Basnett [1]. A more detailed discussion of this is offered in Section 5.3.

2.4 MODELLING THE REHEAT OF THE GLASS

As previously stated the work by Jones [9] indicated that when the hot glass comes into contact with the cooler metal of the mould, the surface layer of the glass can reduce in temperature substantially, before being allowed to reheat after removal from the mould. It was also stated that Trier [10] considers it justifiable to ignore the contribution of conduction during the reheat stage.

The investigation and simulation of the reheat stage is divided into three parts, firstly consideration of the initial mould contact stage to provide a basis for discussion, followed by an observation of the external emissivity on the heat loss during the reheat stage and then a inspection of the effect of not including the contribution to heat loss by conduction in the reheat stage. The simulations are based on the work by Rawson [11], the parameters used for initial conditions and properties are identical to the his investigations and are given in Tables 2.5 and 2.6

Table 2.5 Bands of wavelengths and absorption coefficients as used by Rawson [11] for white glass

Bands	**Absorption coefficient (α)**	**Wavelength (μ)**
Band-1	20 m^{-1}	$\mu < 2.75$
Band-2	400 m^{-1}	(2.75— 4.3) μ

Table 2.6 Initial glass, mould and air temperatures and the properties of glass and steel used in the mould and plunger as used by H. Rawson [11] for radiation

Property	Units	Glass (fluid)	Mould and plunger steel (solid)	Air (fluid)
Density	Kg/m^3	2500	8000	0.0242
C_p (Specific heat)	J/Kg K	1350	500	1000
Thermal conductivity	W/m K	1.45	200	1.225
Heat transfer coefficient	W/m^2 K	-	1600	10
Absorption coefficient	m^{-1}	20-400	-	-
Refractive index	-	0.5	-	-
Initial temperature	°C	1050	490	20
Thickness	mm	10	20	10
Time	Seconds	2 and 3	2 and 3	2 and 3

2.4.1 Investigating the temperature drop during the glass-mould press (conduction-radiation)

Glass with an initial temperature of 1050 °C is simulated in order to show the surface and centre temperature drop during the first 3.0 seconds in a mould with an initial temperature of 490 °C, both conduction and radiation are considered.

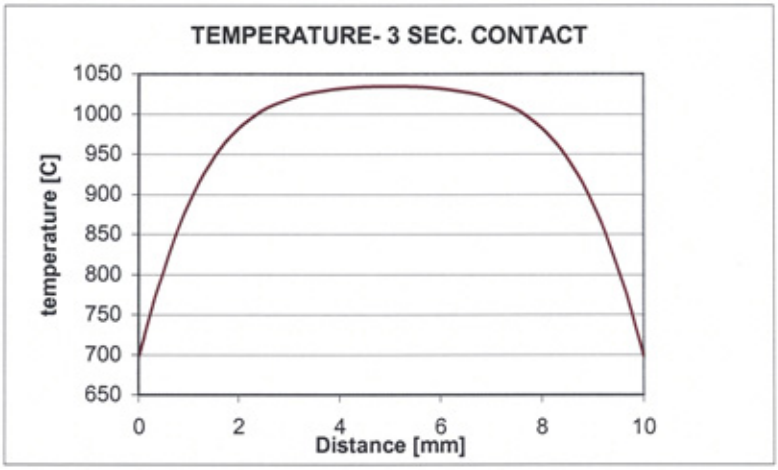

Figure 2.5 Temperature fall during the glass cooling between mould and plunger at 490 °C for 3 seconds and the glass HTC 1600 W/m^2 K

Figure 2.5 shows the temperature distribution through the glass after a period of 3 seconds in the mould, falling to around 700 °C at the glass surface. It is seen that the glass is cooled symmetrically at both edges by the mould. A summary of the surface temperatures obtained over the 3 second period is given in Table 2.7. The central temperature has also dropped after 3 seconds, to 1020 °C, the results shown in Table 2.7 were the same as those published by Rawson [11]. A surface temperature drop to 650 °C in 3.0 seconds for the same conditions was published by Curran and Farag [16].

Table 2.7 Glass surface temperatures during the cooling

Time seconds	0.0	0.5	1.0	1.5	2.0	2.5	3.0
Surface temp °C	1050 °C	850 °C	780 °C	750 °C	730 °C	710 °C	700 °C

2.4.2 Investigating the temperature rise during the glass reheat (Radiation)

Glass with an initial temperature of 1050 °C is simulated in order to show the surface and centre temperature drop during the first 3.0 seconds in air with an ambient temperature of 20 °C, only radiation transfer is considered. Two cases are considered, firstly case I considers when the mould remains close to the glass during the reheat period, in this case the air is not at ambient temperature but is at 490 °C and so has an effect on the external emissivity, it becomes 0.8. Case II considers when the mould has been completely removed and so the air is at ambient temperature, the external emissivity is 0.

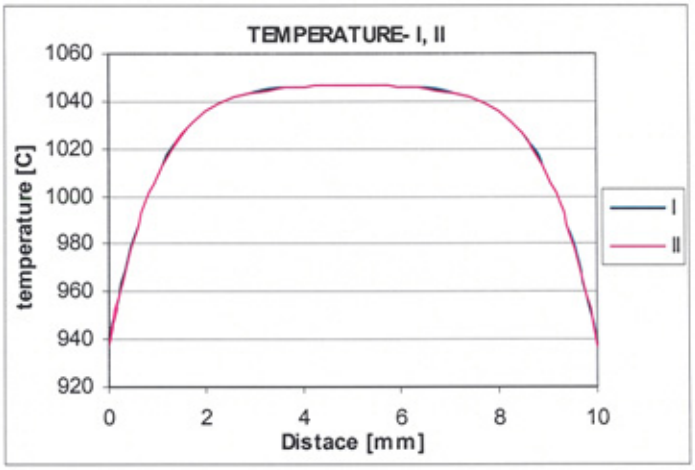

Figure 2.6 Temperature drop of glass cooling in the air the surface temperature drop from 1050 –940 ° C

Figure 2.6 shows that in both cases the temperature distributions follow the same trend with the centre temperatures dropping to 1033 °C from 1050 °C and the surface temperature dropping to 940 °C after 3 seconds. The summary of the results shown in Table 2.8 are the same as those produced by Rawson [11] for the radiation only case. The difference between the two cases throughout the glass was very small.

Table 2.8 Results of temperature and time of glass cooling for 3 seconds in the reheat case HTC is reduced to 10 W/m^2 K, air at temperature of 20 °C

Time seconds	0.0	0.5	1.0	1.5	2.0	2.5	3.0
Surface temp °C	1050 °C	1000 °C	982 °C	970 °C	960 °C	950 °C	940 °C

2.4.3 Investigating the effect of the absence of conduction on the reheat of the glass surface blank open Stage (reheat)

In this section, the simulation is concerned with how the temperature distribution though the glass changes in the 2 seconds immediately following its removal from the mould. The glass is set with an initial centre temperature of 1050 °C and initial surface temperature of 730 °C, as previously stated Rawson showed that when the parison is released from the mould during the press-blow process, the rate of rise of surface temperature may be as high as 250 K/s.

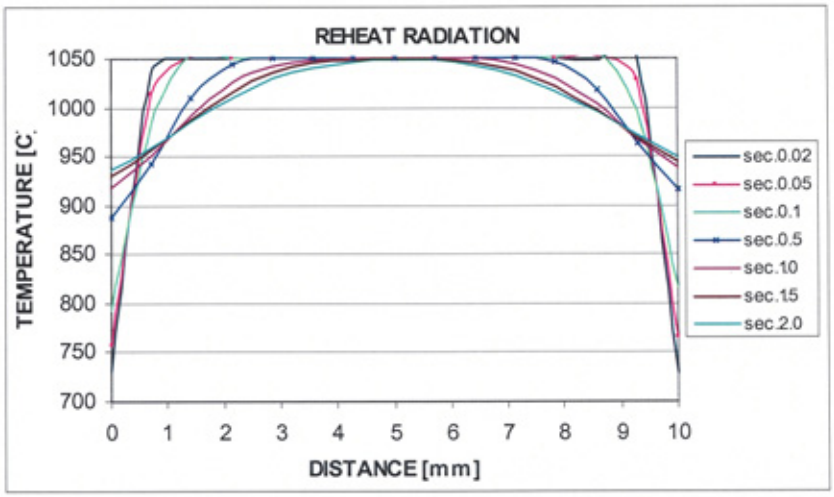

Figure 2.7 Surface temperature rises from 730- 945 °C whether the centre temperature drops from 1050-1048 °C in 2 second (reheat)

Figure 2.7 shows the temperature time curves at the glass surface over a reheat time of 2 seconds. Only radiation is considered and the ambient air temperature is taken as 20 °C. After 2 seconds it is seen that the surface heats from 730 °C to 945 °C. Over the same time period the centre temperature falls from 1050 °C to 1048 °C. Most of the heat is lost from the centre of the glass to the surface by radiation. The summary of these results shown in Table 2.9 were the same as those produced by Rawson [11]. Curran

and Farag [16] stated the surface heated from 650 °C to 950 °C in 2 seconds using a similar simulation

Table 2.9 Results of temperature and time of glass cooling for 2 seconds in the reheat case, and air at temperature of 20 °C, from figure 2.7

Time in (seconds)	0.0	0.5	1.0	1.5	2.0
Surf. temp.(R)	730°C	889°C	920°C	933°C	945°C
Cen. temp. (R)	1050°C	1050°C	1049°C	1049°C	1048°C

2.4.4 Investigating the glass surface temperature rise during reheat, in the absence and presence of conduction heat transfer

In this section, glass with and initial surface temperature of 730 °C and initial centre temperature of 1050 °C is simulated for the 2 seconds immediately following the removal of the glass from the mould in order to show the effect of the presence and absence of conduction heat transfer on the glass surface temperature during the reheat phase in an ambient air temperature of 20 °C. The heat transfer coefficient of the glass was 10 $W/m^2 K$.

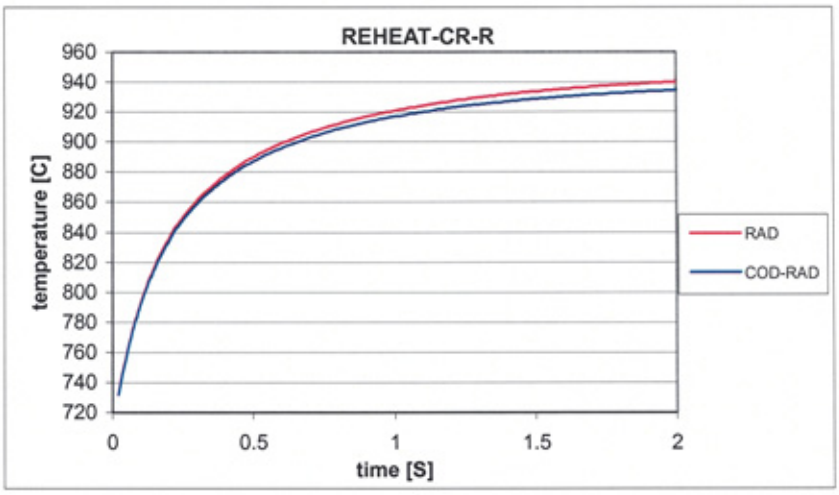

Figure 2.8 Surface temperature rise from 730-945 oC in the radiation case and from 730-930 oC in the radiation conduction at HTC 10 W/m2 K. (in 2 sec reheat)

Figure 2.8 shows the temperature time curves at the glass surface over a reheat time of 2 seconds. In the presence of both conduction and radiation the surface heated from 730 °C to 930 °C in 2 seconds, however with only radiation present, the surface heated from 730 °C to 945 °C in 2 seconds. The 15 °C temperature difference between the two cases is the same as the difference obtained by Rawson [11], a summary of the results is given in Table 2.10.

Table 2.10 Surface temperature rise against reheat time of 2.0 seconds of the two cases radiation and radiation-conduction for HTC 10 W/m^2 K

Time in (seconds)	0.0	0.5	1.0	1.5	2.0
Sur. temp.(R)	730°C	889°C	920°C	933°C	945°C
Sur. temp.(C-R)	730°C	887°C	916°C	928°C	930°C
Temp. diff. (R-CR)	0.0 °C	3 °C	4 °C	5 °C	15 °C

2.5 THE EFFECT OF THE GLASS THICKNESS ON THE HEAT TRANSFER

Gardon [12] has shown that, in the tempering of glass plates 6 mm thick, radiation plays an important role in terms of heat loss. On the other hand, according to McGraw [17] in the pressing of a parison radiation is seen to have little influence. The effect of glass thickness on the glass surface temperature during 5 seconds of glass-mould-plunger contact time is observed through simulation. The flux induced through the glass-mould interface is also observed over the 5 second period for varying glass thickness. Three glass thicknesses are investigated, 10, 25, 50 mm, with the same initial conditions applied in each model as given in Table 2.11. The results of these simulations can be seen in Figures 2.9 and 2.10.

Table 2.11 Initial glass and mould temperatures and the properties of glass and steel used in the mould and plunger as used by McGraw [17]

Property	**Units**	**Glass (fluid)**	**Mould and plunger steel (solid)**
Density	Kg/m^3	2500	8000
C_p (Specific heat)	J/Kg K	1350	500
Thermal conductivity	W/m K	1.45	200
Heat transfer coefficient	$W/m^2 K$	-	1500
Absorption coefficient	m^{-1}	23-45-100	-
Refractive index	-	1.0	-
Temperature	°C	1077	490
Thickness	mm	10, 25, 50	20
Time	Seconds	4	4

on the fall in surface glass temperature and the rate of change of heat flux during the press cooling between glass and plunger, in 5 second contact time.

2.5.1 Investigating the change of glass thickness effect on surface temperature and flux during the glass-mould press.

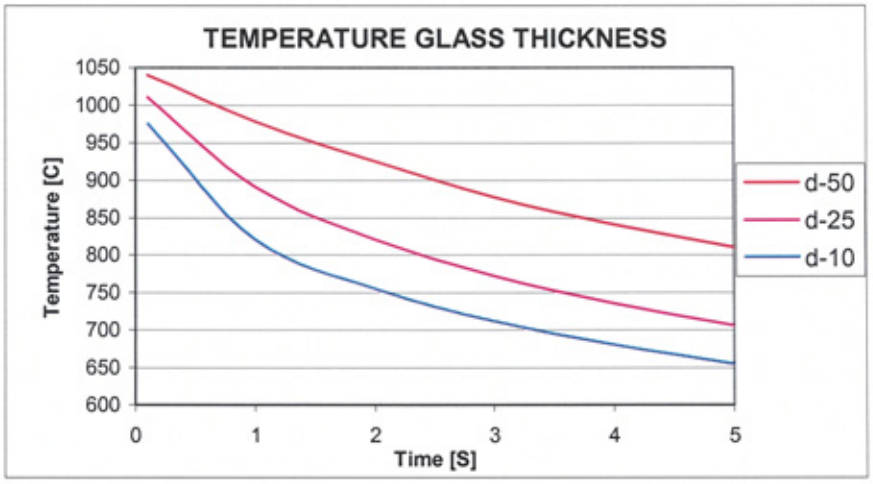

Figure 2.9 Effect of glass thickness on the surface temperature through 10-50 mm glass thickness during 5 sec cooling

Figure 2.9 shows the effect of the thickness of the glass on the fall in surface temperature over 5 seconds of glass-mould-plunger contact time. It can be seen that as the glass thickness reduces the glass surface temperature lost during the 5 seconds increases and more heat is transferred from the glass to the mould i.e. as the thickness of the glass reduces the surface contact temperatures decrease, (experimental work in Section 7.5 regarding cooling and heating shows that as glass thickness reduces the rate of heating and cooling increases). A summary of the results is provided in Table 2.12.

Table 2.12 Surface temperature drop against glass thickness of 10, 25, 50 mm during 5 seconds of cooling between glass and plunger

Time in (seconds)	0.1	1.0	2.0	3.0	4.0	5.0
Surface T (d-50 mm)	1040°C	980°C	920°C	880°C	840°C	810°C
Surface T (d-25 mm)	1010°C	890°C	820°C	770°C	735°C	705°C
Surface T (d-10 mm)	975°C	820°C	750°C	710°C	680°C	650°C

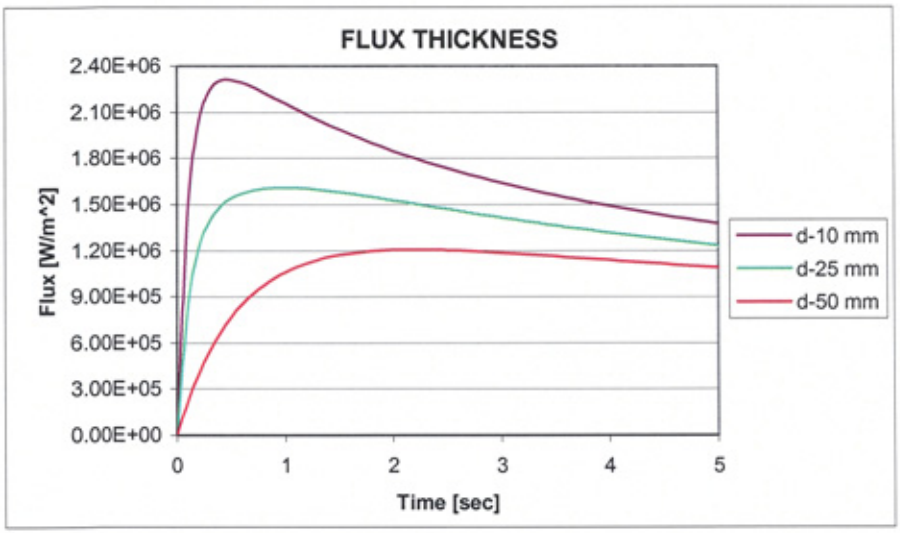

Figure 2.10 Effect of glass thickness on the surface heat flux through. 10-50 mm glass thickness during 5 seconds

Figure 2.10 shows the effect of glass thickness on the heat flux through the contact line between the glass and the mould. From Figure 2.9 it has been seen that as the thickness reduces the glass surface temperature decreases and more heat is transferred from the glass to the mould. This is also corroborated by the flux over the 5 second period shown in Figure 2.10 in that, as the thickness of the glass reduces the significance of radiation increases. This confirms the results produced by McGraw [6]. This also confirms experimental work done later in Section 7.5 as the glass thickness decreases the rate of heating and cooling increases Figures 7.6, 7.7, and 7.8. Table 2.13 provides a summary of the flux characteristics shown in Figure 2.10.

Table 2.13 Surface heat flux against glass thickness of 10, 25, 50 mm during 5 seconds of cooling between glass and plunger

Time (seconds)	0.1	1.0	2.0	3.0	4.0	5.0
d-50 mm.W/m^2	6.50x10^5	1.05 x10^6	1.20 x10^6	1.15 x10^6	1.10 x10^6	1.05 x10^6
d-25 mm.W/m^2	1.55 x10^6	1.60 x10^6	1.53 x10^6	1.40 x10^6	1.30 x10^6	1.22 x10^6
d-10 mm.W/m^2	2.30 x10^6	2.15 x10^6	1.85 x10^6	1.65 x10^6	1.50 x10^6	1.35 x10^6

2.6 THE EFFECT OF THE INITIAL MOULD TEMPERATURE ON THE TEMPERATURE DROP AND HEAT FLUX DURING THE GLASS MOULD CONTACT

In the manufacturing process of glass containers and pressed ware, heat is extracted from the glass by bringing it into contact with the surface of a metal mould or plunger, the temperature of which is considerably lower than that of the glass. The many factors determining the rate of heat extraction interact in a complicated way and they include the initial difference between the temperatures of the glass and the metal surfaces, the thermal resistance of the glass metal interface, the thermal properties of the glass and the metal, and the radiation absorption and emission properties of the glass. This interface has been investigated by both Fellows and Shaw [3] and Babcock and McGraw [13]. Simulations are carried out to show the effect of varying the initial mould temperature on the surface temperature of hot glass over a 4 second period from the point of contact. The initial mould temperatures considered are 545, 300 and 42 °C, and for each the same initial conditions are applied in each simulation, these are given in Table 2.14. The results obtained are shown in Figures 2.11 and 2.12.

Table 2.14 Initial glass and mould temperatures and the properties of glass and steel used in the mould and plunger is used by Fellows and Shaw [3]

Property	Units	Glass (fluid)	Mould and plunger steel (solid)
Density	Kg/m^3	2450	8000
C_p (Specific heat)	J/Kg K	1350	500
Thermal conductivity	W/m K	1.44	200
Heat transfer coefficient	W/m^2 K	-	1600
Absorption coefficient	m^{-1}	100-300	-
Temperature	°C	1077	42, 300, 545
Thickness	mm	10	20
Time	Seconds	4	4

2.6.1 Investigating the effect of the initial mould surface temperature on the surface temperature drop and heat flux during the glass plunger contact

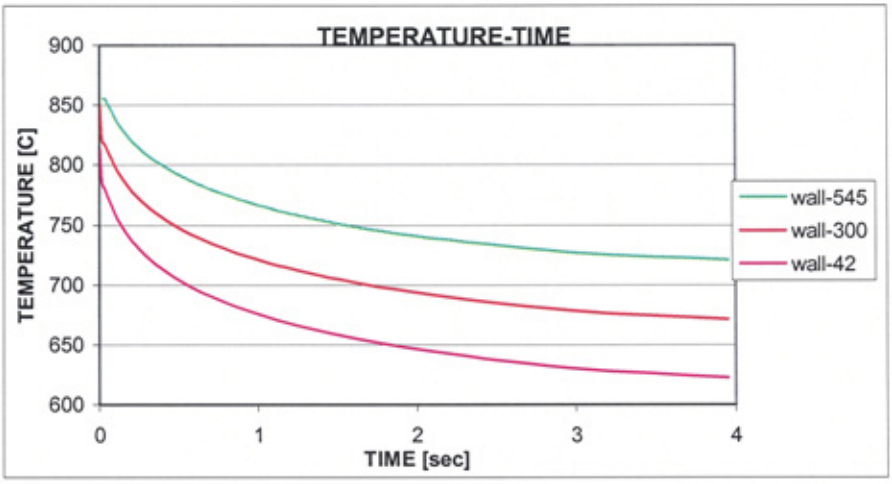

Figure 2.11 Variation of the glass surface temperature with time, initial mould surface temperatures was 42 °C Purple line and 300 °C red line and 545 °C green line

Figure 2.11 shows the effect of the initial mould temperature on the heat transfer through the surface. As the initial temperature of the mould decreases the glass surface temperature decreases. A summary of the results is given in Table 2.15. The results support the findings of Fellows and Shaw. [3] (This effect is further discussed in Section 6.3).

Table 2.15 Results of glass surface temperature drop with three values of initial mould surface temperatures, and glass initial temperature was 1077 °C

Time (seconds)	0.0	1.0	2.0	3.0	4.0
Mould-42 °C.	805 °C	675 °C	645 °C	630 °C	620 °C
Mould -300 °C.	825 °C	720 °C	692 °C	677 °C	670 °C
Mould -545 °C.	855 °C	765 °C	740 °C	725 °C	720 °C

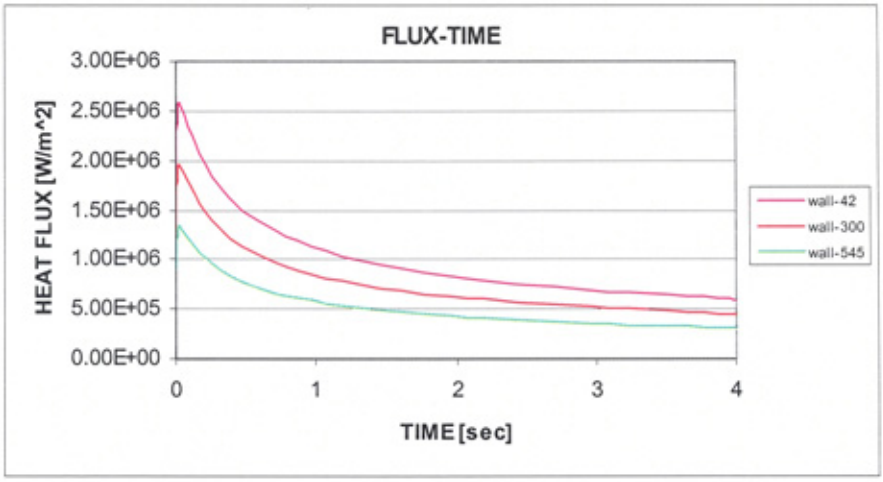

Figure 2.12 Variation of the glass surface flux with time, initial mould surface temperatures was 42 °C Purple line and 300 °C red line and 545 °C green line

Figure 2.12 shows the effect of the initial mould temperature on the heat flux over the 4 seconds preceding the initial mould glass contact. Greater heat fluxes were observed for lower initial mould temperatures, but this effect becomes less pronounced over longer contact times. After 4 seconds of contact, the heat flux for the lowest initial mould temperatures maintains the highest heat flux. A summary of the flux results are shown in table 2.16 and were the same as those observed by Fellows and Shaw [3] (this is further discussed in Sections 6.3 and 6.4).

Table 2.16 Results of flux at the surface with mould initial surface temperature of 42 °C, 300 °C, 545 °C and glass temperature was 1077 °C

Time (seconds)	0.1	1.0	2.0	3.0	4.0
Mould -42 °C. Flux W/m^2	2.5×10^6	1.1×10^6	8.0×10^5	7.0×10^5	6.0×10^5
Mould -300 °C. Flux W/m^2	2.0×10^6	5.8×10^5	6.0×10^5	5.0×10^5	4.5×10^5
Mould-545°C. Flux W/m^2	1.3×10^6	5.1×10^5	4.0×10^5	3.5×10^5	3.0×10^5

2.7 THE EFFECT OF INITIAL PLUNGER TEMPERATURE ON THE HEAT LOSS FROM GLASS

Kent [4] used laboratory investigations to measure the heat transfer in glass during pressing and casting, these results were then used to develop numerical methods for computing surface heat fluxes. These numerical methods assume an initial uniform temperature distribution over the plunger. However, in many forming operations the plunger is not at an initially uniform temperature and the analysis of plunger temperature data to calculate heat fluxes is extremely difficult. Simulations will be performed to show the effect of the initial plunger temperature on the heat transfer from the glass surface over a 5.0 second contact time. Initial plunger temperatures of 560 °C and 490 °C will be investigated and other initial conditions in both cases are as shown in Table 2.17. The results obtained are shown in Figures 2.13 and 2.14.

Table 2.17 Initial glass and plunger temperatures and the properties of glass and steel used in the plunger as used by Roger Kent [4]

Property	Units	Glass (fluid)	Mould and plunger steel (solid)
Density	Kg/m^3	2500	8000
C_p (Specific heat)	J/Kg K	1300	500
Thermal conductivity	W/m K	1.50	200
Heat transfer coefficient	K W/m^2	-	1600
Absorption coefficient	m^{-1}	100-300	-
Refractive index	-	0.5	-
Initial temperature	°C	1015	490, 560
Thickness	mm	10	20
Time	Second	0.5	0.5

2.7.1 Investigating the effect of the initial plunger surface temperature on the surface temperature drop and heat loss during the glass plunger contact

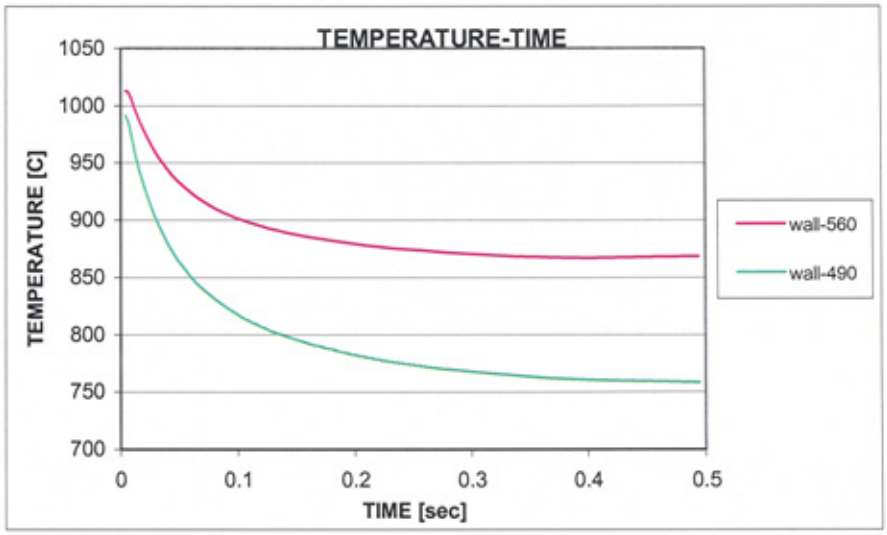

Figure 2.13 Variation of the glass surface temperature with time, initial mould surface temperatures was 560 °C Purple line and 490 °C green line

Figure 2.13 shows that for an initial plunger temperature of 490 °C, the glass surface temperature falls from 1015 °C to 760 °C in the 5 second period and when the plunger initial temperature is 560 °C, the glass surface temperature falls to 870 °C in the same time period. Therefore it is clear that as the initial surface temperature of the plunger decreases then the heat loss increases, as indicated by Kent [4] (this is also discussed in Sections 6.3 and 6.4). Table 2.18 contains a summary of the results in Figure 2.13.

Table 2.18 Results of glass surface temperature drop with initial mould surface temperatures of 490 °C and 560 °C and glass initial temperature was 1015 °C

Time (seconds)	0.01	0.1	0.2	0.3	0.4	0.5
Wall-560 °C.	990 °C	900 °C	880 °C	875 °C	873 °C	870 °C
Wall-490 °C.	1000 °C	810 °C	780 °C	775 °C	770 °C	760 °C

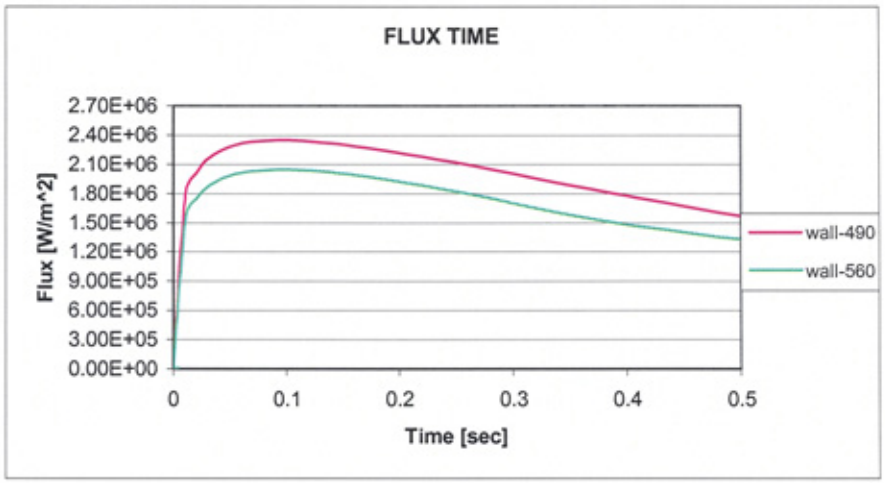

Figure 2.14 Variation of the glass surface flux with time, initial mould surface temperatures was 560 °C Purple line and 490 °C green line

Figure 2.14 shows the heat flux through the glass-plunger interface over the same 5 second period immediately preceding the first contact. Starting with the same initial glass temperature the initial plunger temperature of 490 °C generates a heat flux change from 2.25 $x10^6$ to 1.35 $x10^6$ W/m^2 and the initial plunger temperature of at 560 °C generates a heat flux change from 2.03 $x10^6$ to 1.16 $x10^6$ W/m^2. This shows that the lower the initial plunger temperature the higher the heat flux that is generated. This concurs with the findings from Figure 2.13 since more temperature is lost from the glass for the lower initial plunger temperature. This result confirms that obtained by Roger Kent [4] the results are summarised in Table 2.19.

Table 2.19 Results of flux at the surface with mould initial surface temperature of 490 °C and 560 °C and glass temperature was 1015 °C

Time (seconds)	0.1	0.2	0.3	0.4	0.5
Wall-490 °C. Flux W/m^2	2.38 $x10^6$	2.22 $x10^6$	1.90 $x10^6$	1.75 $x10^6$	1.60 $x10^6$
Wall-560 °C. Flux W/m^2	1.95 $x10^6$	1.85 $x10^6$	1.72 $x10^6$	1.50 $x10^6$	1.30 $x10^6$

Table 2.20 Results of flux at the surface with mould initial surface temperature of 490 °C and the temperature decrease of the glass surface

Time (seconds)	0.1	0.2	0.3	0.4	0.5
Wall-490 °C.	1000 °C	810 °C	780 °C	775 °C	770 °C
Wall-490 °C. Flux W/m^2	2.38 x10^6	2.22 x10^6	1.90 x10^6	1.75 x10^6	1.60 x10^6

All of the results arising from experiments and simulations carried out by the referenced works are complied and summarised in the Tables 2.21–2.23. The tables contain details of the simulation or experimental conditions, the properties being considered and their effect on the surface and centre temperatures of the glass over a given time period. This information is for the readers benefit, allowing convenient comparison of different bodies of work.

Table -2.21 Summary of the glass properties (literature review)

(Glass) Properties	Density Kg/m^3	Specific Heat J/Kg-K	Thermal Conductivity W/m-K	Initial Glass Temp °C	Absorption Coefficient m^{-1}	Refractive index	Thickness mm	Time sec	Centre temp. drop °C	Surface temp. drop °C
Jones and Basnett [12]	2500	1350	1.45	1050	32, 45, 100 white glass	0.5	10	5	1050-1015	1050-650
					32, 45, 300 opaque glass				1050-1030	1050-650
Rawson [27]	2500	1350	1.45	1050	20-400 white glass	–	10	3	1050-1035	1050-700
								2	1050-1048	1050-730
McGraw [55]	2500	1350	1.45	1050	32, 45, 100 white glass	–	10, 25, 50	5	1050-1030	1050-650
Fellows and Shaw [19]	2450	1350	1.44	1077	100, 300 white glass	1.0	10	4	---	1077-720
Kent [18]	2500	1300	1.50	1015	100, 300 white glass	–	10	0.5	---	1015-760

Table -2.22 Summary of the mould properties (literature review)

(Mould) Properties	Density Kg/m^3	Specific Heat J/Kg-K	Thermal Conductivity W/m-K	Heat Transfer Coefficient W/m^2-K	Initial mould Temperature °C	Flux at the surface W/m^2
Jones and Basnett [12]	8000	500	200	1500 (0.0375cals./cm^2s.°c)	490	---
Rawson [27]	8000	500	200	1500	490	-----
Fellows and Shaw [19]	8000	500	200	1600	42, 300, 545	2.0E+06 to 4.5E+05 (Time from 0.1 to 4.0 sec.)
Kent [18]	8000	500	200	1600	490, 560	2.38E+06 to 1.60E+06 (Time from 0.1 to 0.5 sec)
McGraw[55]	8000	500	200	1500	490	2.30E+06 to 1.35E+06 (Time from 0.1 to 5.0 sec)

Table -2.23 Summary of the air properties (literature review)

(Air) Properties	Density Kg/m^3	Specific Heat J/Kg-K	Thermal Conductivity W/m-K	Heat Transfer Coefficient W/m^2-K	Initial Temperature °C	Radiation (reheat) °C
Rawson [27]	0.024	1000	1.20	10	20	730-940
McGraw [3]	0.024	1000	1.225	10	20	---

2.8 DISCUSSIONS

Figures 2.1 and 2.3 show the temperature distributions during pressing through 10 mm thick opaque and white glass from 0.1 to 5.0 seconds. The initial centre temperature for both types of glass was 1050 °C, at the end of the pressing period the temperature at the centre of the opaque glass had dropped to 1015 °C and to 1030 °C for the white glass. These results are as obtained by Jones and Basnett [1]. The wavelength spectrums of white and opaque glass are shown in tables 2.2 and 2.3. For white glass the absorption coefficient α = 23, 45, 100 m^{-1} and for opaque glass α = 23, 45, 300 m^{-1}. Therefore at shorter wavelengths, white glass absorbs less energy than opaque glass. In terms of cooling, the opaque glass looses heat energy faster than the white glass over, the same time period. White and opaque glasses both have similar thermal properties except for colour, where white glass is completely transparent while opaque glass is not. This means that the higher the absorption coefficient of the glass, the greater its ability to absorb or lose heat energy. The absorption coefficients for white and half green (opaque) glass are presented later in Figures 3.6 and 3.7. Hagy [23] shows that the radiative thermal conductivity of half green glass is higher than that of white glass. The experimental results in chapter 8 and the discussion of the differences between white and green glass during the cooling process highlight a similar relationship.

Figure 2.5 shows the reheat calculations for a model in which white glass is cooled symmetrically from both surfaces for 3.0 seconds between a steel mould and plunger. The initial temperature of the glass was 1050 °C and the temperature of the metal surface in contact with the glass was maintained at 490 °C. The centre temperature of

the glass drops to 1020 °C in this time while the surface temperature reaches 935 °C. These results closely follow those produced by Rawson [11].

Figure 2.6 shows the change in centre temperature of the white glass for the 3 seconds after it is removed from the mould for two cases. Firstly, when the air temperature is at the same temperature as the mould and plunger giving an external emissivity of 0.8 and secondly when the air temperature is ambient and external emissivity is 0. In both cases the centre temperature drops from 1050 °C to 1033 °C and the surface temperature increases to 940 °C from 700 °C after 3 seconds. Again the results match those produced by Rawson [11].

Considering the two cases of heat transfer during the reheat stage of conduction-radiation and radiation only, Figures 2.7-2.8 show the temperature distributions through the glass over a time of 2 seconds, which is about the actual time taken during glass manufacture. Comparing the increase in glass surface temperature for each of the heat transfer cases a difference of 15 °C was observed, with the reheat for conduction-radiation going from 730 °C to 930 °C and for radiation only from 730 °C to 945 °C in 2 seconds. Therefore when only radiation is considered the reheat stage sees a greater increase in glass surface temperature than when both radiation and conduction is considered. The effect of conduction is hence very small and most of the heat lost from the centre of the glass to the surface is by radiation as shown by Rawson [11]. Reheat occurs because the centre of the glass is hotter than the surface this leads to heat transfer from the centre of the glass to the surface and in the absence of conduction from the surface to the mould or plunger, the temperature of the glass increases again. This means that when the glass cools in the air with no metal contact heat transfer by radiation is dominant.

Figure 2.9 shows the effect of different thicknesses of glass (10, 25, and 50 mm) on the glass surface temperature during mould plunger contact over a period of 5 seconds. As the thickness reduces the centre temperature drops and more heat is transferred from the glass to the mould, the same occurs with the flux in Figure 2.10, and as the thickness of the glass reduces the significance of radiation increases. In McGraw [6] it is shown that the glass thickness has a great influence on the heat transfer from the centre of the glass to the surface. As seen from Table 2.12, when the glass thickness is 10 mm, more heat is transferred from the centre to the surface in comparison to a thickness of 50 mm. The greater the temperature drops the more heat that is transferred from the glass to the mould. Also the centre temperature drops faster for smaller thicknesses of glass, as the high transfer of heat between the glass and the mould causes a high temperature gradient, and high heat flux see Table 2.14.

Figures 2.11 and 2.12 show the effect of the initial mould temperature on the heat transfer through the surface between mould and glass. As the initial mould temperature decreases more heat is transferred from the hot glass to the mould and so the glass temperature decreases more also. With an initial glass surface temperature of 1077 °C and initial mould surface temperatures of 545, 300 and 42 °C, the glass surface temperature is seen to decrease as the mould surface temperature decreases during a 4 seconds period. This is because the higher the initial temperature gradient is between the centre of the hot glass and the mould the faster the heat is lost and hence the faster the glass surface temperature cools. The same results were observed by Fellows and Shaw [3]. As the contact time observed is increased from 0.1 seconds, then the rate of heat transfer begins to decrease, and the difference between the surface temperatures for each initial mould temperature also reduces. To summarise, this means that the effect of

the initial mould temperature on the glass surface temperature is of most importance over short contact times and more heat is lost from the glass for cooler initial mould temperatures. As time increases and heat is transferred to the mould, increasing the mould temperature, then the temperature gradient between the centre of the glass and the mould reduces, which in turn reduces the heat flux and hence the amount of heat transferred to the mould. Over a sufficiently large time period a point of equilibrium would be reached, where the mould has absorbed enough heat from the glass that its temperature has increased and the glass temperature has decreased to the same point resulting in a temperature gradient of 0, ending heat transfer.

Figures 2.13 and 2.14 show the effect of initial plunger temperature on the surface temperature and surface flux of over a 5 second period. Starting with an initial glass temperature of 1015 °C and an initial plunger temperature of 490 °C a fall of 255 °C to 760 °C is observed at the glass surface over the 5 second period and for an initial plunger temperature of 560 °C a fall of 145 °C to 870 °C over the same period. Therefore, the increase in operating temperature of the plunger by approximately 70 °C decreases the temperature loss at the glass surface by approximately 110 °C. Kent [4] repeated the work by Fellows and Shaw. [3], using different initial glass and plunger temperatures and observed a cooling time of only 0.5 seconds. As with the mould at the initial point of contact there is a large temperature gradient between the plunger and the centre of the glass which induces heat transfer and the cooler the initial plunger temperature the greater the temperature gradient and hence the greater the flux. Again as time increases the plunger temperature increases and the glass centre temperature decreases reducing the flux and heat transfer. Comparing the temperature loss over the first 0.1 seconds for an initial plunger temperature of 490 °C the drop is 205 °C and at

an initial plunger temperature of 560 °C the drop is 115 °C, signifying the much steeper gradient for the lower initial temperature. Over the following 0.4 second period the surface temperature only drops a further 50 °C and 30 °C for the initial plunger temperatures of 490 °C and 560 °C respectively. The dominant period of heat transfer is therefore very short, of the order of 0.1 seconds and is large for lower initial plunger temperatures.

2.9 SUMMARY

Observation of the cooling of both white and opaque glass over a 5.0 second period between a mould and plunger shows that the centre temperature of white glass decreases more rapidly than that of opaque glass, due to the higher absorption coefficient of opaque glass; as presented in Sections 2.3.1 and 2.3.2.

During the reheat stage, blank open, consideration of external emissivity introduced by the effect of the moulds temperature on the surrounding air temperature results in a minimal change in heat transfer characteristics. This will be discussed further later.

The rate of surface temperature cooling of 10 mm thick glass over a 3 second period during blank open is faster when both conduction and radiation transfer mechanisms are considered than when only radiation is considered This is due to the concession of an extra 10 W/m^2 K thermal conductivity between the glass and air; as presented in Section 2.4.3 and 2.4.4.

After contact with the mould different glass thicknesses of 10, 25, 50 mm are seen to cool at different rates. As the thickness reduces the glass centre and the surface temperatures decrease faster and more heat transferred from the glass to the mould; as presented in Section 2.5.

Reducing the initial mould temperature at the time of contact, causes a higher temperature gradient and results in greater heat transfer, reducing the glass surface temperature and increasing the heat flux. The dominant period of heat loss from the glass is over the initial 0.1 seconds, at which time the temperature gradient has reduced due to the increased mould and decreased glass temperatures; as presented in Section 2.6.

Reducing the initial plunger temperature at the time of contact, causes a higher temperature gradient and results in greater heat transfer, reducing the glass surface temperature and increasing the heat flux. The dominant period of heat loss from the glass is over the initial 0.1 seconds, at which time the temperature gradient has reduced due to the increased plunger and decreased glass temperatures; as presented in Section 2.7.

CHAPTER THREE – GLASS PROPERTIES

3.1 INTRODUCTION

During the formation of glass containers, heat from the glass melt needs to be extracted by the mould at a high enough rate such that the parison formed holds its shape. The amount of heat extracted from the glass melt has been shown to be dependent on parameters such as, the properties of the glass including: density, viscosity, specific heat, thermal conductivity and heat transfer coefficients at the glass-mould and glass-air interfaces, the characteristics of the mould material, and the time of contact between the metal mould and glass melt. The initial temperature of the mould will affect the heat flux as was shown in Sections 2.5.1-2.5.3.

This chapter provides an understanding of how the thermal and mechanical properties of glass change with respect to temperature. This discussion is preceded by an examination of the composition of the soda lime glass on which the work in this thesis is based. The chapter also aims to obtain typical values for the different properties based on the work that has been published previously. The density of glass changes as it is heated and pressed, the effect of this is considered in Section 3.3.1.

The way in which the viscosity of the melt glass changes with temperature is of primary importance. The viscosity of the glass melt is affected by both temperature and its composition. As a glass cools, it transforms from a liquid to a stiff solid at the glass transformation temperature. The viscosity-temperature relationship is presented in Section 3.3.2.

The effect of the absorption coefficient on the heat energy lost during the glass tool contact is also studied for two types of glass (white and green). The green glass has a higher absorption coefficient than the white glass; the three wave bands are presented in section 3.7.

The heat flux at the glass mould interface depends on the temperature difference between the glass melt and the mould during the contact between the glass and mould and during the reheat case where the glass is cooled in the air and is presented in Section 3.3.4.

The other glass properties: refractive index; external emissivity, heat capacity, specific heat, and thermal conductivity and radiation are presented in the remainder of Section 3.3.

The glass mechanical properties: Coefficients of linear thermal expansion and the temperature effect on the linear expansion at the strain point are presented in Section 3.4.1. The elastic properties for white glass, Young's modulus (E), and the variation of Young's modulus with the temperature below the working range are presented in Section 3.4.2. The modulus of rigidity (Shear modulus) (G) is also presented in Section 3.4.2 along with the bulk modulus (K) and Poisson's ratio (μ).

3.2 GLASS COMPOSITION

Figure 3.1 shows the chemical composition of soda lime Glass, Si O_2 –Al_2 O_3 –Na_2 O – K_2 O –Ca O –Mg O typically used in the manufacture of glass containers. The glass compositions were expressed as weight contents. X-ray analysis of a typical glass sample is shown in Figure 3.1.

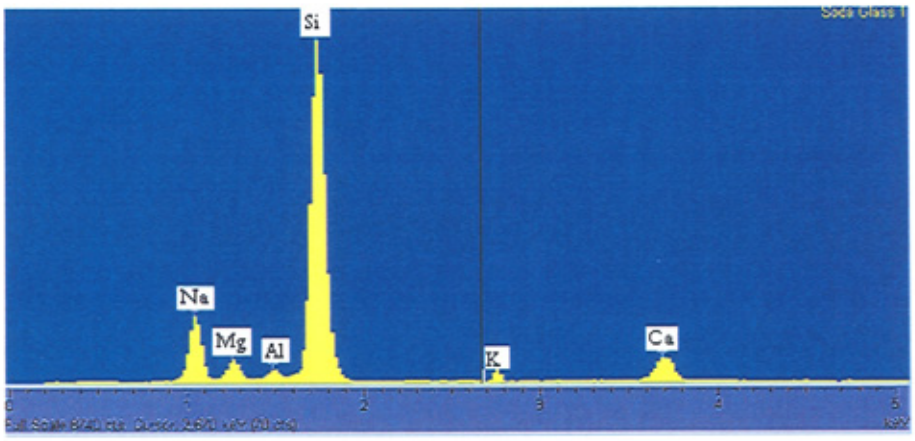

Figure 3.1 Percentage values of the glass composition elements

Table 3.1 Soda lime glass percentages of elements by weight

Composition	Si O_2	Na_2 O	K_2 O	Ca O	Mg O	Al_2 O_3
Wt % Composition(1)	72.58	13.22	0.54	10.52	1.31	1.27
Wt % Composition(2)	72.85	12.95	0.52	10.84	1.36	1.34

Calculation of the oxygen gram mole of silica glass composition

$Si\ O_2$ (gram mole) % = 28 + 16 x 2 = 60 x 0.7285 = 43.71

Na_2O (gram mole) % = 23 x 2 + 16 = 62 x 0.1295 = 8.029

K_2O (gram mole) % = 39 x 2 + 16 = 49 x 0.0052 = 0.255

Ca O (gram mole) % = 40 + 16 = 56 x 0.1084 = 6.070

Mg O (gram mole) % = 24 + 16 = 40 x 0.0136 = 0.544

Al_2O_3 (gram mole) % = 27 x 2 + 16 x 3 = 86 x 0.0134 = 1.152

Total gram mole

Total (gram mole) = 373 Total (gram mole) % = 59.76

Total (oxygen gram mole)

$(O_2 + O + O + O + O + O_3) = (16 \times 2 + 16 + 16 + 16 + 16 + 16 \times 3)$

Total (Oxygen gram mole) = 144

$O_2 = (144 \times 59.76) / 373 = 23.07$

Oxygen % (gram mole)

23.07 / 144 = 0.160

0.160 x 100 = 16

3.3 GLASS THERMAL PROPERTIES

3.3.1 DENSITY

The density of glass is usually expressed in terms of kilograms per cubic metre. Silica glass has a density at room temperature of 2203 Kg/m^3. The addition of other oxides to the silica to form silicate glasses will, in nearly all cases, increase the density. Exceptions are found in glasses that have 96% silica content and in low-loss borosilicate glasses, which have densities of 2180 Kg/m^3 and 2130 Kg/m^3 respectively. The densities of Soda-lime glasses are around 2500 Kg/m^3. For very dense lead silicate glass, used for optics and for the absorption of high-energy radiations, densities can exceed 6000 Kg/m^3.

The density of glass is subject to variation as a result of thermal treatment. Density is at its greatest when the glass is stable at the lowest practicable temperatures for glass forming. The volume of a specific body of glass will increase with temperature. The volumetric change is inversely proportional to the change in density. It is three times the linear change of dimension with temperature.

According to Hagy [23], densities of glasses can vary from 2.5 gm/cm^3 to 8.0 gm/cm^3. The densities of some typical glasses are shown in Table 3.2. The density of most glasses decreases with temperature; a typical example being given in Figure 3.2

From the literature review, Jones and Basnett [1], Rawson [11], McGraw [6] and Kent [4], have used a glass density of 2500 Kg/m^3 at a temperature of 1050 °C, and Fellows and Shaw [3], used a density of 2450 Kg/m^3, these are reviewed in Table 2.21.

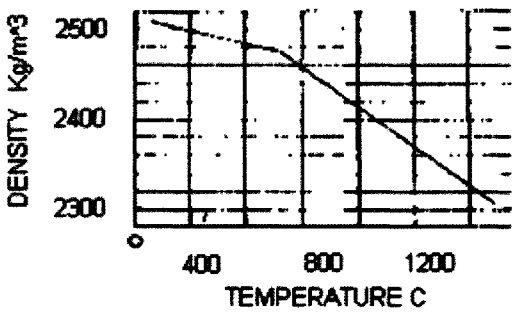

Figure 3.2 Temperature and density change Hagy [23]

Glass	Density Kg/m^3
Fused Silica	2200
Borosilicate Glass	2230
Container Glass	2460
Plate Glass	2460
Dense Flint	4800

Table 3.2 Densities of typical glasses Hagy [23]

3.3.2 VISCOSITY

The viscosity characteristics of glass are important to the study of the vitreous state. From the practical stand point of glass manufacture, knowledge of these characteristics is vital in determining compositions favourable to melting and fabricating operations. They are also useful in determining proper annealing temperatures. The viscosity of glass varies continuously from the molten state to the lowest temperature at which structural adjustment is perceptible. The viscosity curves of several different glasses are shown in Figure 3.3. The curve is roughly hyperbolic in form, with an empirical expression determined by Fulcher [19] as equation (1).

$$\log \eta = -A + \frac{B}{T - T_0} \qquad (1)$$

Where η = viscosity at any temperature, A and B are constants, T_o is the room temperature constant, T the temperature considered.

3.3.2.1 LAKATOS GLASS VISCOSITY

Viscosity can be determined using equation (1) rearranged in terms of temperature.

$$T = T_0 + \frac{B}{\log \eta + A}$$

Figure 3.3 Shows the viscosity-temperature relationship of a glass melt calculated using the Fulcher [19] and Lakatos [20] equations (where B=3848, A=1.47 and T_o = 287°C derived from the chemical composition by weight shown in Table 3.3).

The viscosity-temperature characteristics of the glass melt can be modelled using the Fulcher equation (1). The three constants from the Fulcher equation (A, B and T_o) can be calculated from the known composition of the glass melt using the equations of T.

Where, based upon the molar wt%;

$$B = -6039.7\ Na_2O - 1439.6\ K_2O - 3919.3\ CaO + 6285.3\ MgO + 2253.4\ Al_2O_3 + 5736. \quad (2)$$

$$A = -1.4788\ Na_2O + .8350\ K_2O + 1.6030\ CaO + 5.4936\ MgO - 1.5183\ Al_2O_3 + 1.4550 \quad (3)$$

$$T_0 = -25.07\ Na_2O - 321.0\ K_2O + 544.3\ CaO - 384.0\ MgO + 294.4\ Al_2O_3 + 198.1 \quad (4)$$

The constants value for soda lime glass A=1.59, B = 4263.53 and C = 271.59

Table 3.3 Shows the chemical composition of glass weight %

Composition	$Si O_2$	$Na_2 O$	$K_2 O$	Ca O	Mg O	$Al_2 O_3$
Wt % Composition	72.85	12.95	0.52	10.84	1.36	1.34

During the formation of glass containers, heat needs to be withdrawn from the surface of the glass melt to form a skin. Examining the viscosity-temperature characteristics, shown in Figure 3.3, it can be seen that the surface temperature must fall from the initial 1050°C (approximate viscosity 16 Kg/m-s) to at least 700°C (corresponding to an approximate viscosity of 3.0×10^5 Kg/m-s)

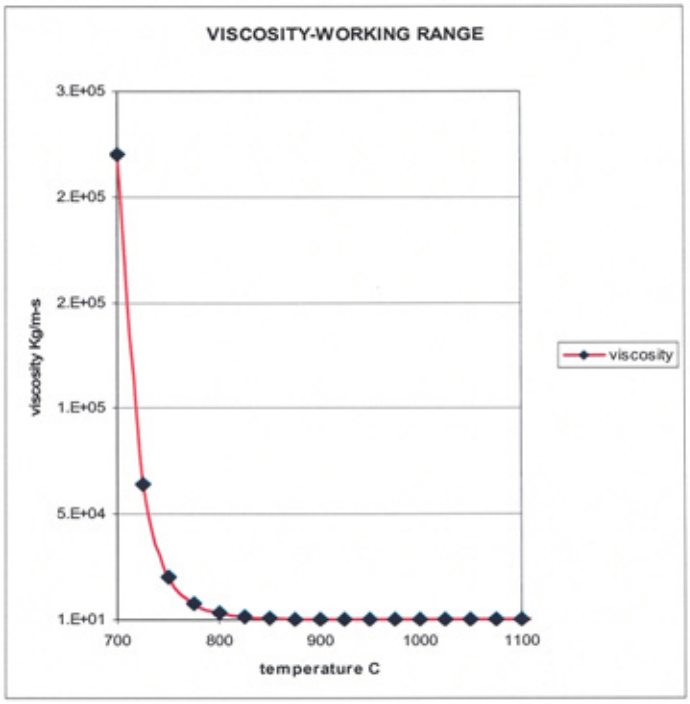

Figure 3.3 Temperature and viscosity working range

This effect has been demonstrated by Lillie [21] who measured the changes in viscosity in glass fibres with a diameter of 0.8 mm over a period of 2000 min. at a temperature of 486 °C. This is almost 9 °C below the stabilized glass temperature of 477 °C.

ANNEALING POINT

This represents the temperature at which the internal strains in glass are reduced to 10^6 Pa-s. An acceptable commercial time limit for the glass to reach this point is 15 min.

STRAIN POINT

This is the temperature at which the internal stresses are reduced to less than 10^{13} Pa-s. A commercially acceptable time limit for the glass to reach this is 4 hrs. At this viscosity, the glass is substantially rigid. The data for determining the strain point are taken with the same procedures used for the annealing point, but for a slower rate of fibre elongation.

FLOW POINT

Lillie [21] has noted the need for an additional reference point to the softening point, to depict a lower level of viscosity. He has proposed the softening point to be a viscosity of 8.0 $x10^7$ poise (5.6 $x10^{12}$) Kg/m-s. This reference point has not yet been established as a standard.

NOTE: The annealing point was formerly taken as a viscosity of 5.0 x 10^{13} poise (5.2 $x10^{10}$ (5.2 x 10^{10}) Kg/m-s and the strain point as 2.0 $x10^{15}$ poise (8.0 x 10^7) Kg/m-s. Much of the data published for glasses are made using these values. The differences in temperatures for these two conditions amount to only a few degrees.

SOFTENING POINT

At the softening point, the low viscosity of the glass permits its stabilization during measurement. At the annealing and strain points, with their higher viscosities, complete stabilization is not attained at the cooling rate employed. The corresponding

temperatures will be slightly lower than for the same glass after stabilization. In the case of one soda-lime glass, Lillie [21] has found the temperature differences to be roughly 15°C at the strain point and less than 5°C at the annealing point.

For most commercial glasses, the annealing point temperature is 35 to 40°C above that of the strain point. Glasses which have a large temperature interval between the flow point and the softening point are said to have a long "working range" and are generally easier to fabricate in the viscous state than glasses such as the alumino-silicates which have a short working range. Although silica glass has a long working range when expressed in degrees, the working temperature is so high that the glass cools very rapidly and makes ordinary fabricating operations very difficult. Table 3.4 summarizes the fixed point's values.

Table 3.4 Summarises the temperature values strain, annealing, softening working and melting point Lillie [21]

Temperature	Strain point	Annealing point	Softening point	Working point	Melting point
T[°C]	536 °C	563 °C	735 °C	1033 °C	1457 °C
poise	3.0×10^{15}	5.0×10^{13}	8.0×10^{7}	1.0×10^{5}	1.0×10^{3}

The viscosity of soda-lime glass in the working range from 700 °C to 1100 °C is 8.0×10^{7} to 1.0×10^{4} poise (or 1.40×10^{4} to 1.04 Kg/m-s) as seen in Figure 3.4. As the temperature of the glass increases the value of viscosity decreases, this is as seen in figure 3.4, where, for a working range temperature of 700 °C to 1100 °C the viscosity is 1.40×10^{5} to 1.04 Kg/m-s.

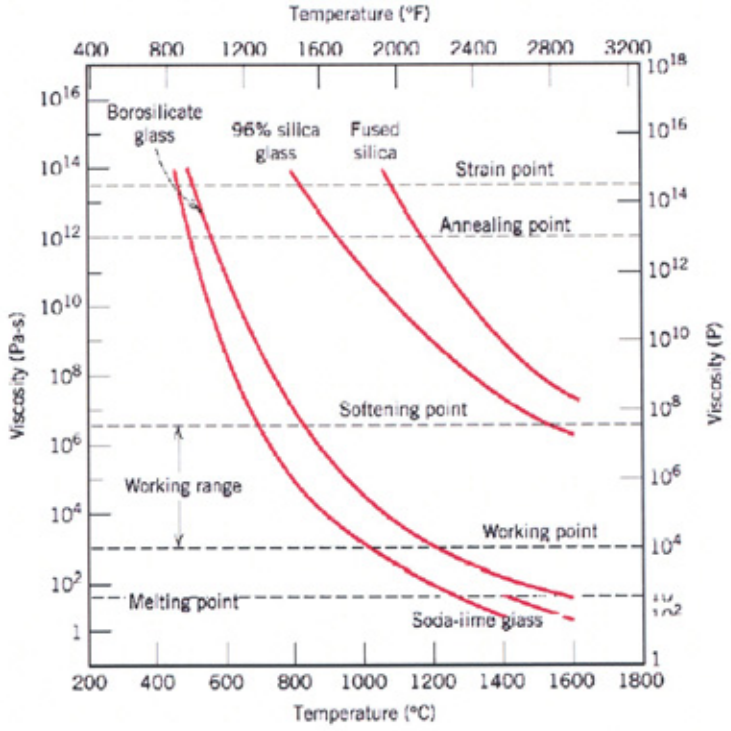

Figure 3.4 Viscosity curves of commercial glasses the numbers indicated listed in Table 3.5 Lillie [21]

Table 3.5 Summarizes viscosity values strain, annealing, softening working and melting point

viscosity	Strain point	Annealing point	Softening point	Working point	Melting point
T[°C]	536 °C	563 °C	735 °C	1033 °C	1457 °C
poise	3.0×10^{15}	5.0×10^{13}	8.0×10^{7}	1.0×10^{5}	1.0×10^{3}
Kg/m-s	5.6×10^{12}	5.2×10^{10}	1.40×10^{4}	1.041×10^{2}	1.041

During the pressing operation, the glass melt will tend to be forced to flow by the surface of the plunger. The glass melt will therefore flow to try and follow the texture of the plunger until the surface of the glass melt becomes so viscous that the pressing pressure used cannot force the glass melt to flow any further.

Pressing glass at low plunger temperatures will mean that initially the heat will be withdrawn faster from the surface of the glass melt than when the glass is pressed using a higher initial plunger temperature.

On formation of the glass, the temperature at the surface of the glass is lower than that at the interior due to the temperature gradients produced between the glass and the relatively cool mould. The surface of the glass therefore gains a very viscous surface layer with a relatively fluid interior; the solid layer enables the glass to keep its shape during the formation process.

3.3.3 ABSORPTION COEFFICIENT

The ability of glass to absorb radiation is characterized by its absorption coefficient (α), defined by the familiar Lambert-Bougure law $I_x = I_o e^{-\alpha x}$. In which (I_o) is the intensity of monochromatic radiation entering a transparent body at right angles to its surface and (I_x) the residual intensity after radiation has penetrated a distance x in to the body.

Many of the present considerations were triggered by the experimental work of Grove and Jellyman [48] in Great Britain who measured the temperature dependence of the spectral absorption coefficients of glasses and thus made it worthwhile to elaborate theoretical consideration of radiant heat transfer in hot glass. Figure 3.5 shows the temperature variation and the wavelength of the absorption coefficients of the white soda lime glass, Figure 3.6 shows green soda lime glass, as presented by Endrys, Geotti and Luka [22].

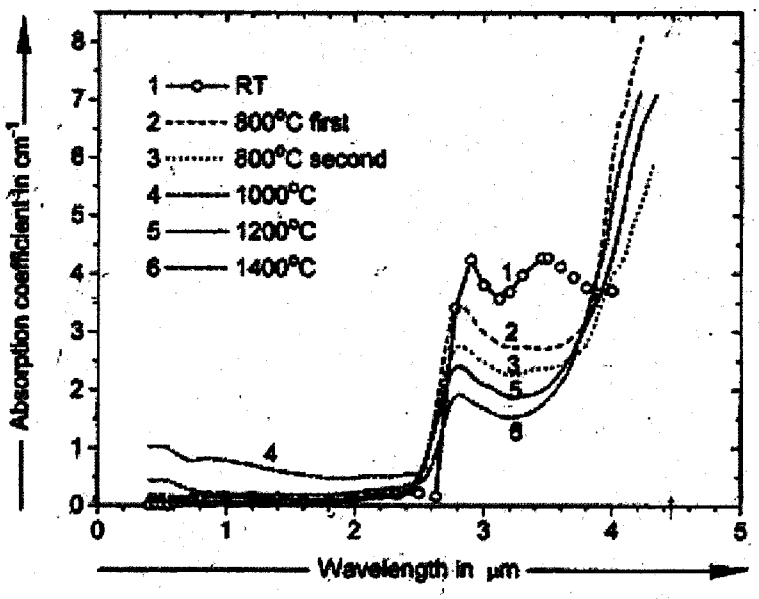

Figure 3.5 Absorption coefficients and wavelengths white soda lime glass Geotti, and Riu [22]

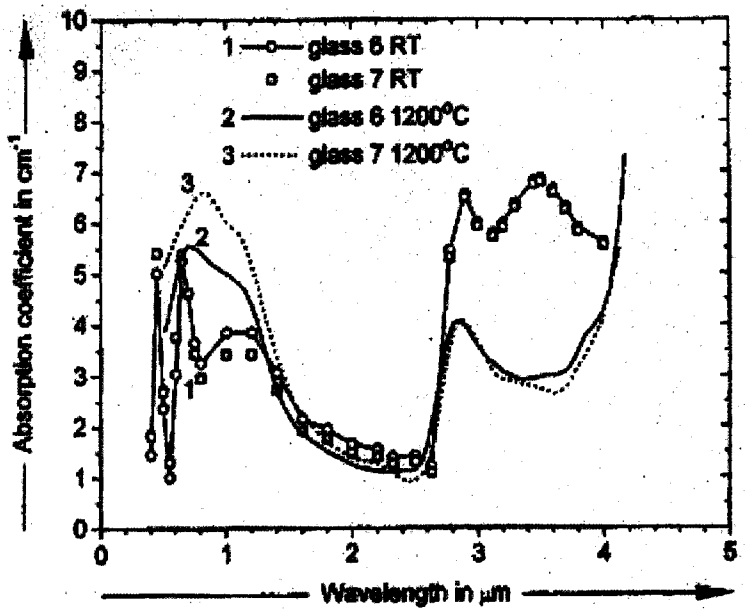

Figure 3.6 Absorption coefficients and wavelengths green soda lime glass Geotti, and Riu [22]

Figure 3.5 shows the value of the Absorption Coefficient for white glass in the three wave bands, α = 32, 45, 100 m^{-1}, and Figure 3.6 shows value of the Absorption Coefficient for green glass in the three wave bands, α = 200, 100, 300 m^{-1}, these values are used in chapter 8 comparison between the white and green glass due to cooling, Table 8.4.

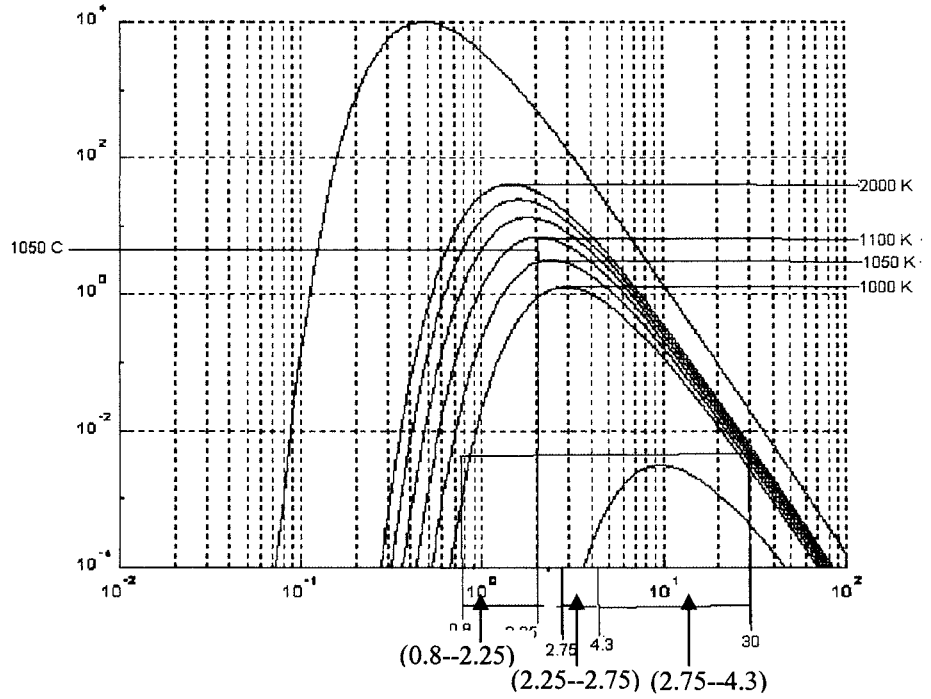

Figure 3.7 Three wave bands of absorption coefficients of white soda-lime glass at maximum temperature of 1100 °C table below shows the values of each band

The three wave bands are indicated in Figure 3.7 and summarised in Table 3.6.

Table 3.6 Bands of wavelengths and absorption coefficients, used by Basnett [1], for white glass seen in Table 2.21

Bands	Absorption coefficient (α)	Wave length (μ)
Band-1	23 m^{-1}	(0.8--2.25) μ
Band-2	45 m^{-1}	(2.25--2.75) μ
Band-3	100 m^{-1}	(2.75--4.3) μ

From previous studies of Basnett [1], $\alpha = 32, 45, 100\ m^{-1}$ for white glass and $\alpha = 32, 45, 300\ m^{-1}$ for opaque glass, in each of the three bands as defined in Table 3.6. The absorption coefficients for white glass used by other authors considered in this work were given in Table 2.21.

3.3.4 HEAT TRANSFER COEFFICIENT

The conductive heat transfer depends on the heat-transfer coefficient at the glass/mould interface and the temperature difference between the mould and the glass surfaces, whereas radiative transfer only depends on the temperature distribution within the glass. A low heat-transfer coefficient would result in a higher radiative influence. McGraw [6] found that the rate of heat removed from glass is controlled to a great extent by the glass-mould interface.

Naughton and McGraw [18] analysed heat transfer in glass-pressing operations using a heat-balance technique. The surface area of the glass in actual contact with the metal surface was thought to be the major factor in the transfer of heat. Jones [24] simulated the glass forming process by computer to determine the dominant factors affecting heat transfer; he later applied the existing theories to forming problems by making simplifying assumptions, but no computer simulation details are given.

Different values of heat transfer coefficient have been applied through the various publications researched. In the studies by Jones and Basnett [1], and Rawson [11], of glass surface temperature changes due to contact with the mould and plunger, a heat transfer coefficient for the mould and plunger of 1500 $W/m^2\ K$ was used by Fellows and Shaw [3] and Kent [4], used a higher heat transfer coefficient of 600 $W/m^2\ K$ in their

studies of the cooling of the glass between the plunger and the mould for different initial mould and plunger temperatures.

Rawson [11] and McGraw [6], in their consideration of the open blank (reheat) stage after a period of 2-3 seconds, considered the ambient air temperature (of 20 °C) to have a thermal conductivity of 1.20 W/m K and a heat transfer coefficient of 10 W/m^2 K.

3.3.5 THE REFRACTIVE INDEX

Refractive Index $n = \sin(\theta_1) / \sin(\theta_2)$.

Where (θ_1), angle of incidence and (θ_2), angle of refraction, as shown in figure appendix. C6-1. Fellows and Shaw [3] have used a refractive index of 1.0 and Jones and Basnett [1] used a Refractive index 0.5. See app. C6 Figure C6-1

3.3.6 THE EXTERNAL EMISSIVITY

The emission of radiation by diathermanous materials is a bulk, not a surface, phenomenon. The ability of the material to emit radiation is characterized by its volume emissive power. This is the rate at which the radiation is emitted in all directions by a unit volume of the material. For an ideal grey material, the volume emissive power is given by $J = 4 \alpha n^2 \sigma T^4$. In this expression n is the refractive index of the material, α its absorption coefficient, T the absolute temperature of the radiating volume element, and σ the (Stefan) Boltzman constant. The volume emissive power of the material is thus seen to be proportional to its absorption coefficient and to $n^2 * \sigma * T^4$, which is the emissive power of a black body radiator in to the radiating material Gardon [12].

3.3.7 HEAT CAPACITY AND SPECIFIC HEAT

Specific heat has been discussed in detail by Sharp and Ginther [25], it increases with temperature and approaches zero at zero absolute temperature. The accepted data for silica glass are those given by Sosman [26]. Values for other glasses have been computed using the additive method by Sharp and Ginther [23] and confirmed by the experimental data of Parmelee and Badger [27].

The best available data on the true and mean specific heats of several commercial glass types are found in the Handbook of Glass Manufacture (Hagy and Barney [23]). The heat content of a substance is a measure of the quantity of heat per unit mass that the substance possesses. The heat content will vary with temperature and the instantaneous rate of change is termed true heat capacity. This can be measured for a constant volume, C_v, or constant pressure, C_p. The heat capacity when referred to the heat capacity of water, between 17 °C and 18 °C, is called the relative specific heat. If the heat content is measured between two temperatures the derived quantity is the mean specific heat. This will approach the true specific heat for small temperature intervals. For larger temperature intervals, the mean specific heat will be roughly equal to the true specific heat at the mean temperature of the measurement. The mean specific heat is of more practical importance to the glass technologist. The total heat capacity, and especially, C_v and C_p are of more theoretical interest. The units of heat capacity in the S.I systems are J/Kg K.

The behaviour of the specific heat of glasses can be illustrated by the data for a borosilicate glass, Corning Code 7740; this is illustrated in appendix B Table B3-1. At temperatures below 5K, the heat capacity follows the T^3 law. Its Debye characteristic temperature, T_d, is 325K. Most glasses will exhibit the same general temperature

dependence. The mean specific heat of several commercial glasses is shown in Table 3.7. Figure 3.8 shows the working temperature range from 500 °C to 1200 °C against the value of the specific heat which varies from 0.27-0.31 Cal/gm °C or 1260 to 1360 J/Kg K Hagy [23].

From the previous study, Jones and Basnett [1], Rawson [11], McGraw [6], and, Fellows and Shaw [3], used the specific heat of 1350 J/kg K, and a lower value of 1300 J/kg K was used by Kent [4].

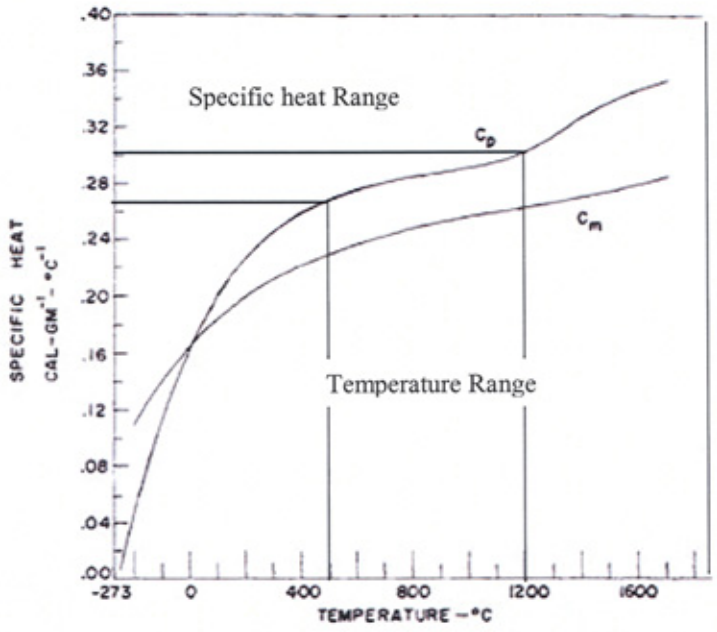

Figure 3.8 Temperature range against the specific heat range E. Hagy [23]

Table 3.7 Shows C_p [J/Kg K] against temperature °C conversion from Figure 3.8

Temperature °C	500	600	700	800	900	1000	1100	1200
C_p [Cal/gm °C]	0.270	0.275	0.285	0.293	0.296	0.300	0.306	0.310
C_p [J/Kg K]	1260	1280	1290	1300	1310	1320	1340	1360

3.3.8 THERMAL CONDUCTIVITY

The thermal conductivity is the rate of heat flow per unit area under the existence of a temperature gradient in the glass. The SI Units used to express this are W/m K.

Experimentally the measurement of thermal conductivity presents difficulties and accuracies better than 5 % are hard to attain. The heat flow through a specified area must be known as well as the temperature gradient. Any extraneous heat transfer must be made negligible and an excellent technique in thermometry is needed. Some of the methods used involve plates, discs and rods, and heat transfer may be axial or radial, and the measurements absolute or comparative. The Thermal Comparator developed by R. W. Powell is a convenient and rapid method for making comparative measurements.

The characteristic of thermal conductance in glasses differs considerably from those found in crystalline materials. For glasses the conductivity drops steadily with temperature and reaches very low values in the neighbourhood of absolute zero. For crystals, the conductivity continues to rise with decreasing temperature until very low temperatures are reached (Kittle [28]).

At low temperatures glass is a relatively poor conductor of heat and this property is inherent in the random structure of glass. Figure 3.9, is illustrative of the general nature of this property, for glasses at cryogenic temperatures the conductivity is extremely low, but rises monotonically with temperature. Near room temperature, the change with temperature is small. At high temperatures radiation plays the dominant role, this is further discussed later, thermal conductivity is not a strong function of composition and ranges from 1.5×10^{-3} to 3×10^{-3} joules/Kg K.

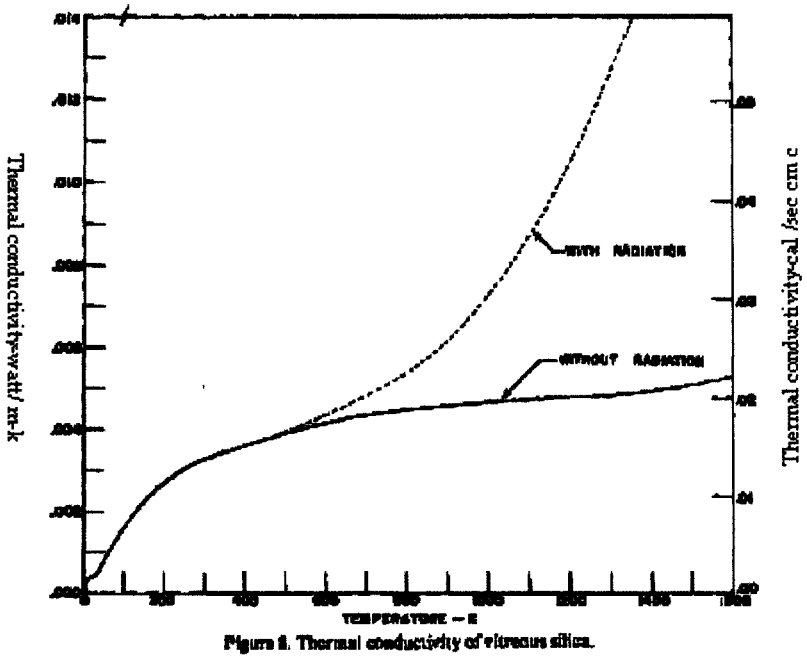

Figure 3.9 Thermal conductivity against the temperature, the dotted line shows with radiation and the solid line shows without radiation Hagy [23]

At temperatures in excess of 600°C, radiant heat transfer may occur in addition to that of the normal conduction mechanism. This is illustrated in Figure 3.9 and by the curve for vitreous silica. A review of this has been given by Gardon [12]. When radiative effects occur the "apparent thermal conductivity" depends on the size of the specimen and the experimental condition and cannot be considered a true physical property of the material.

3.3.8.1 Conduction thermal conductivity

For heat transfer under glass forming conditions both conduction and radiative heat transfer must be considered if a complete understanding of the process is to be obtained. The relative importance of these two transport mechanisms is not at all clear from the literature that exists on the subject.

The method used by Gardon [12] has shown that, in the tempering of glass plates 6 mm thick, radiation is important. In the pressing of the parison, 4.75 mm thick, radiation is completely negligible according to McGraw [2].

The thermal conductivity of glass is important for many applications, either in the conductive or radiative case, from the previous studies by Basnett [1], Rawson [11], and McGraw [6]. They used a thermal conductivity of 1.45 W/m K, due to the glass cooling between the plunger and mould, though they used different initial mould temperatures. Fellows and Shaw [3] used a thermal conductivity of 1.44 W/m K and Kent [4] a higher value of 1.5 W/m K.

3.3.8.2 Radiative thermal conductivity

A simplified approach to the incorporation of the effect of radiative heat transfer may be considered by use of an equivalent thermal conductivity. For a grey material this is obtained from Geotti, and Riu [22] by $K_r = 16\ n^2\ \sigma\ T^3 / 3\alpha$, where $\sigma = 5.67 \times 10^{-8}$ is the Stefan-Boltzman constant and α is the mean absorption coefficient, which actually has three wave-bands covering three distinct regions of soda lime glass transmission spectra, see Figure 3.7. Figure 3.9 shows the nature of the relationship between a true conductivity (without radiation) and the equivalent thermal conductivity (with radiation).

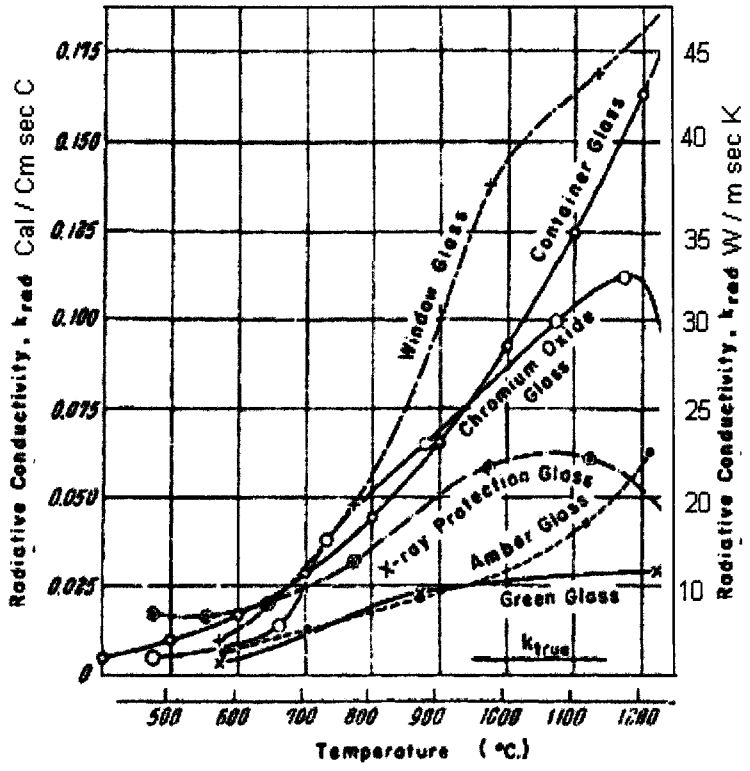

Figure 3.10 Radiative thermal conductivity against the temperature of different silica glasses Hagy [23]

3.4 GLASS MECHANICAL PROPERTIES

3.4.1 COEFFICIENT OF LINEAR THERMAL EXPANSION

The Handbook of Glass Manufacture Henery and Hagy [23], measured the coefficients of linear thermal expansion. The slope of the linear thermal expansion curve is a continuously changing function with temperature. This is shown in Figure 3.11 a plot of the instantaneous expansion coefficient vs. temperature for a borosilicate crown glass. Starting at room temperature, the coefficient rises fairly rapidly. From somewhat above room temperature to above 400°C, the value increases slowly and linearly. Then a rapid increase occurs, starting just below the strain point of the glass.

The thermal expansion of glass is affected markedly by heat treatment. The largest changes that can be accomplished with a thermal history occur in what is known as the transformation range, where a time dependent expansion mechanism is effective. Generally, the transformation range is about 100°C in width, being centred near the strain point of the glass. In this work a value of 1.35×10^{-5} m/m/°C is adopted for the expansion coefficient shown in Table 3.8.

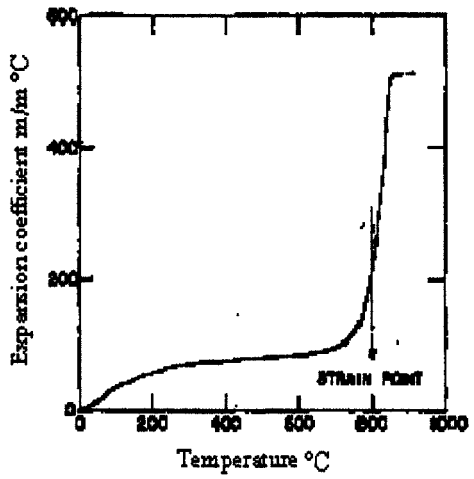

Figure 3.11 Instantaneous expansion coefficients Hagy [23]

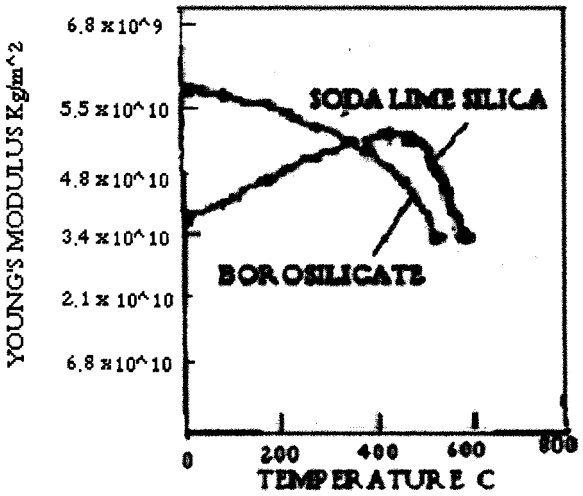

Figure 3.12 Young's modulus verses temperature for silica glass Hagy [23]

3.4.2 ELASTIC PROPERTIES

The fundamental elastic properties of glass are connected by certain definite relationships. The elastic constants themselves may be defined as:

Young's modulus (E)

The ratio of stress to elastic strain or unit elongation for the condition of uniaxial stress the units are that of stress.

Modulus of rigidity (Shear modulus) (G)

Is the ratio of shear stress to the unit angular deformation for the condition of pure shear, the units are the same as for Young's modulus. The value used in this work is 3.98×10^{10} Pascal (N/m^2).

Bulk modulus (K)

Is the ratio of stress, triaxial and equal in all directions (e.g. hydrostatic pressure) to the unit volume deformation the units are again the same as for Young's modulus.

Poisson's ratio (μ)

The ratio of lateral unit strain to longitudinal unit strain, under the condition of uniform and uniaxial longitudinal stress, as stated above, for isotropic bodies such as glass these constants are related in the following manner:

$\mu = (E / 2G) - 1$. The value used in this work is 0.45 for soda lime glass the range of Poisson's ratio for liquids over 700 °C is (0.45), and for solids less than 600 °C is (0.23)

$K = E / 3(1 - 2\mu)$.

These relationships permit the complete description of the above elastic constants by the knowledge of any two constants, Hagy [23].

Table 3.8 Glass constants Young's modulus (E), modulus of rigidity (G), Poisson's ratio (μ) as used by Wakatsuki [29]

Mechanical properties	units	Glass	Mould and plunger steel (solid)
Young's modules(E)	Pascal (N/m^2)	7.8×10^8	1.85×10^6
Poisons ratio(μ)	----	0.45	0.36
Expansion coefficient	m/m/°C	1.35×10^{-5}	1.35×10^{-3}
Shear modules(G)	Pascal (N/m^2)	3.98×10^6	4.7×10^{10}

Above room temperature, the glass also shows an increasing modulus with temperature as indicated in Figure 3.12 Hagy [23] the relationship between Young's Modulus and observed practical strength.

3.5 SUMMARY

The density of glass is subject to variation as a result of thermal treatment. Density is greatest when the glass is stable at the lowest practicable temperatures for forming.

The viscosity of glass varies continuously from the molten state to the lowest temperature at which structural adjustment is perceptible.

The values of the absorption coefficient for white and green glass through the three wave bands have been stated, and will be used in chapter 8. The absorption coefficient of green glass is higher than that of white glass in the highest wave band.

A set of typical values for each of the glass properties discussed for soda-lime glass has been established, and are summarised in Table 3.9

Table 3.9 Glass properties for soda-lime glass taken for this study

Density at 1600 °C	2500 Kg/m^3
Viscosity at 735 °C (softening point)	6.40 x 10^4 Kg/m.s
Viscosity at 1200 °C (melting point)	1.00 Kg/m.s
Heat-transfer coefficient (glass-mould interface)	1500 W/m^2 K
Heat-transfer coefficient (glass-air interface)	10 W/m^2-K
Refractive index	0.5 to 1.0
External emissivity	0.8 to 1.0
Heat capacity and specific heat (at high temp)	990 to 1350 J/Kg K.
Thermal conductivity	1.45 to 2.5 W/m K

CHAPTER FOUR – THE COMPARISON BETWEEN FOUR RADIATIVE MODELS (RO, DTRM, P-1, DO)

4.1 INTRODUCTION

In this chapter a Computational Fluid Dynamic modelling software package, 'Fluent', is used to simulate the heat transfer process from the glass during the blank open phase of glass manufacture when heat transfer by radiation is dominant. This software incorporates different radiative heat transfer mathematical models which may be applied, to solving the case. In this work, four methods will be used to solve the same model and their results compared with each other as well as with experimental work that matches the model as closely as possible. The four approaches are Rosseland (RO), Discrete Transfer Model (DTRM), P-1 and Discrete Ordinates (DO) and in each case the same set of initial conditions have been applied to the model.

Prior to performing the modelling and discussing the results, it is useful to consider the optical thickness of the glass in question as this is known to have an affect on modelling results. Previously published work has highlighted that each of the models behaves differently depending on the thickness and that only selected models are appropriate for modelling at particular thicknesses; this is discussed in Section 4.2.

Section 4.3 provides a description of each of the four radiation models detailing its relative advantages and limitations; it also discusses the boundary conditions used in the calculations.

In Section 4.5 the parameters of the model are stated, including the material properties of the glass and the model initial conditions. The model parameters are based around the

experimental work that will be performed later in Chapter 7. This is followed in Section 4.6 by a discussion of the results obtained for the glass surface temperature drop by applying each of the mathematical methods (RO, DTRM, P-1 and DO) to the same model and then a comparison of these results. A comparison is also made with experimental results that will be later presented in Chapter 7, to show which mathematical model performs the best in this case.

4.2 OPTICAL THICKNESS

The optical thickness (L) is a good indicator of which mathematical model to use in a simulation. For an optical thickness (L) of more than 30 mm, the Rosseland model is the most efficient and has been shown to be more accurate Viskanta and Song [31] than the P-1 approximation. However, at thicknesses of less than 20 mm the Rosseland model does not correctly predict the shape of the temperature profile. This is a result of two diffusion approximations made by Moon and Song [30] in the Rosseland formulation. Both the DTRM and the DO model work across the range of optical thicknesses and they are the only appropriate models at optical thicknesses of less than 20 mm.

In this work, 10 mm thick soda-lime glass, which has an optical thickness< 20 mm, suggests that the DO model is best suited.

4.3 THE FOUR TYPES OF MODELS

In this investigation four different mathematical methods are applied to solve a model using the 'Fluent' software, these models are: Rosseland (RO), the Discrete Transfer (DTRM), the P-1, and the Discrete Ordinates (DO). The model under examination is that of a hot glass body radiating into the ambient air, this presents a heat transfer coefficient of 10 $W/m^2 K$. The thermal properties and initial conditions applied to the model are the same as those applied in the work published by Rawson [11]. A discussion of each of the mathematical methods is now provided.

4.3.1 THE ROSSELAND RADIATION MODEL (RO)

The Rosseland or diffusion approximation for radiation is valid when the optical thickness is greater than 30 mm. It is derived from the P-1 model equations, with some added approximations. This section provides details about the Rosseland model.

The Rosseland model needs solve one less transport equation for the incident radiation than the P-1 model. In having to solve one less equation the Rosseland model is faster than the P-1 model and also requires less memory.

4.3.2 THE DISCRETE TRANSFER RADIATION MODEL (DTRM)

The main assumption of the DTRM is that the radiation leaving the surface element in a certain range of solid angles can be approximated by a single ray.

The primary advantages of the DTRM are threefold: it is a relatively simple model, increased accuracy is achieved by increasing the number of rays considered, and it applies to a wide range of optical thicknesses.

The user should be aware of the following limitations when using the DTRM model:

- DTRM assumes that all surfaces are diffuse. This means that the reflection of incident radiation at the surface is isotropic with respect to the solid angle.
- The effect of scattering is not included.
- The implementation assumes grey radiation.
- Solving a problem with a large number of rays is CPU intensive.

4.3.3 THE (P-1) RADIATION MODEL

The P-1 radiation model is the simplest case of the more general P-N model, it is based on the expansion of the radiation intensity (I) into an orthogonal series of spherical harmonics.

The P-1 model has several advantages over the DTRM. Firstly, the use of an easy to solve diffusion equation requires little demand on the CPU. The model includes the effect of scattering. For combustion applications where the optical thickness is large, the P-1 model works reasonably well. In addition, the P-1 model can easily be applied to complicated geometries with curvilinear coordinates.

The user should be aware of the following limitations when using the P-1 radiation model:

- The P-1 model assumes that all surfaces are diffuse. This means that the reflection of incident radiation at the surface is isotropic with respect to the solid angle.
- The implementation assumes grey radiation.
- There may be a loss of accuracy, depending on the complexity of the geometry, if the optical thickness is small.
- The P-1 model tends to over predict radiative fluxes from localized heat sources or sinks.

4.3.4 THE DISCRETE ORDINATES RADIATION MODEL (DO)

The discrete ordinates DO radiation model solves the radiative transfer equation for a finite number of discrete solid angles, each associated with a vector direction $\vec{s}$ fixed in the global Cartesian system (x, y, z).

The DO model spans the entire range of optical thicknesses, and allows a range of problems to be solved, from surface-to-surface radiation to participating radiation in combustion problems. It can also provide solutions to radiation in semi-transparent media such as glass. Both computational cost and memory requirements are moderate for typical angular discretizations. The current implementation is restricted to either grey radiation or non-grey radiation using a grey-band model. Solving a problem with a fine angular discretization may be CPU intensive.

The non-grey implementation in the software is intended for use with participating media with a spectral absorption coefficient (α), which varies in a stepwise fashion

across spectral bands, but varies smoothly within the band. Glass, for example, displays banded behaviour of this type. For the purposes of the current investigation, this will allow the anisotropic semi-transparent nature of the model to be included in the simulation. However, the non-grey implementation assumes a constant absorption coefficient within each wavelength band.

4.3.4.1 Beam irradiation

As mentioned above, the software (Fluent) allows the specification of the irradiation at semi-transparent boundaries. The irradiation is applied in terms of an incident radiant heat flux (W/m^2) by specifying the solid angle over which the irradiation is distributed, as well as the vector of the centroid of the solid angle. To indicate whether the irradiation is reflected specularly or diffusely, the diffuse fraction may be specified.

4.3.4.2 The diffuse fraction

At semi-transparent boundaries, the software allows the specification of the fraction of the incoming radiation that is treated as diffuse. The diffuse fraction is reflected diffusely, using the treatment described above; the transmitted portion is also treated diffusely. The remainder of the incoming energy is treated in a specular fashion.

4.4 SUMMARY OF ADVANTAGES AND LIMITATIONS OF EACH MODEL

1. Scattering and emissivity: The P-1, Roseland, and DO models account for scattering, while the DTRM neglects it.
2. Semi-transparent media and secular boundaries: Only the DO model allows specular reflection and calculation of radiation in semi-transparent media such as glass.
3. Non-grey radiation: Only the DO model allows the computation non-grey radiation using a grey band model.
4. Localized heat sources: In models containing with localized sources of heat the DO model is probably the best suited for computing radiation.

In this study of 12 mm thick glass which has an optical length of <20 mm, it is predicted that the DO model is best suited to computing the radiation, although the DTRM with a sufficiently large number of rays, should also produce acceptable results.

4.5 MODELLING AND SIMULATION PARAMETERS

Each of the four mathematical techniques discussed will be applied to a model to predict the heat loss by radiation from glass when it is in the air. The simulation results will be compared with practical results, discussed in Chapter 7. Therefore the model used is constructed in such a way as to reflect the practical work carried out.

The analysis to be performed is of a piece of soda-lime glass with a thickness of 12 mm. Starting with an initial temperature of 1100 °C the heat lost by radiation from one

surface of the glass to the surrounding environment, which consists of air (20 °C), over a period of 50 seconds is calculated. This is approximately the time it takes for the glass to cool from 1100 to 500 °C in air, this will be seen later in Chapter 7. The temperature at the centre of the glass (at a depth of 6 mm from the surface), from the glass surface is also calculated.

Tables 4.1 to 4.9 present the simulation parameters and material properties required for the creation of the model and Figure 4.1 shows the physical layout of the model.

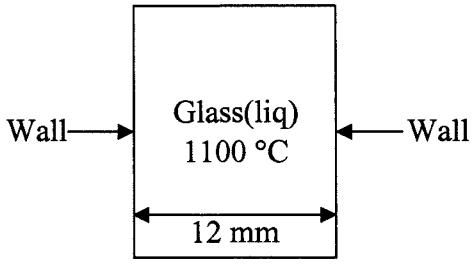

Figure 4.1 Liquid glass at 1100 °C cooled in air

The modelling parameters are listed in Table 4.1; these parameters are used to specify the treatment the model will apply to each model element.

Table 4.1 Types of models used and settings

Model	Settings
Space	2D
Time	Unsteady, 1st-order implicit
Viscous	Laminar
Heat Transfer	Enabled
Solidification and melting	Disabled
Radiation	Discrete ordinate model
Species transport	Disabled
Coupled dispersed phase	Disabled
Pollutants	Disabled

Table 4.2 details the boundary conditions applied to each of the interfaces shown in Figure 4.1.

Table 4.2 Modelling boundary conditions of glass, mould and plunger

Zones name	Id-type
Glass	fluid
Wall	wall
Default-interior	interior
Edge	symmetry

The controls that are applied by the software to direct as to which properties it needs to solve are given in Table 4.3

Table 4.3 Solver control equations

Equations	Solved
Flow	No
Energy	Yes
Discrete ordinates	Yes
Numeric	Enabled

The parameters used to define the unsteady state calculations are given in Table 4.4.

Table 4.4 Variables and relaxation factors

Variables	Relaxation factor
Pressure	0.30
Density	1
Body forces	1
Momentum	0.69
Energy	1
Discrete ordinates	1

The parameters used to define the linear state calculations are given in Table 4.5.

Table 4.5 Variable, type, criterion, and tolerance (linear solver)

Variable	Type	Criterion	Tolerance
Pressure	V-cycle	0.1	0.7
X-momentum	Flexible	0.1	0.7
Y-momentum	Flexible	0.1	0.7
Energy	Flexible	0.1	0.7
Discrete ordinates	Flexible	0.1	0.7

The parameters used to define the discrete scheme are given in Table 4.6.

Table 4.6 Variable and discrete scheme

Variable	Scheme
Pressure	Standard
Pressure-velocity coupling	Simple
Momentum	First order upwind
Energy	First order upwind

The limits of the solutions used in the modelling are given in Table 4.7.

Table 4.7 Quantity and solution limits

Quantity	Limit
Minimum absolute pressure	1
Maximum absolute pressure	5000000
Minimum temperature	1
Maximum temperature	5000

Tables 4.8 and 4.9 provide the material properties of the soda-lime glass.

Table 4.8 Bands of wavelengths and absorption coefficients, used by Jones and Basnett [1], for white glass Table 2.22

Bands	**Absorption coefficient (α)**	**Wavelength (μ)**
Band-1	23 m^{-1}	(0.8--2.25) μ
Band-2	45 m^{-1}	(2.25--2.75) μ
Band-3	100 m^{-1}	(2.75--4.3) μ

Table 4.9, Initial glass, mould and air temperatures and the properties was used by Jones and Basnett [1], Rawson [11], McGraw [6], Tables 2.22 and 2.23.

Property	**Units**	**Glass (fluid)**	**Air (fluid)**
Density	Kg/m^3	2500	1.225
C_p (Specific heat)	J/Kg K	1350	1000
Thermal conductivity	W/m K	1.45	0.0242
Temperature	°C	1100	20
Heat transfer coefficient	W/m^2 K	-	10
Absorption coefficient	m^{-1}	23, 45, 100	-
Refractive index	-	0.5	-
Thickness	mm	6	20
Time	Second	50	50

4.6 COMPARING THE FOUR MODELS (RO, DTRM, P-1, DO)

The results obtained by applying each of the four mathematical approaches to the above model are now presented and briefly discussed along with some equivalent experimental results.

4.6.1 ROSSELAND MODEL COOLING OF 6 MM GLASS FOR 50 SECONDS

Figure 4.2 shows the result obtained from the model when applying the Rosseland formulation for both the glass surface and centre temperature, against time over a period of 50 seconds. It can be seen from the figure that the surface and centre temperature range vary from 1100-655 °C and 1100-730 °C over the 50 second period respectively.

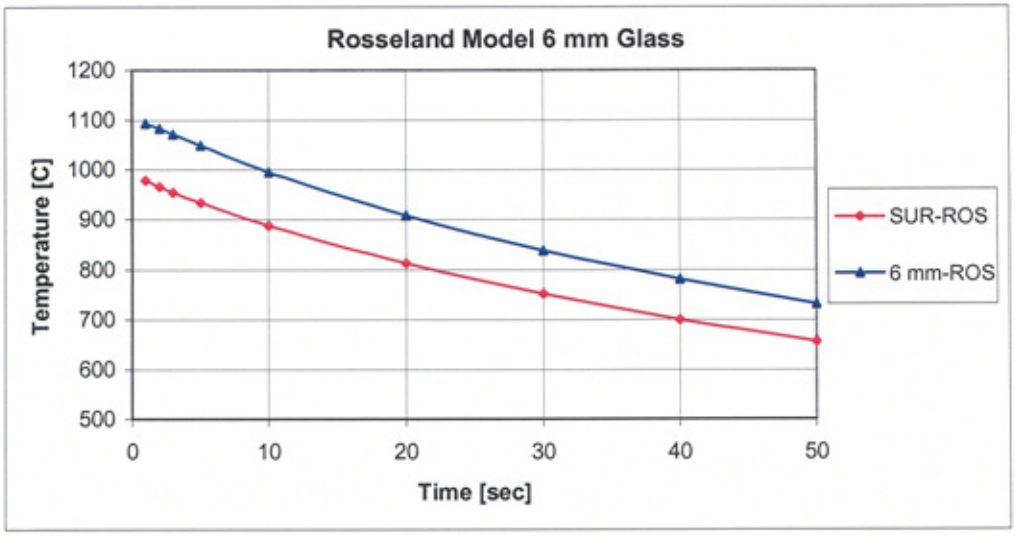

Figure 4.2 Variations of glass (surface and 6 mm) cooling temperatures with 50 seconds, Rosseland model conduction-radiation, HTC between glass and air at 20 °C was 10 W/m^2 K

A summary of the temperatures at the surface and centre of the glass is given in Table 4.10 at 10 second intervals. It is clear from the table that as the time increases the temperature difference between the two point's decreases, starting at a maximum difference of 100 °C dropping to a minimum difference of 75 °C at the end of the 50 second period.

Table 4.10 Surface and centre temperature over 50 seconds cooling (Rosseland)

Time (seconds)	1.0	10	20	30	40	50
6 mm	1100 °C	995 °C	910 °C	840 °C	780 °C	730 °C
Surface	1000 °C	890 °C	810 °C	750 °C	700 °C	655 °C
(Sur.-6 mm)Dif.	100 °C	100 °C	100 °C	90 °C	80 °C	75 °C

4.6.2 DTR MODEL COOLING OF 6 mm GLASS FOR 50 SECONDS

Figure 4.3 shows the results obtained from the DTR model for the glass surface and centre temperatures over a 50 second time period. It can be seen from the figure that the temperatures vary from 1100-655 °C and 1100-730 °C at the surface and centre of the glass over the 50 second period respectively.

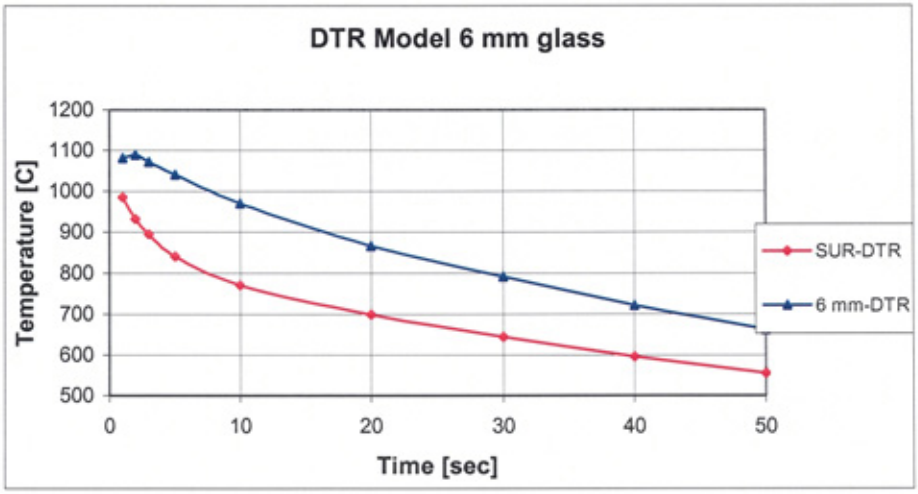

Figure 4.3 Variations of glass (surface and 6 mm) cooling temperatures with 50 seconds, DTR model conduction-radiation, HTC between glass and air at 20 °C was 10 W/m^2 K

A summary of the temperatures at the surface and centre of the glass is given in Table 4.11 at 10 second intervals. It is clear from the table that as the time increases the temperature difference between the two points decreases, starting at a maximum difference of 190 °C dropping to a minimum difference of 100 °C at the end of the 50 second period.

Table 4.11 Surface and centre temperature over 50 seconds cooling (DTR) model

Time (seconds)	1.0	10	20	30	40	50
6 mm	1100 °C	960 °C	860 °C	790 °C	720 °C	660 °C
Surface	1000 °C	770 °C	700 °C	640 °C	600 °C	560 °C
(Sur.-6 mm)Dif.	100 °C	190°C	160°C	150°C	120°C	100°C

4.6.3 P-1 MODEL COOLING OF 6 mm GLASS FOR 50 SECONDS

Figure 4.4 shows the results obtained from the P-1 model for the glass surface and centre temperatures over a 50 second time period. It can be seen from the figure that the temperatures vary from 1100-550 °C and 910-610 °C at the surface and at the centre over the 50 second period respectively.

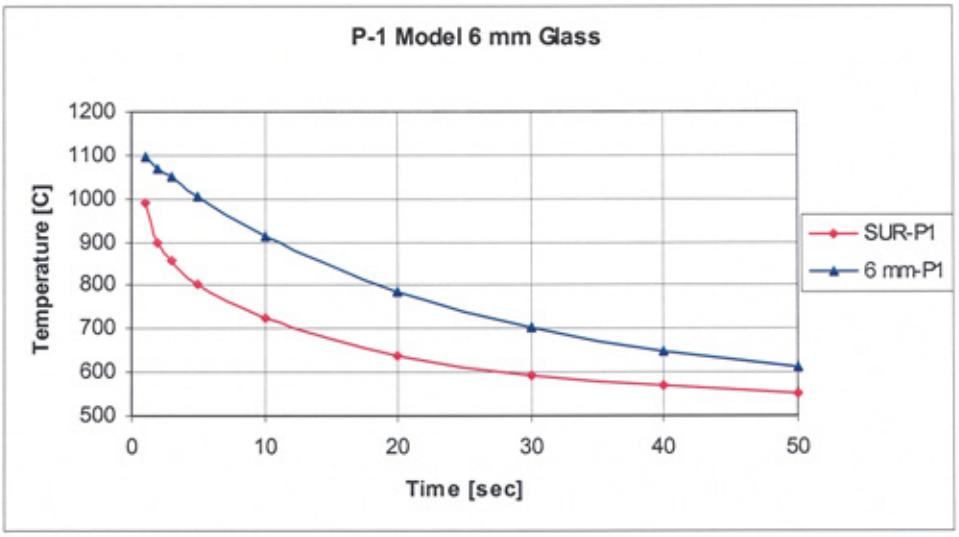

Figure 4.4 Variations of glass (surface and 6 mm) cooling temperatures with 50 seconds, P-1 model conduction-radiation, HTC between glass and air at 20 °C was 10 W/m^2 K

A summary of the temperatures at the surface and at the centre of the glass is given in Table 4.12 at 10 second intervals. It is clear from the table that as the time increases the

temperature difference between the two point's decreases, starting at a maximum difference of 190 °C dropping to a minimum difference of 60 °C at the end of the 50 second period.

Table 4.12 Surface and centre temperature over 50 seconds cooling (P-1) model

Time seconds	1.0	10	20	30	40	50
6 mm	1100 °C	910 °C	790 °C	700 °C	650 °C	610 °C
Surface	1000 °C	720 °C	630 °C	590 °C	570 °C	550 °C
(Sur.-6 mm)Dif.	100 °C	190°C	160°C	110°C	80°C	60°C

4.6.4 DO MODEL COOLING OF 6 mm GLASS FOR 50 SECONDS

Figure 4.5 shows the results obtained from the DO model for the glass surface and centre temperatures over a 50 second time period. It can be seen from the figure that the temperatures vary from 1100-500 °C and 1100-570 °C at the surface and centre of the glass over the 50 second period respectively.

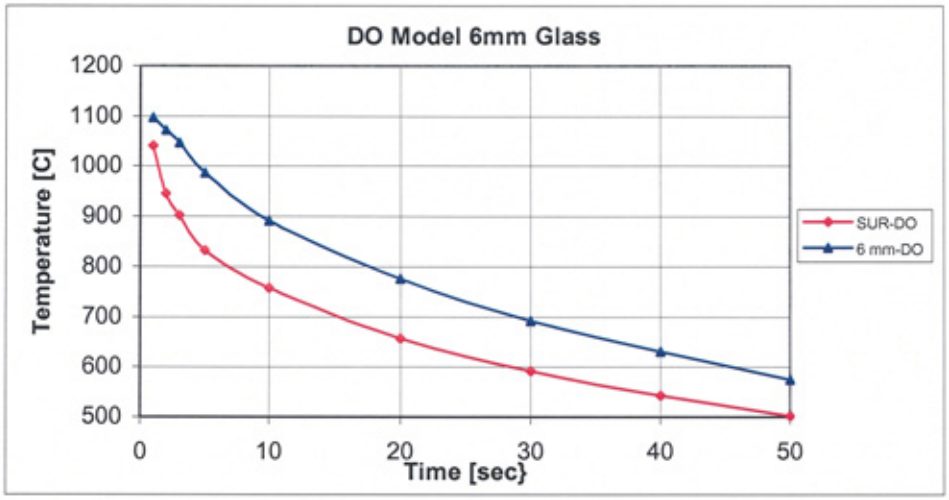

Figure 4.5 Variations of glass (surface and 6 mm) cooling temperatures with 50 seconds; DO model conduction-radiation, HTC between glass and air at 20 °C was 10 W/m^2 K.

A summary of the temperatures at the surface and at the centre of the glass is given in Table 4.13 at 10 second intervals. It is clear from the table that as the time increases the temperature difference between the two points decreases, starting at a maximum difference of 130 °C dropping to a minimum difference of 70 °C at the end of the 50 second period.

Table 4.13 Surface and centre temperature over 50 seconds cooling (DO) model

Time (seconds)	1.0	10	20	30	40	50
6 mm	1100 °C	890 °C	770 °C	690 °C	630 °C	570 °C
Surface	1050 °C	760 °C	650 °C	590 °C	540 °C	500 °C
(Sur.-6 mm)Dif.	50 °C	130°C	120°C	100°C	90°C	70°C

4.6.5 EXPERIMENTAL RESULTS OF COOLING GLASS OF 6 mm FOR 50 SECONDS

The experimental work from which the following results were obtained is presented in Chapter 7. A piece of 6 mm thick white glass is heated to an initial temperature of 1100 °C in a furnace and then removed and cooled in the air at an ambient temperature of 20 °C for 50 seconds. The glass is placed in an insulating material and is allowed to cool from one surface only, equivalent to the simulations above where the 12 mm thick piece of glass is cooled from two opposite surfaces.

Figure 4.6 shows how the surface temperature and the temperature at a depth of 6 mm (equivalent to the centre temperature above) change over a 50 second period. The surface temperature drops rapidly, from 1100-500 °C in the first 50 seconds and the temperature at a depth of 6 mm drops from 1100 °C to 570 °C.

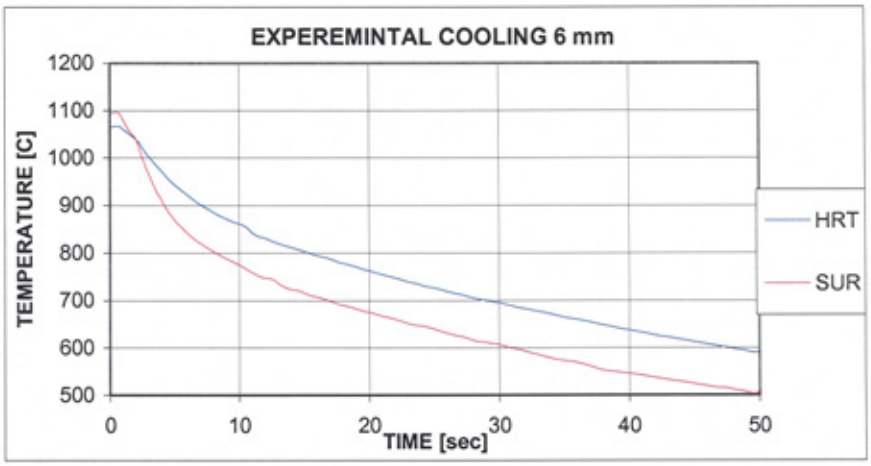

Figure 4.6 Variations of glass (surface and 6 mm) cooling temperatures with 50 seconds, from experimental results

Table 4.14 provides a summary of these results and details the numerical difference between the surface and centre (6 mm depth) temperatures at 10 second intervals. The difference between them is at its maximum after 10 seconds with a value of 100 °C, this falls to a minimum value of 80 °C at the end of the 50 seconds.

Table 4.14 Experimental results of temperature variation with 50 seconds cooling

Time (seconds)	1.0	10	20	30	40	50
6 mm	1100°C	870°C	760°C	690°C	630°C	570°C
Surface	1070°C	770°C	670°C	600°C	540°C	500°C
(Sur.-6 mm)Dif.	30°C	100°C	90°C	90°C	90°C	70°C

4.6.6 COMPARISONS OF MODELLING AND EXPERIMENTAL RESULTS FOR GLASS SURFACE TEMPERATURE DROP

Figure 4.7 shows a comparison of the surface temperatures obtained from the five methods and Tables 4.15, 4.16 and 4.17 provide numerical comparisons. The discussion is separated into two parts; firstly, a comparison between the surface temperatures obtained from the four different mathematical techniques is made and secondly the models are compared with the experimental work presented in Section 4.6.6.

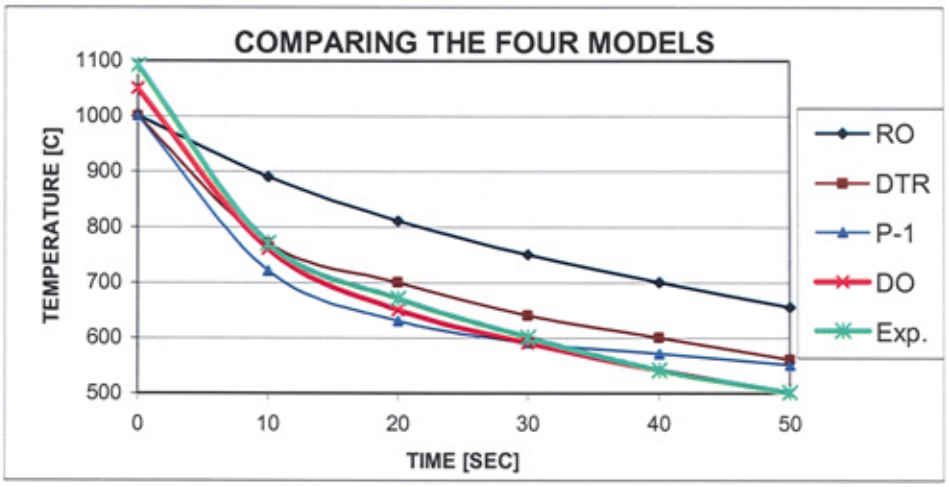

Figure 4.7 Comparing the four models surface temperature results with the experimental results

Table 4.15 Comparing of surface temperatures of the four models

Time (seconds)	1.0	10	20	30	40	50
Rosseland	1100 °C	890 °C	810 °C	750 °C	700 °C	655 °C
DTR	1100 °C	770 °C	700 °C	640 °C	600 °C	560 °C
P-1	1100 °C	720 °C	630 °C	590 °C	570 °C	550 °C
DO	**1100 °C**	**760 °C**	**650 °C**	**590 °C**	**540 °C**	**500 °C**
Experimental	**1100 °C**	**770°C**	**670°C**	**600°C**	**540°C**	**500°C**

Table 4.16 Comparing of 6 mm deep temperatures of the four models

Time (seconds)	1.0	10	20	30	40	50
Rosseland	1000 °C	995 °C	910 °C	840 °C	780 °C	730 °C
DTR	1000 °C	960 °C	860 °C	790 °C	720 °C	660 °C
P-1	1000 °C	910 °C	790 °C	700 °C	650 °C	610 °C
DO	**1050 °C**	**890 °C**	**770 °C**	**690 °C**	**630 °C**	**570 °C**
Experimental	**1070 °C**	**870°C**	**760°C**	**690°C**	**630°C**	**570°C**

Table 4.17 Comparing the temperature differences of the four models and experimental work

Time (seconds)	1.0	10	20	30	40	50
Rosseland	100 °C	100 °C	100 °C	90 °C	80 °C	75 °C
DTR	100 °C	190°C	160°C	150°C	120°C	100°C
P-1	100 °C	190°C	160°C	110°C	80°C	60°C
DO	**50 °C**	**130°C**	**120°C**	**100°C**	**90°C**	**70°C**
Experimental	**30°C**	**100°C**	**90°C**	**90°C**	**90°C**	**70°C**

4.7 DISCUSSIONS

4.7.1 COMPARISON OF MODELLING RESULTS

Comparing the results obtained from the four models, given in Table 4.15, it is clear that over the 50 second cooling period Rosseland model predicts the smallest surface temperature drop, from 1100 °C to 650 °C, while DO predicts the largest, from 1100 °C to 500 °C, a difference of over 150 °C. The other two models predict almost equal surface temperature falls to around the 550 °C. The profile of the temperature decay is inversely exponential in all cases, with the DTR, P-1 and DO models showing the same general trend while the Rosseland model predicts far slower heat loss. The DO model predicts the fastest heat loss.

The centre temperatures predicted by the four models over the 50 second cooling period, given in Table 4.16, show the same trends as the surface temperature, with Rosseland showing the smallest heat loss while DO shows the highest. This should be expected as the DO model formulation allows a greater dissipation of energy from the surface.

For clarification, the difference between the centre and surface temperatures are compared in Table 4.17. This shows that the heat flux predicted in the DTR and P-1 models are much greater than in the Rosseland and DO models, reaching a flux after the first 10 seconds of 190 °C in comparison to the DO model at 130 °C. After the initial rise in flux over the first 10 seconds it steadily decreases as the rate at which heat is transferred from the centre to the surface approaches that being lost by the surface to the air. The DTR model maintains the highest flux level after 50 seconds of 100 °C, while

the P-1 model decreases the temperature gradient most rapidly down to 60 °C from the maximum 190 °C.

4.7.2 COMPARISON OF MODELLING AND EXPERIMENTAL RESULTS

In order to provide some evidence as to which model best predicts the actual heat transfer experimental work has been performed, which is discussed in Chapter 7. The experimental results are shown along with the modelling results in Figure 4.6 and Tables 4.15 – 4.17. It is clear from both the graph of surface temperature and the numerical results given in the tables that the DO model offers the closest prediction to the practical measurements and it is noticeable that as time increases the DO model converges towards the experimental result.

It has been suggested in the literature (Cheong and Song [30] and Viskanta and Song [31]) that the DO model would provide the best approximation to the real world and that this is mainly due to the optical thickness and its effect on the assumptions used in the derivation of the other mathematical models.

4.8 SUMMARY

In this chapter the modelling of heat transfer from a glass surface by radiation has been studied. Four different mathematical techniques have been applied to the same model and the results obtained from each method have been compared with experimental work to show which provides the best estimation to the true result. The model considered the radiative heat loss from glass to air over a 50 second period and this model was mirrored in the experimental work. The temperature of the glass was recorded at the glass surface and at the centre of the glass.

The comparison of the modelling results and the experimental results in Figure 4.7 and Tables 4.15 – 4.17 shows that the DO modelling method provides the closest result to that obtained experimentally. The DTR and P-1 modelling techniques offer reasonable approximations over the 50 second period observed for the most part within a 10% error. However, the Rosseland model is unable to provide a good prediction; it shows heat being lost from the glass too slowly. This has been discussed as resulting from the optical thickness of the glass being too small for the approximations made in the Rosseland formulation. This corroborates work published by Viskanta and Song [31] and Cheong, and Song [30] (DO modelling has been used in Chapters 2, 5, 6 7 and 8).

CHAPTER FIVE – MODELLING GLASS PROPERTIES

5.1 INTRODUCTION

During the formation of glass containers it is necessary to obtain a suitable level of heat transfer through the glass melt-mould interface in order that the glass holds its shape when it is removed from the mould. The amount of heat extracted from the glass is dependent on many factors, including: the properties of the glass material, (i.e. density, viscosity), the heat transfer coefficients at the glass-mould and glass-air interfaces, the characteristics of the mould material, and the glass-mould contact time. To demonstrate the impact of such factors, a computer model for the one dimensional heat flow process was presented and discussed in Chapter 4. This model was evaluated using four mathematical approaches, of which DO was shown to provide the best approximation to the experimental data.

In this chapter, the glass thermal and mechanical properties are studied to investigate the effect of temperature on the behaviour of these properties. Two cases of heat transfer are presented: (a) Conduction between the glass and the mould and internal radiation within the glass bulk and (b) Radiation within the glass and to the surrounding air. The model used in this study is presented in section 5.2, along with the definition of the modelling parameters used and a model diagram.

To show the effect of the glass absorption coefficient on the cooling of the centre and surface temperatures of the glass in both heat transfer cases, two different values of absorption coefficient are modelled in Section 5.3. The two values used represent those of white glass and opaque glasses.

The effect of the refractive index on heat loss from the surface and centre of the glass is investigated in Section 5.4. Two values of refractive index are considered and a comparison of the fall in surface and centre temperatures for both heat transfer cases is made.

The effect of varying the heat transfer coefficient on the glass surface and centre temperatures is modelled in Section 5.5. Two values of heat transfer coefficient are simulated in order to show how these affect the cooling of the glass centre and the surface temperatures in each of the heat transfer cases.

In Section 5.6 the effect of external emissivity on the glass surface and centre temperatures is modelled. Two values of external emissivity are used to show how the cooling of the glass surface and centre temperatures change for heat transfer by conduction-radiation.

An investigation of the effect of specific heat on the surface and centre glass temperature is modelled in Section 5.7. Three values of specific heat are used in the simulation to show how the cooling of the glass surface and centre temperatures change in both cases of heat transfer.

The effect of thermal conductivity on the surface and centre glass temperature is modelled in Section 5.8. Two values of thermal conductivity are used to show how it affects the cooling of the glass surface and centre temperatures in both heat transfer cases.

Finally, a compilation of the results is provided in a table in Section 5.9 followed by some further discussion and a summary in Sections 5.10 and 5.11.

5.2 METHOD AND DESCRIPTION OF MODELLING

In this section the model used to study the effect of the glass properties (absorption coefficient, refractive index, heat-transfer coefficient, external emissivity, specific heat and thermal conductivity between the glass and the mould-plunger) under the two cases of heat transfer i.e. conduction-radiation and radiation only is defined.

Firstly, conduction-radiation which occurs during the time when the glass is in contact with the mould and plunger, for a period of 5 seconds, is considered (Conduction between the glass and the mould and internal radiation within the glass bulk). The model is shown in Figure 5.1 (a), the initial glass temperature is set at 1050 °C and the mould-plunger initial temperatures are 490 °C. These are the same initial conditions used in the works published by Jones and Basnett [1], Rawson [11] Secondly, the radiation case (Radiation within the glass and to the surrounding air) is considered. The model is shown in Figure5.1 (b), the initial glass temperature is set at 1050 °C and the air is at an ambient temperature of 20 °C. These are the same initial conditions used in works published by Rawson [11] and McGraw [6]. The initial thermal properties of the glass, steel and air used in this model are provided in Table 5.1.

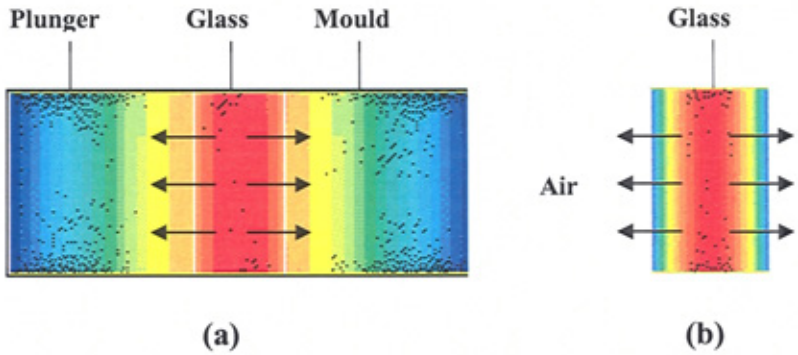

Figure 5.1 Two different stages the (press) conduction-radiation (a) and radiation only (b)

In their work on the cooling of glass between the mould and plunger Jones and Basnett [1] made a comparison between white and opaque glass over a period of 5.0 seconds. McGraw [6] also used a period of 5 seconds in his observation of the cooling of white glass during contact with the mould and plunger. Fellows and Shaw [3] used a period of only 4 seconds while investigating the effect of varying the initial mould temperature. In considering the blank open phase (reheat) Rawson [11] looked at the cooling of the glass over the initial 2-3 seconds.

5.2.1 MODELLING AND SIMULATION PARAMETERS

This section presents the material properties and parameters that have been used in the modelling. This modelling work is performed using the commercial software package 'Fluent' CFD finite volume package.

A diagrammatic representation of the structure of the model is shown in Figure 5.2. The glass is seen sandwiched between the plunger and the mould while externally the mould and plunger are shown as walled. The walls in this case are non-heat conducting. The shadow interfaces are used by the model to allow mathematical treatment of the flow of heat through each side of the interface.

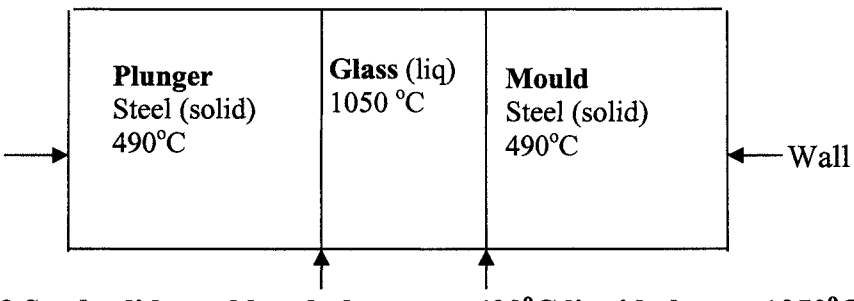

Figure 5.2 Steel solid mould and plunger at 490°C liquid glass at 1050°C

5.2.2 MATERIAL PROPERTIES GLASS, MOULD, PLUNGER AND AIR

The initial thermal properties used to describe the glass, steel and air used in this model are provided in Table 5.1.

Table 5.1 Initial glass and mould temperatures and the properties of glass and mould (steel) and plunger and air as used by Basnett [1], H. Rawson [11], McGraw [6], seen in Tables2.22 and 2.24

Property	**Units**	**Glass (fluid)**	**Mould and plunger steel (solid)**	**Air (fluid)**
Density	Kg/m^3	2500	8000	1.225
C_p (Specific heat)	J/Kg K	1350	500	1000
Thermal conductivity	W/m K	1.45	200	0.0242
Viscosity	Kg/m s	10	-	10
Temperature	°C	1050	490	20
Heat transfer coefficient	$W/m^2 K$	-	1500	10
Absorption coefficient	m^{-1}	23, 45, 100	-	-
Refractive index	-	0.5	-	-
Thickness	mm	10	20	20
Time	Second	5	5	5

5.3 MODELLING THE EFFECT OF THE ABSORPTION COEFFICIENT AT THE CENTRE AND SURFACE GLASS TEMPERATURE

To study the effect of varying the absorption coefficient of the glass on the cooling of the glass, two types of glass are modelled, white and opaque. The absorption coefficients of the two types of glass in the three bands, as given in chapter 2 Table 2.2, vary only in the third band, where white glass is 100 m^{-1} and opaque glass is 300 m^{-1}. The model uses a glass thickness of 10 mm and observes the heat lost over 5 seconds for two cases of heat transfer; (a)-Conduction between the glass and the mould plus the internal radiation within the glass bulk (b)-Radiation within the glass and to the surrounding air. The results obtained from the model for the conduction radiation and the radiation only cases are shown in Figures 5.3 and 5.4 respectively and summaries of the results are also provided in Tables 5.2 and 5.3

5.3.1 Conduction-Radiation (a)

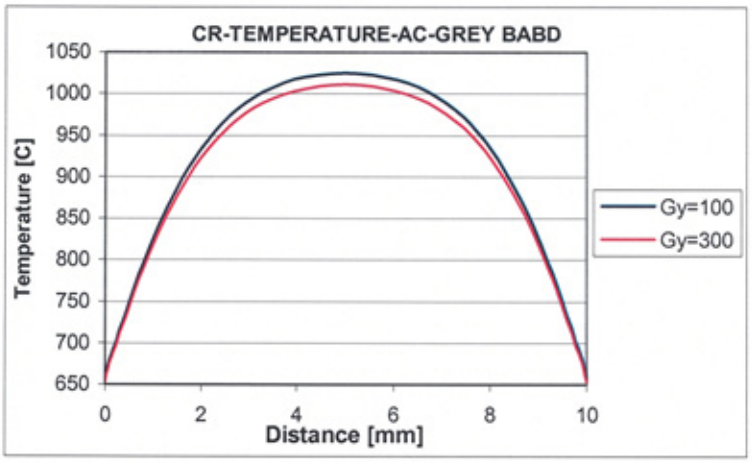

Figure 5.3 Variation of temperature with white glass α=100 m^{-1} and opaque glass α=300 m^{-1} during 5 seconds (glass-to-mould) cooling, conduction-radiation

From Figure 5.3 it can be seen that the change in absorption coefficient results in a significant change in the temperature distribution. The white glass having a lower absorption coefficient is seen to have lost the least temperature, dropping from the initial 1050 °C by 20 K to 1030 °C, while the centre temperature of the opaque glass with the higher absorption coefficient drops from 1050 °C by 35 K to 1015 °C. The surface temperatures show little difference in heat loss with the surface of the white glass falling by 338 K to 652 °C and the opaque glass by marginally more 400 K to 650 °C. It should be expected that a change in absorption coefficient would influence the glass bulk temperature more than the surface temperature. (The results obtained in Table 5.2 are also discussed in sections 2.3.1 and 2.3.2)

Table 5.2 Temperature drop results due to change of absorption coefficient(C-R)

A.C	Band 1	Band 2	Band 3	Centre temp. drop	Surface temp. drop
Opaque glass	α=23 m^{-1} (0.8--2.25) μ	α= 45 m^{-1} (2.25--2.75) μ	α= 300 m^{-1} (2.75--4.3) μ	(1050-1015)°C	(1050-650) °C
White glass	α=23 m^{-1} (0.8--2.25) μ	α= 45 m^{-1} (2.25--2.75) μ	α= 100 m^{-1} (2.75--4.3) μ	(1050-1030)°C	(1050-652) °C

5.3.2 RADIATION (B)

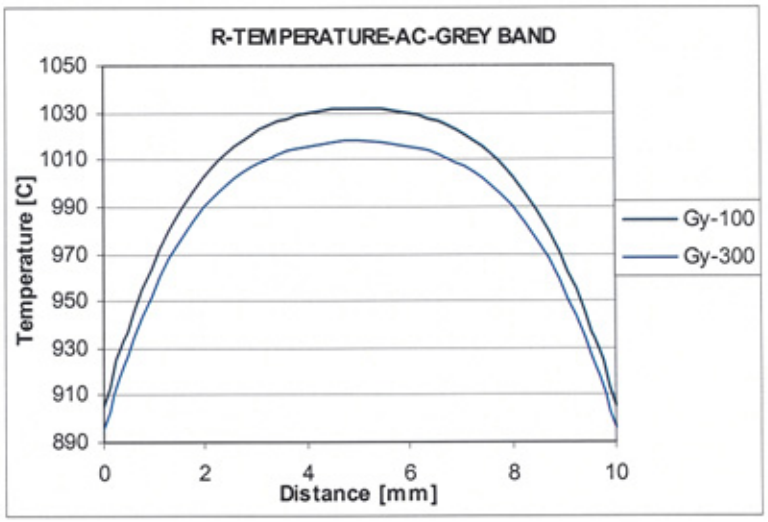

Figure 5.4 Variation of temperature with white glass α =100 m^{-1} and opaque glass α =300 m^{-1} during 5 seconds (glass-to-air) cooling, radiation

Figure 5.4 shows the temperature distribution results obtained from the model used in the radiation only case. Again, there is a significant difference in the temperature drops observed as a result of the change in absorption coefficient. The centre temperature of the white glass falls from 1050 °C by 18 K to 1032 °C while the centre temperature of the opaque glass falls more, from 1050 °C by 32 K to 1018 °C. The surface temperatures fall from 1050 °C by 140 K and 154 K for white and opaque glass respectively. As in the conduction-radiation case observed in Figure 5.3, the temperature drops more rapidly for higher absorption coefficients.

Table 5.3 Temperature drop results due to change of absorption coefficient (R)

A.C	Band 1	Band 2	Band 3	Centre temp. drop	Surface temp. drop
Opaque glass	α=23 m^{-1} (0.8--2.25) μ	α= 45 m^{-1} (2.25--2.75) μ	α= 300 m^{-1} (2.75--4.3) μ	(1050-1018) °C	(1050-896) °C
White glass	α=23 m^{-1} (0.8--2.25) μ	α= 45 m^{-1} (2.25--2.75) μ	α= 100 m^{-1} (2.75--4.3) μ	(1050-1032) °C	(1050-910) °C

Comparing the results from the two different heat transfer cases (Tables 5.2 and 5.3), the temperature drop observed in radiation case is less that the drop in the conduction-radiation case. These results confirm those published by Rawson [11], as discussed in Section. 2.3.3.

5.4 MODELLING THE EFFECT OF THE REFRACTIVE INDEX ON THE SURFACE AND CENTRE TEMPERATURE

To study the effect of varying the refractive index of the glass on the cooling of the glass, two values will be investigated, 0.5 and 1.0. The model uses a glass thickness of 10 mm and observes the heat lost over 5 seconds for two cases of heat transfer; (a)-Conduction between the glass and the mould plus the internal radiation within the glass bulk (b)-Radiation within the glass and to the surrounding air. The results obtained from the model for the conduction radiation and the radiation only cases are shown in Figures 5.5 and 5.6 respectively and summaries of the results are also provided in Tables 5.4 and 5.5

5.4.1 CONDUCTION RADIATION (A)

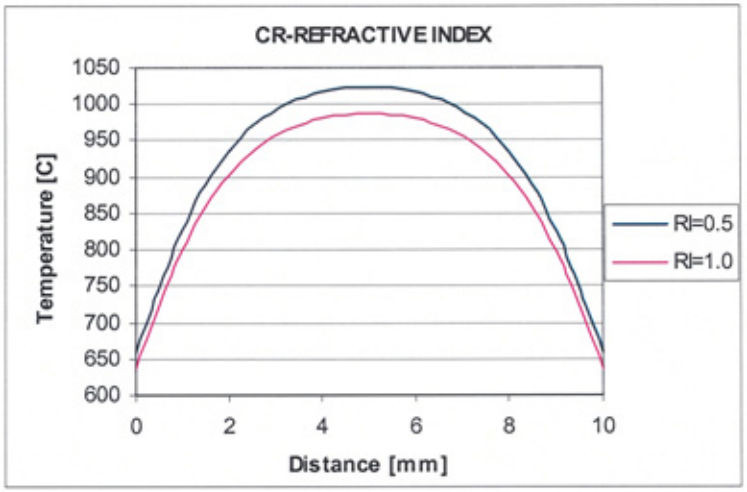

Figure 5.5 Glass temperature against refractive index 0.5 and 1.0 over 5 seconds (glass-to-mould) cooling, conduction-radiation

From Figure 5.5 it can be seen that the change in refractive index results in a significant change in the temperature distribution. The lower the refractive index the lower is the heat loss. For a refractive index of 0.5 the centre temperature drops from the initial 1050 °C by 30 K to 1020 °C, while the glass with refractive index of 1.0 drops from 1050 °C by 60 K to 990 °C. The surface temperatures show little difference in heat loss falling by 400 K to 650 °C and 425 K to 625 °C for the refractive indexes of 0.5 and 1.0 respectively. It should be expected that a change in refractive index would influence the glass bulk temperature more than the surface temperature. The refractive index used can vary between 0.5 and 1.0. As described in Section 2.3.2. (Also discussed in section 3.3.5 glass properties).

Table 5.4 Temperature drop results due to change of refractive index (C and R)

Refractive index	Centre temp. drop	Surf. Temp. drop
0.5	(1050--1020) °C	(1050--650) °C
1.0	(1050—990) °C	(1050—625) °C

5.4.2 RADIATION (B)

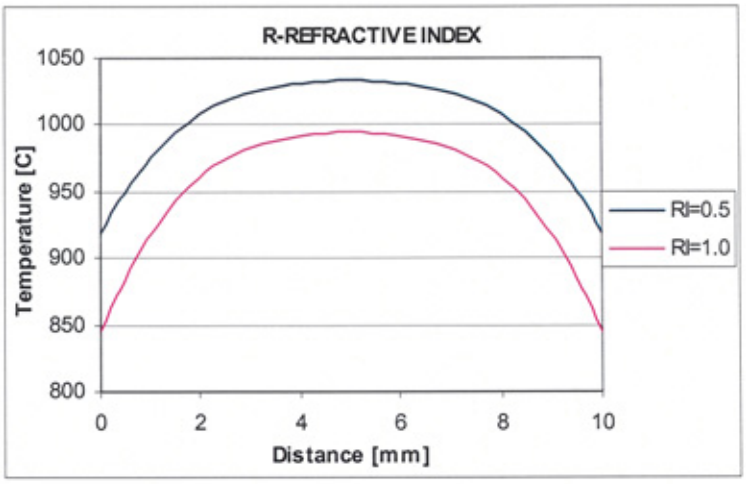

Figure 5.6 Glass temperatures against refractive index, 0.5 and 1.0 over 5 seconds (glass-to-air) cooling, radiation

Figure 5.6 shows the temperature distribution results obtained from the model used in the radiation only case. Again, there is a significant difference in the temperature drops observed as a result of the change in refractive index. The centre temperature of the glass with refractive index 0.5 falls from 1050 °C by 18 K to 1032 °C while the centre temperature of the glass with refractive index 1.0 falls from 1050 °C by 50 K to 1000 °C. The surface temperatures fall from 1050 °C to 918 °C and 850 °C for the glasses with refractive index's 0.5 and 1.0 respectively. As in the conduction-radiation case observed in Figure 5.5, the temperature drops more rapidly as the refractive index increases. In the radiation case it would be expected that the change in refractive index would influence the surface temperature more than the centre. (The results are summarised in Table 5.5, comparable results were obtained by Rawson [11] as shown in Table 2.21).

Table 5.5 Temperature drop results due to change of refractive index (R)

Refractive index	Centre temp. drop	Surf. Temp. drop
0.5	(1050--1032) °C	(1050--918) °C
1.0	(1050—1000) °C	(1050—850) °C

5.5 MODELLING THE EFFECT OF THE HEAT TRANSFER COEFFICIENT ON THE CENTRE AND SURFACE GLASS TEMPERATURE

Conductive heat transfer depends on the heat-transfer coefficient at the glass/tool interface and the temperature difference between the tool and the glass surfaces. Whereas, radiative transfer only depends on the temperature distribution within the glass, a low heat-transfer coefficient would result in a proportionally higher radiative influence. The effect of varying the heat transfer coefficient is modelled using identical sets of initial conditions as seen in Table 5.6. Two values of heat transfer coefficient are used in the modelling to allow a comparison to be drawn with previously published works.

Firstly, Jones and Basnett [1] and Rawson [11] used a heat transfer coefficient of 1500 W/m^2 K in the modelling of the conduction-radiation case and then secondly, Rawson [11] also used 10 W/m^2 K in the radiation only case. In this case values of 1500 and 20 W/m^2 K will be used. The lower the heat transfer coefficient is, then the higher the radiative influence of the glass. The results obtained from the modelling of the heat transfer coefficients are shown in Figure 5.7, with a summary of the results in Table 5.6.

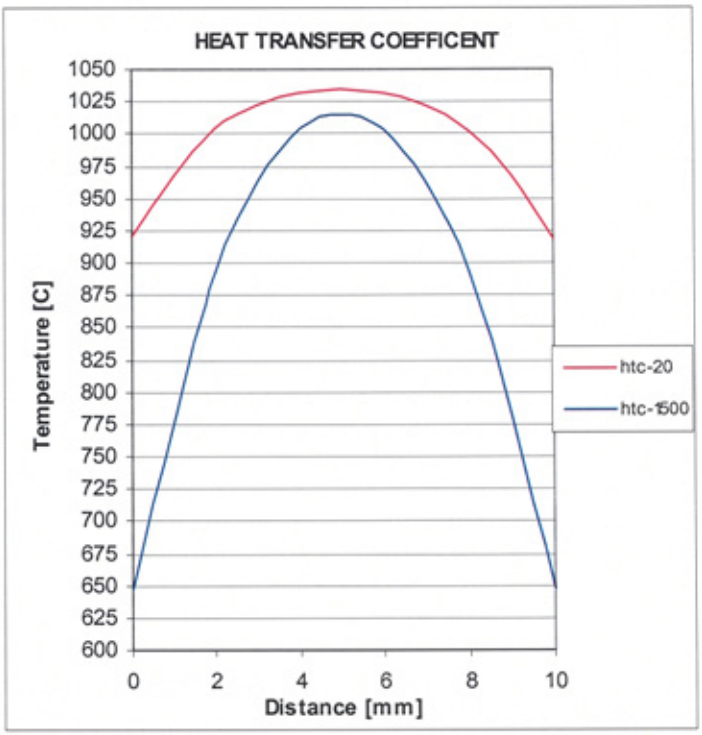

Figure 5.7 Variation of glass temperature with two values of heat transfer coefficients 20 and 1500 W/m^{2}K during 5 seconds (glass-to-mould) cooling conduction-radiation

It is seen from Figure 5.7 that the effect of varying the heat transfer coefficient is significant. When the HTC is low (20 W/m^2 K), radiation is the dominant mode of heat conduction and the decrease in temperature is very small; around 15 K at the centre (see Table 5.6), as opposed to a decrease of 35 K when the HTC is at 1500 W/m^2 K. The variation is especially apparent at the surface where there is contact with the mould, temperature decreases of 130 K and 400 K for HTC of 20 W/m^2 K and 1500 W/m^2 K respectively.

It would be expected that the change in HTC would influence the surface temperature more than the centre. Results shown in Table 5.6 for a HTC of 1500 W/m^2 K are comparable to those in (Table 2.21), where the centre temperature drop was 35 K and the surface temperature drop is 400 K. The results for HTC of 20 W/m^2 K are similar to the reheat case shown by Rawson [11].

Table 5.6 Temperature drop results due to change of HTC (C and R)

HTC	Centre temp. drop	Surf. Temp. drop
20	(1050—1035) °C	(1050—920) °C
1500	(1050—1015) °C	(1050—650) °C

5.6 MODELLING THE EFFECT OF EXTERNAL EMISSIVITY ON THE CENTRE AND SURFACE TEMPERATURE

To investigate the effect of external emissivity on the heat transfer from the glass, two values of external emissivity 0.8 and 1.0 will be employed in the modelling while all other initial conditions are kept the same. The temperature variation at both the surface and centre of the 10 mm thick glass will be observed for each case of heat transfer (a)-Conduction between the glass and the mould and internal radiation within the glass bulk (b)-Radiation within the glass and to the surrounding air.

5.6.1 CONDUCTION-RADIATION (A)

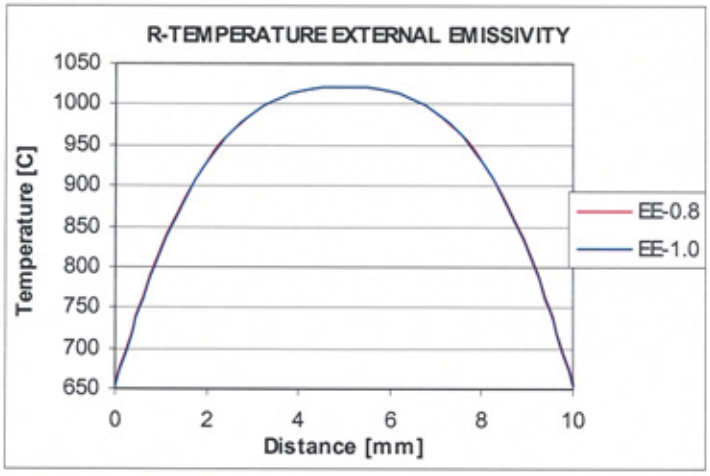

Figure 5.8 Variation of glass temperature with external emissivity 0.8 and 1.0 during 5 seconds (glass-to-mould) cooling conduction-radiation

Figure 5.8 shows the effect of the external emissivity on the temperature decrease of the glass in the conduction-radiation case, a summary of the results is provided in Table 5.7. For an External Emissivity (EE) = 0.8 the centre temperature drop 28 K and the surface temperature drop 400 K. For EE =1.0 the centre temperature drop 29 K and the surface temperature drop 401 K. The change of the external emissivity has little effect on the centre temperature and on the glass-mould surface heat loss.

Table 5.7 Temperature drop results due to change of external emissivity (C-R)

E.E.	Centre temp. drop	Surf. Temp. drop
0.8	(1050-1022) °C	(1050-650) °C
1.0	(1050-1021) °C	(1050-649) °C

5.6.2 RADIATION (B)

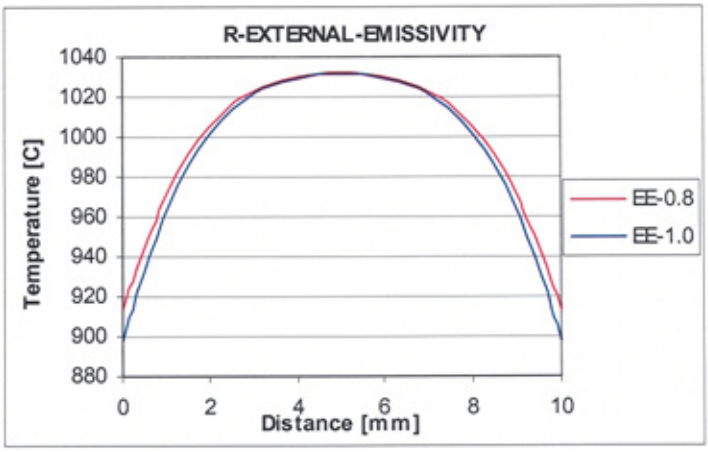

Figure 5.9 Variation of glass temperature with external emissivity 0.8 and 1.0 during 5 seconds (glass-to-air) cooling radiation

Figure 5.9 shows the effect of the external emissivity on the temperature decrease of the glass in the radiation case, a summary of the results is provided in Table 5.8. For EE = 0.8 the centre temperature drops 18 K and the surface temperature drops 132 K. For EE

=1.0 the centre temperature drops 19 K and the surface temperature drops 150 K. The difference in centre temperature drop is 1 K, this remains small as in the conduction radiation case, however the difference in surface temperature drop is now of some significance at 18 K. The working range used for external emissivity is generally between 0.9 and 1.0 the value used in the previous study was 0.95.

Table 5.8 Temperature drop results due to change of external emissivity (R)

EE	Centre temp. drop	Surf. Temp. drop
0.8	(1050-1032) °C	(1050-918) °C
1.0	(1050-1031) °C	(1050-900) °C

5.7 MODELLING THE EFFECT OF SPECIFIC HEAT ON THE SURFACE AND CENTRE GLASS TEMPERATURE

The effect of the specific heat on the heat lost from the centre and surface of 10 mm thick soda-line glass over a 5.0 second period is now investigated. Three values of specific heat are used, two constant at 1300 and 1500 J/kg K and one temperature dependent, are modelled. Two cases of heat transfer are considered (a)-Conduction between the glass and the mould and internal radiation within the glass bulk (b)-Radiation within the glass and to the surrounding air.

5.7.1 CONDUCTION RADIATION (A)

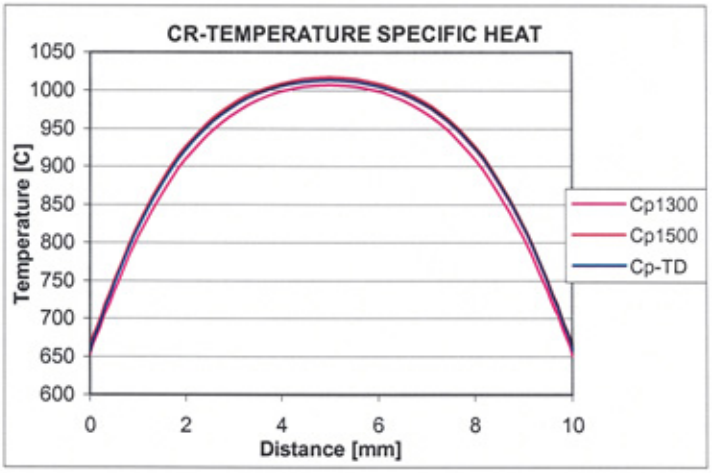

Figure 5.10 Variation of glass temperature with two values of specific heat 1300 and 1500 J/Kg K during 5 seconds (glass-to-mould) cooling, conduction-radiation

Figure 5.10 shows the effect of varying the specific heat on the temperature profile through the glass in the conduction-radiation, these results are summarised in Table 5.9. As the specific heat increases the centre and surface temperature decreases.

For specific heat = 1300 J/Kg K the centre temperature drops 44 K and the surface temperature drops 390 K. For specific heat =1500 J/Kg K the centre temperature drops 34 K and the surface temperature drops 400 K. For temperature dependent specific heat, the centre temperature drops 38 K and the surface temperature drops 395 K. Change in specific heat influences the centre temperature more than the surface temperature. Comparable results were obtained by Jones and Basnett [1] (as descried in Section 2.3.2. and shown in Table 2.21).

Table 5.9 Temperature drop results due to change of specific heat C_p (C & R)

Specific heat C_p	Centre temp. drop	Surf. Temp. drop
1300	(1050—1006) °C	(1050—660) °C
1500	(1050—1016) °C	(1050—650) °C
TD	(1050—1012) °C	(1050—655) °C

5.7.2 RADIATION (B)

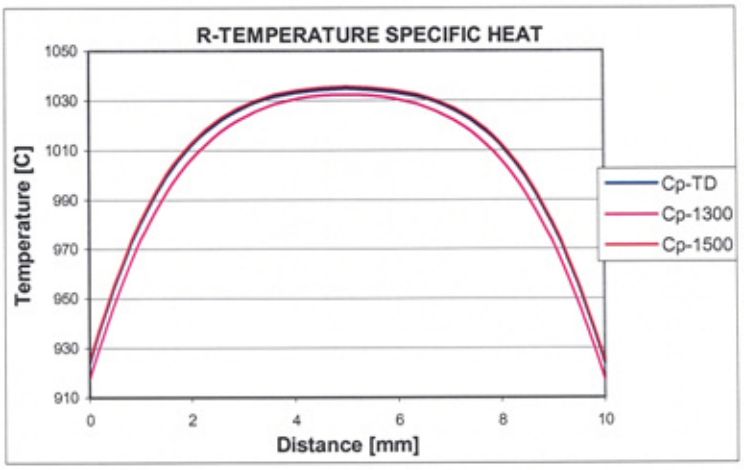

Figure 5.11 Variation of glass temperature with two values of specific heat 1300 and 1500 J/Kg K during 5 seconds (glass-to-air) cooling, radiation

Figure 5.11 shows the effect of specific heat on the temperature profile though the glass drop of the glass, in the radiation case, these results are summarised in Table 5.10.

For specific heat = 1300 J/Kg K the centre temperature drops 18 K and the surface temperature drops 132 K. For specific heat =1500 J/Kg K the centre temperature drops 15 K and the surface temperature drops 125 K. For temperature dependent specific heat, the centre temperature drops 16 K and the surface temperature drops 126 K. As the specific heat increases the surface and centre temperature decreases, the results in the radiation case show a lower drop in the centre and surface temperatures than in the

conduction-radiation case. Generally as the specific heat increases the temperature drop decreases.

Table 5.10 Temperature drop results due to change of specific heat C_p (Radiation)

Specific heat C_p	Centre temp. drop	Surf. Temp. drop
1300	(1050—1032) °C	(1050—918) °C
1500	(1050—1035) °C	(1050—925) °C
TD	(1050—1034) °C	(1050—924) °C

5.8 MODELLING THE EFFECT OF THERMAL CONDUCTIVITY ON THE SURFACE AND CENTRAL GLASS TEMPERATURE

To study the effect of varying the thermal conductivity on the cooling of the glass, two constant values 1.45 and 2.0 W/m K and a temperature dependant value are used in the model, and the variation of cooling temperature through the 10 mm thick glass is observed over a 5 second period. Two cases of heat transfer are simulated (a)-Conduction between the glass and the mould and internal radiation within the glass bulk (b)-Radiation within the glass and to the surrounding air.

5.8.1 CONDUCTION RADIATION (A)

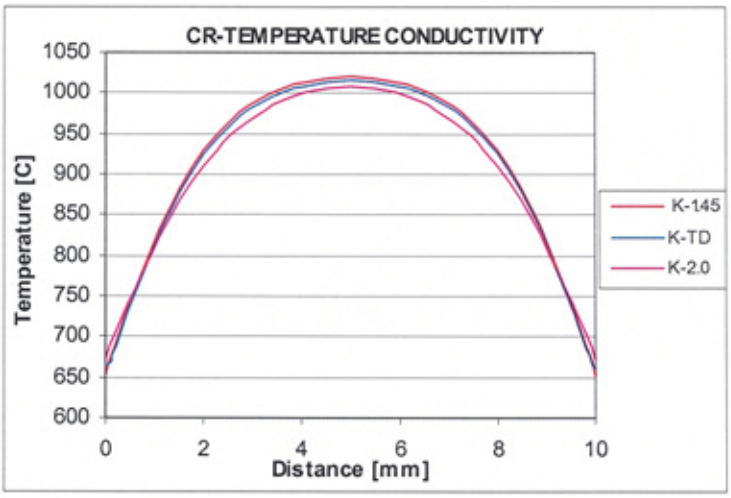

Figure 5.12 Variation of glass temperature with two of thermal conductivity 1.45 and 2.0 W/m K over 5 seconds (glass-to-mould) cooling conduction-radiation

Figure 5.12 shows the effect of the thermal conductivity on the centre and surface temperature in the conduction-radiation case; the results are summarised in Table 5.11. For thermal conductivity = 1.45 W/m K the centre temperature drops 20 K and the surface temperature drops 400 K. For thermal conductivity = 2.0 W/m K the centre temperature drops 43 K and the surface temperature drops 378 K. For temperature dependent thermal conductivity the centre temperature drops 35 K and the surface temperature drops 390 K. Changes in thermal conductivity influence the centre temperature more than the surface temperature. It can be seen that as the thermal conductivity increases then the heat loss decreases. Comparable results were obtained and descried in Section 2.3.2, and shown in Table 2.21.

Table 5.11 Temperature drop due to change of thermal conductivity (C and R)

Thermal conductivity	Centre temp. drop	Surf. Temp. drop
1.45	(1050--1022) °C	(1050--650) °C
2.0	(1050—1007) °C	(1050—672) °C
TD	(1050—1015) °C	(1050—660) °C

5.8.2 RADIATION (B)

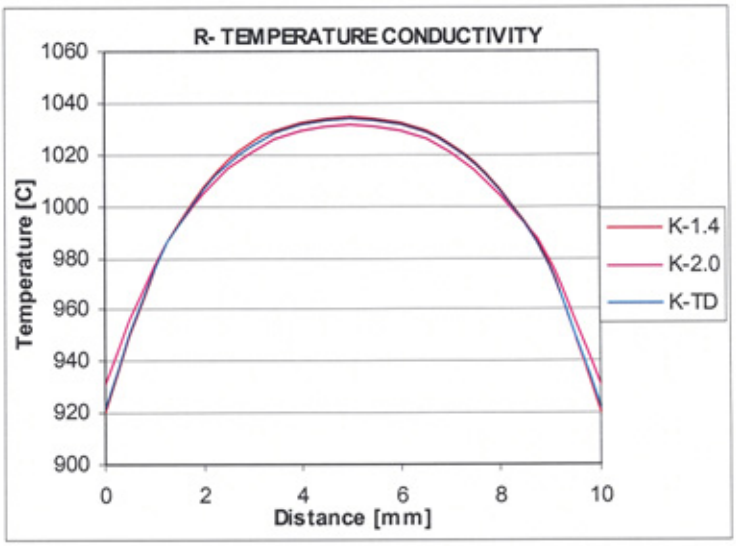

Figure 5.13 Variation of glass temperature with two of thermal conductivity1.45 and 2.0 W/m K during 5 seconds (glass-to-air) cooling radiation

Figure 5.13 shows the effect of varying the thermal conductivity on the temperature profile through the glass in the radiation case, these results are summarised in Table 5.12.

For thermal conductivity = 1.45 W/m K the centre temperature drops 15 K and the surface temperature drops 130 K. For thermal conductivity = 2.0 W/m K the centre temperature drops 19 K and the surface temperature drops 119 K. For temperature dependent thermal conductivity the centre temperature drops 16 K and the surface temperature drops 128 K. As the thermal conductivity increases the surface and centre

temperature drop decreases. The heat loss in the radiation case is lower than that obtained in the conduction-radiation case.

Table 5.12 Temperature drop due to change of thermal conductivity (R)

Thermal conductivity	Centre temp. drop	Surf. Temp. drop
1.45	(1050--1035) °C	(1050--920) °C
2.0	(1050—1031) °C	(1050—931) °C
TD	(1050—1034) °C	(1050—922) °C

A higher surface temperature fall is observed in the conduction-radiation than in the radiation case as expected, however, the centre temperature recorded a higher drop in the radiation case than conduction-radiation.

Table 5.13 Summary of the modelling results

Glass properties	(Radiation) Case		(Conduction- radiation) Case	
Absorption Coefficient	**Centre temp. drop**	**Surface temp. drop**	**Centre temp. drop**	**Surface temp. drop**
$\alpha = 100\ m^{-1}$	(1050-1032) 18 K	(1050-910) 140 K	(1050-1030) 20 K	(1050-652) 398 K
$\alpha = 300\ m^{-1}$	(1050-1018) 32 K	(1050-896) 154 K	(1050-1015) 35 K	(1050-650) 400 K
Refractive Index				
0.5	(1050-1032) 18 K	(1050-918) 132 K	(1050-1020) 30 K	(1050-650) 400 K
1.0	(1050-1000) 50 K	(1050-850) 200 K	(1050-990) 60 K	(1050-625) 425 K
External Emissivity				
0.8	(1050-1032) 18 K	(1050-918) 132 K	(1050-1022) 28 K	(1050-650) 400 K
1.0	(1050-1031) 19 K	(1050-900) 150 K	(1050-1021) 29 K	(1050-649) 401 K
Specific heat				
1300	(1050-1032) 18 K	(1050-918) 132 K	(1050-1006) 44 K	(1050-660) 390 K
1500	(1050-1035) 15 K	(1050-925) 125 K	(1050-1016) 34 K	(1050-650) 400 K
TD	(1050-1034) 16 K	(1050-924) 126 K	(1050-1012) 38 K	(1050-655) 395 K
Thermal conductivity				
1.45	(1050-1035) 15 K	(1050-920) 130 K	(1050-1022) 28 K	(1050-650) 400 K
2.0	(1050-1031) 19 K	(1050-931) 119 K	(1050-1007) 43 K	(1050-672) 378 K
TD	(1050-1034) 16 K	(1050-922) 128 K	(1050-1015) 35 K	(1050-660) 390 K
Heat Transfer Coefficient				
20	(1050-1035) 15 K	(1050-920) 130 K	-	-
1500	-	-	(1050-1015) 35 K	(1050-650) 400 K

5.9 DISCUSSION

In Section 5.3, Figures 5.3 and 5.4 show the variation in temperature through 10 mm thick white and opaque soda-lime glass after 5 seconds. The difference in absorption coefficient between the two types of glass was seen to have an effect on the rate of cooling of the glass during heat transfer by both conduction radiation and radiation only. The absorption coefficient (α) varies according to the wavelength of the hot glass, and is defined into pre-specified bands (grey bands). As indicated in chapter 2 Table 2.5 and Table 2.21, the opaque glass has a higher absorption coefficient than the white glass in the upper band. From the figures it is clear that the opaque glass loses energy faster than the white glass and so it can be concluded that the higher the absorption coefficient the faster the heat energy can be lost. Conversely, the glass with the higher absorption coefficient can absorb heat energy at a faster rate. This is regardless of the mode of heat transfer under consideration i.e. conduction radiation or radiation only. These results confirm the work by Jones and Basnett [1] (as presented in Section 2.3.2).

Comparing the two results in Tables 5.2 and 5.3 the variation of the temperature at central and surface is smaller in the conduction-radiation than radiation only case. When the glass is cooled between the mould and the plunger most of the heat energy is transferred by conduction, the influence of radiation is very small in comparison. When the glass is cooled in the air and there is no conduction, most of the heat energy is lost by radiation. In both cases the temperature lost by the glass surface is higher than that lost from the centre of the glass.

In Section 5.4, Figures 5.5 and 5.6 show the effect of varying the refractive index of a 10 mm thick piece of soda-lime glass on the temperature lost from the glass during heat transfer by both conduction-radiation and radiation only. The two values of refractive index applied were 0.5 and 1.0. From the figures it is clear that the fall at the surface of the glass is greater than at the centre of the glass in all cases. However, it is also clear that as the refractive index increases the heat loss also increases. The refractive index represents the reflection of heat energy, as the reflection increases more energy lost from the glass (see Table 2.21 refractive index 1.0 by Jones and Basnett [1] and 0.5 by Fellows and Shaw [3]; See Table 5.13 for comparison). More energy is lost when both conduction and radiation are present in the heat transfer,

(See Table 5.13 for comparison).

In Section 5.5 Figure 5.7 showed the effect of varying the heat transfer coefficient of the surrounding environment on the cooling of a 10 mm thick piece of soda-lime glass during heat transfer by conduction-radiation. Two values of heat transfer coefficient were investigated 1500 W/m^2 K and 20 W/m^2 K. When the heat transfer coefficient is large then conduction is the dominant mode of heat transfer. When the heat transfer coefficient is 20 W/m^2 K the results appear close to those obtained in the case of radiation only, with only a 6 K difference, most of the heat is transferred by radiation. It can be seen from Table 5.6 that the difference between the centre temperatures obtained in each case is only 15 K. However, the difference at the glass surface between the two cases is 270 K, with the higher heat transfer coefficient resulting in a temperature drop of 400 K. Therefore it can be said that as the heat transfer coefficient increases then conduction becomes by far the most dominant mode of heat transfer. Comparable results were obtained (See Table 5.13).

In Section 5.6 Figures 5.8 and 5.9 showed the effect of varying the external emissivity of the surrounding environment on the cooling of a 10 mm thick piece of soda-lime glass during heat transfer by conduction-radiation and by radiation only. Two values of external emissivity were used in the model, 0.8 and 1.0. In the case of heat transfer by conduction-radiation the change in external emissivity results in a difference in the resulting centre and surface glass temperatures of only 1 K. This effect is negligible and can be ignored. In the case of radiation only, again the centre temperature sees only a 1 K change between the two values of external emissivity, however at the surface of the glass a more significant effect is apparent and a difference of 18 K is observed (Tables 5.7 and 5.8), this cannot be ignored. The working range used for external emissivity is 0.9 to 1.0; the value used in previous studies was 0.95. Comparable results to these were obtained in (Section.2.3.2), and (See Table 5.13 for comparison).

In Section 5.7 Figures 5.10 and 5.11 showed the effect of varying the specific heat of a 10 mm thick piece of soda-lime glass during heat transfer by conduction-radiation and by radiation only. Two constant values were used to represent the specific heat 1300 and 1500 J/kg K and a temperature dependant value was also used. From the figures it is seen that as the specific heat increases then so the heat loss from the glass decreases. This effect is more apparent at the centre of the glass than at the surface, it is also noticeable that the heat loss is greater in the conduction radiation case than it is in the radiation only case. Comparable results were obtained (as discussed in Section 2.3.2). and (See Table 5.13 for comparison).

In Section 5.8 Figures 5.12 and 5.13 showed the effect of varying the thermal conductivity of a 10 mm thick piece of soda-lime glass during heat transfer by conduction-radiation and by radiation only. Two constant values of thermal

conductivity were used in the model, 1.24 and 2.0 as well as a temperature dependant value. The figures in both heat transfer cases show that as the thermal conductivity increases then the centre of the glass undergoes an increasing drop in temperature, whereas the surface of the glass undergoes a decreasing temperature drop. It is also noticeable that there is a greater temperature loss in the conduction-radiation case in comparison to the radiation only case. The change in thermal conductivity would influence the temperature centre more than the surface. Comparable results were obtained and descried in Section 2.3.2) and (See Table 5.13 for comparison)

5.10 SUMMARY

In this chapter the effect of glass properties on heat transfer under conditions of conduction-radiation, which concerns the heat transfer by conduction through the glass-mould/plunger interface along with internal radiation and then radiation only concerning only heat transferred by radiation to ambient air. The investigation was performed by modelling the heat profile through a 10 mm thick piece of soda-lime glass using the same initial conditions but varying the property under inspection accordingly. The properties being observed were the absorption coefficient, the heat transfer coefficient, the external emissivity, the specific heat and the thermal conductivity. The following conclusions can be drawn in each case:

- As the absorption coefficient (α) increases the centre temperature of the hot glass decreases in both the conduction-radiation and radiation only cases. The results show the variation of the temperature at central and surface is smaller in the conduction-radiation than radiation case.

- As the refractive index increases the centre and surface temperatures decrease, however the rate of decrease is higher at the surface than in the centre, this is the case for both conduction-radiation and radiation only.

- As the heat transfer coefficient increases the heat lost from the glass also increases. The significance of the change in heat transfer coefficient on the heat loss increases moving from the centre towards the surface of the glass.

- As the external emissivity increases little effect is seen over the whole profile in the case of conduction-radiation and little effect is also seen on the centre temperature in the radiation only case. The increase in external emissivity has a significant effect on the surface temperature of the glass in the case of radiation only. A drop in temperature of 40 K results between the change from 0.8 to 1.0 approximately 5 % of the surface temperature.

- As the specific heat increases the heat lost from the centre and surface of the glass increases in both conduction-radiation and radiation only cases of heat transfer.

- As the thermal conductivity increases the heat lost from the centre of the glass decreases more rapidly and the heat lost from the surface of the glass decreases more slowly. This is because as the thermal conductivity increases the heat is transferred from the centre of the glass to the surface more rapidly.

CHAPTER SIX – HEAT FLUX AND STRESS

6.1 INTRODUCTION

This chapter investigates by modelling, the change in both flux and stress in a glass sample during cooling. The flux is investigated for three cases of heat transfer, firstly in the case of conduction and internal radiation when the glass is in contact with the mould, secondly in the case of conduction only when the glass is in contact with the mould, finally in the case of radiation only while the glass is in the reheat stage. The glass properties and initial conditions used in the model are similar to those used in the literature Tables (2.21, 2.22 and 2.23) to allow relevant comparisons to be drawn.

The modelling is performed using the Elfen software package. This software offers an advantage in simulation as it allows consideration of the coupling between temperature and internal stress inside the hot glass. By using the semi-coupled conditions of thermal and mechanical coupling between temperature, and stress, for the three cases of heat transfer, a comparison can be made of the stress and temperature though the profile of a glass sample.

In Section 6.3 the modelling parameters are defined these include the Thermal Loadings, Constrains, Controls, Mesh type, problem type, model and analysis type.

In Section 6.4 the results obtained for the flux under the first two cases of heat transfer are presented and discussed. These are conduction-radiation and conduction only during the glasses contact time with the mould. The radiation only case during the reheat stage is presented and discussed in Section 6.5.

The investigation of the rate of change of stress at the glass surface during cooling by radiation only (reheat stage) is presented in Section 6.6. Further discussion and conclusions are provided in a Sections 6.7 and 6.8.

6.2 THE EFFECT OF RADIATION IN LOSING HEAT BETWEEN THE GLASS AND MOULD

Jones and Basnett [1] performed simulations to show the heat flux through a 10 mm thick piece of glass during the pressing process. During pressing initially the glass has a firm contact with the mould and so the conduction at the surface of the glass is high and hence so is the flux through the surface. As the glass cools then it begins to contract, the result of which is an air gap between the mould and the glass. As a result of this air gap the flux at the glass surface begins to fall as little conduction is present. Instead heat is transferred from the surface via convection. Figures 6.1 and 6.2 show the flux through the glass obtained by the simulations of Jones and Basnett [1] when the heat transfer mechanisms considered were conduction and internal radiation and conduction only respectively. They performed the simulation by changing the boundary conditions at the surface of the glass as time increased to mimic the introduction of an air gap between the glass and mould as the glass contracts.

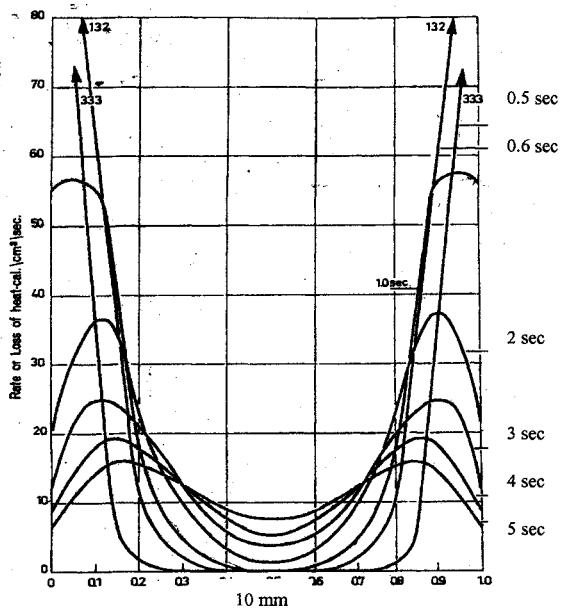

Figure 6.1 flux distribution in pressing at various times surface conduction-radiation Basnett [1]

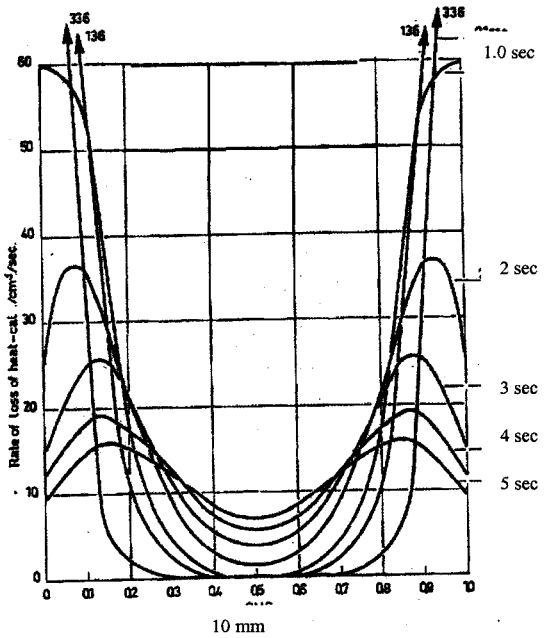

Figure 6.2 flux distribution in pressing at various times, surface conduction Jones and Basnett [1]

From Figures 6.1 and 6.2 it can be seen that initially up to a time of 0.6 seconds, the flux at the surface of the glass is very large indicating a high level of conduction. Then as the air gap is introduced from 1 second onwards, the flux at the surface begins to fall and the maximum flux appears at a depth of 0.4-0.5 mm from the surface. This shows that the level of heat transfer from the glass surface by conduction is falling. Between the two cases, it is seen that when internal radiation is considered, the surface layers of the glass lose heat energy slightly faster. In the centre of the glass the flux is almost identical for both cases.

Table 6.1 Flux variation of hot glass (C and C-R) 5 seconds Jones and Basnett [27]

Time seconds	0.1	1.0	2.0	3.0	4.0	5.0
Flux- W/m^2 (C)	2.5×10^6	1.0×10^6	6.7×10^5	5.0×10^5	4.1×10^5	4.0×10^5
Flux- W/m^2(C-R)	2.3×10^6	1.3×10^5	5.0×10^5	3.7×10^5	2.9×10^5	2.5×10^5

6.3 METHOD AND DESCRIPTION OF MODELLING

The software chosen to perform the modelling of heat flux is (Elfen), this is because it offers the ability to consider the coupling between the temperature and internal stress inside the hot glass. By using the semi-coupled conditions of thermal and mechanical coupling between temperature, flux and stress, in the two cases of heat transfer to the mould, conduction-radiation and conduction only, a comparison can be made of the flux and temperature through a 10 mm thickness of glass.

The material properties and parameters used in this simulation are presented in Tables 6.2 – 6.6 below. The glass properties initial conditions and parameters used are the same as those used in previous literature; see Table 2.22 as used by Basnett [1] and Shaw [3] Chap.2 Figure 2.9 and Kent [4] Chap.2 Figure 2.12.

Table 6.2 Radiation boundaries, emissivity, Stefan B-constant, and ambient temperature

Line	Emissivity	Stefan Boltzman-constant	Ambient temp.
Line-1	0.98	5.67×10^{-8} W/m^2 K^4	20 °C
Line-2	0.98	5.67×10^{-8} W/m^2 K^4	20 °C

Table 6.3 Constrains, surface temperature, initial temp

Surface temperature	Initial temp.
Sur-1	1050 °C
Sur-2	490 °C
Sur-3	490 °C

Table 6.4 Control, element order, and linear

Element order	Linear
Mesh type	Unstructured
Problem type	Semi-coupled
Model type	Plain stress
Analysis type	Implicit
Controls	Implicit non-linear transient

Table 6.5 Initial glass, mould and air temperatures and the properties of glass and steel used in mould and plunger was used by Jones and Basnett [1], H. Rawson [11], McGraw [6], as shown in Table 2.22

Property	Units	Glass (fluid)	Mould and plunger steel (solid)	Air (fluid)
Density	Kg/m^3	2500	8000	1.225
C_p (Specific heat)	J/Kg K	1350	500	1000
Thermal conductivity	W/m K	1.45	100	0.0242
Heat transfer coefficient	$W/m^2 K$	-	1500	10
Absorption coefficient	m^{-1}	23, 45, 100	-	-
Initial temperature	°C	1050	490	20
Thickness	mm	10	20	10
Time	Second	5	5	5

Table 6.6 Mechanical Properties of glass, steel, and plunger as used by Hirrosh Wakatsuki [29]

Mechanical properties	Units	Glass-(liquid)	Mould- Plunger steel (solid)
Young's modules	Pascal (N/m^2)	7.8×10^8	1.85×10^{10}
Poisons ratio	----	0.45	0.36
Expansion coefficient	cm/cm/°C	1.35×10^{-5}	1.35×10^{-3}
Shear modules	Pascal (N/m^2)	3.98×10^{10}	4.7×10^{10}

6.4 HEAT FLUX BETWEEN THE GLASS AND MOULD BY CONDUCTION RADIATION AND CONDUCTION ONLY

In this section, the simulation carried out shows the change of heat flux through a 10 mm thick piece of glass as it is cooled over a period of 5.0 seconds between the mould and plunger. Two mechanisms of heat transfer are considered in this section, conduction- radiation and conduction only. The surface value has not been reported due to the mathematical description, in the software, of the boundary conditions used, in this case the value at 0.5 mm is taken to be the surface. The flux through the glass at different times up to 5.0 seconds for each case of heat transfer is shown in Figures 6.3 and 6.4 for conduction-radiation and conduction only respectively.

6.4.1 Conduction-radiation case

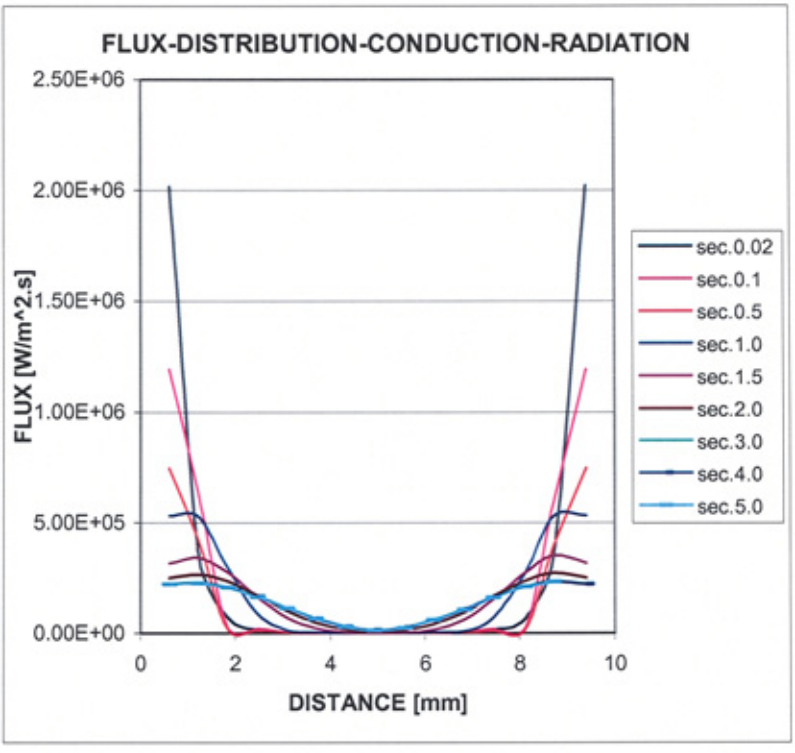

Figure 6.3 Heat flux in the hot glass conduction-radiation case through the 10 mm distance, maximum flux at 0.5 mm from the surface

6.4.2 Conduction-case

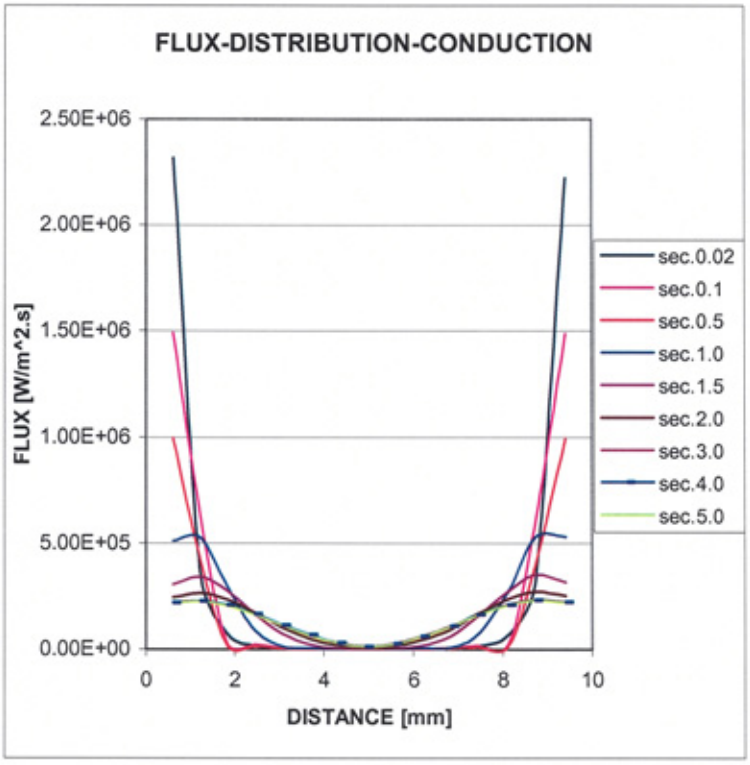

Figure 6.4 Heat flux in the hot glass conduction case through the 10 mm distance, maximum flux at 0.5 mm from the surface

The results obtained in Figures 6.3 and 6.4 are comparable to those obtained for the initial two time steps by Jones and Basnett [1] (as shown in Figures 6.1 and 6.2 respectively). They are only comparable to the initial steps as in this simulation the boundary conditions have not been manipulated to imitate the shrinking of the glass and hence the introduction of an air gap between the glass surface and mould. As in the case the plunger force during pressing is maintained.

The flux is high at the glass surface and decreases as the depth into the glass increases in both cases of heat transfer. At the surface of the glass the flux observed in the case of conduction only is greater than that of the case of conduction-radiation. This is because

the internal radiation acts as a thermal supply from the centre of the glass to its surface. A comparison of the flux at the surface of the glass over the 5.0 second time period in both cases of heat transfer is shown in Figure 6.5. The difference in flux at the centre of the glass for the two cases of heat transfer is negligible. As time increases the flux towards the centre of the glass also increases. This is because most of the heat is transferred from the glass surface to the mould in the first 2.0 seconds of contact due to the initial high temperature difference, as the mould gets hotter and the glass cooler, the temperature gradient deeper into the glass increases as must the flux. The results obtained for the surface flux results for both cases are summarised in Table 6.7.

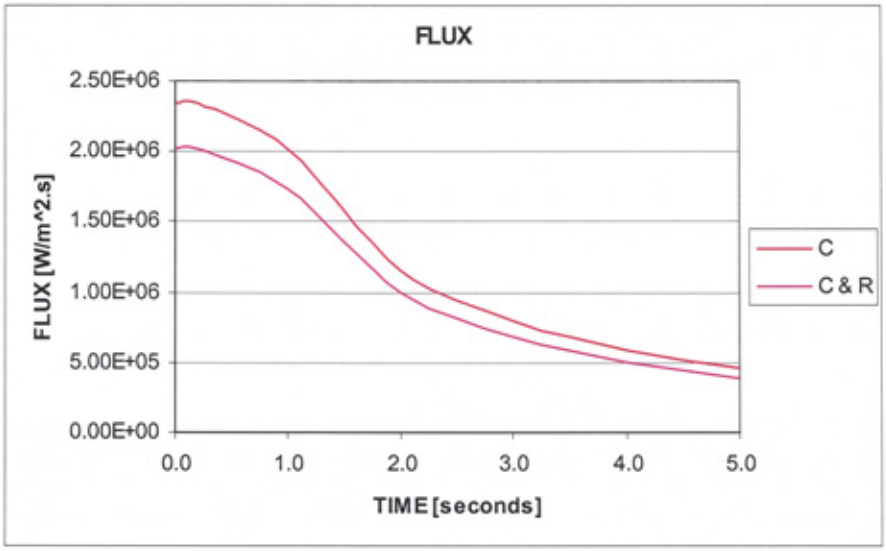

Figure 6.5 Heat flux in the hot glass for both heat transfer by conduction-radiation and conduction only against 5.0 seconds, a maximum flux at the surface 2.4 x10^6 W/m^2 about 0.2 seconds of time (C only)

Table 6.7 Shows flux variation in the hot glass (C and C-R) cases during 5 seconds.

Time (seconds)	0.1	1.0	2.0	3.0	4.0	5.0
Surface W/m^2 (C)	2.3 x10^6	2.0 x10^6	1.2 x10^6	8.0 x10^5	6.0 x10^5	5.0 x10^5
Surface W/m^2 (C-R)	2.0 x10^6	1.8 x10^6	1.0 x10^6	7.0 x10^5	5.0 x10^5	4.0 x10^5

In comparison to previously published works by Kent [4] (Section 2.7, Table 2.19 glass-mould contact from 0.1 to 0.5 seconds the flux was given as 2.38 x 10^6 to 1.60 x 10^6 W/m^2), Fellows and Shaw [3] (Section 2.6.1, Table 2.17 glass-mould contact from 0.1 to 4.0 seconds the flux was given as 2.0 x 10^6 to 4.5 x 10^5 W/m^2) and McGraw [6] (Section 2.5.1, Table 2.14 glass-mould contact from 0.1 to 5.0 seconds the flux was given as 2.30 x 10^6 to 1.35 x 10^6 W/m^2), the results obtained are close. (The previously published works quoted here were discussed in sections 2.6.1 and 2.7.1. Differences in result in part are due to the effect of the initial mould surface temperature used in the models by Fellows and Shaw [3] And Kent [4]).

6.5 HEAT FLUX FROM DIFFERENT PARTS IN THE GLASS RADIATION CASE

In this section, modelling is performed using the relevant parameters given in Section 6.3 to allow the change in heat flux through the profile of a 10 mm glass sample to be found as the glass cools in air over a 5.0 second period. In this case the heat transfer mechanism is by radiation only as the glass is cooling in air, in comparison to the model in Section 6.4 this means that the thermal conductivity is reduced from 1500 W/m^2 K to 10 W/m^2 K. As in the case of Section 6.4 the actual glass surface flux is

not reported on due to the mathematical description of the boundary conditions. As such the same as before surface is taken to be at a depth of 0.5 mm.

Figure 6.6 shows the flux through the profile of the glass at given time intervals up to 5.0 seconds. The results show that the heat flux at the surface is initially the maximum, as in the two cases of conduction, and that it is high in comparison to the heat flux deeper into the glass. However the maximum value of heat flux in this radiation only case (4.50 x 10^4 W/m^2 s) is around 50 times less than that of the maximum for the conduction only case (2.40 x 10^6 W/m^2 s). Again the flux through the glass increases with time as the surface temperature falls and the glasses internal thermal gradient increases.

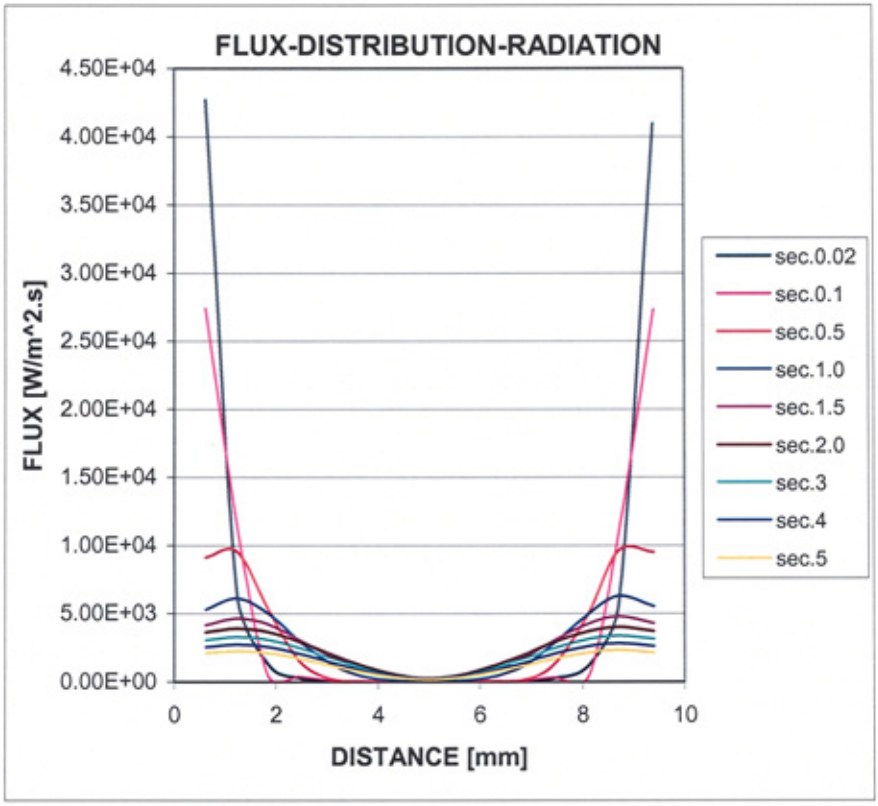

Figure 6.6 Heat flux in the hot glass by radiation through the 10 mm distance

Figure 6.7 shows the change in flux at the glass surface over the 5.0 second time period. It shows the same surface flux profile as those obtained in the conduction-radiation and conduction only cases of Figure 6.5 but is proportionally smaller, a summary of these surface flux results is given in Table 6.8 (Related literature and discussions can be found in section 6.2.1 the effect of radiation on the flux, Basnett [1]).

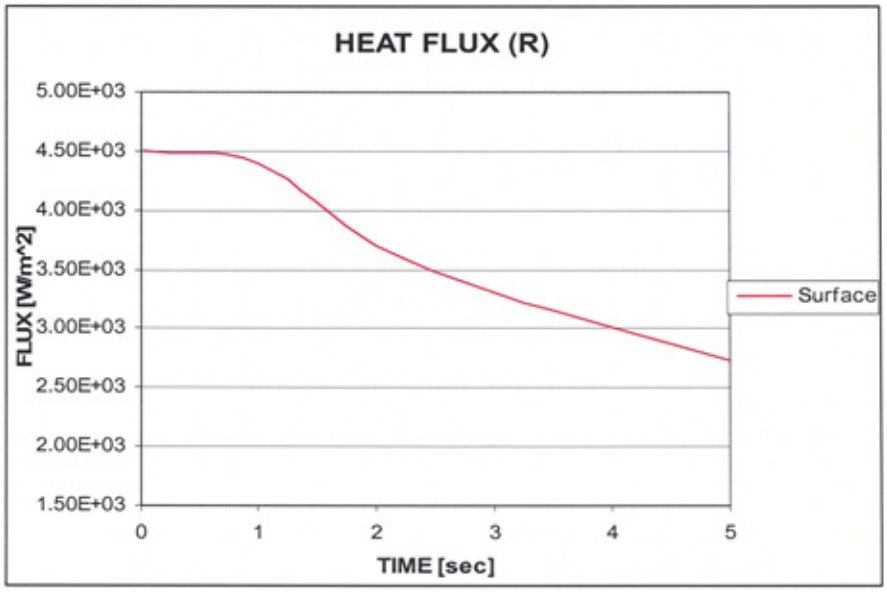

Figure 6.7 Heat flux in the hot glass radiation case against 5.0 seconds, a maximum flux at the surface 4.50 x10^4 W/m ^{2}s about 0.2 seconds of time (Radiation)

Table 6.8 Variation of heat flux in the hot glass, 5 seconds (radiation) case

Time (seconds)	0.2	1.0	2.0	3.0	4.0	5.0
Surface W/m^2	4.50 x10^4	4.50 x10^4	3.75 x10^4	3.30 x10^4	3.00 x10^4	2.73 x10^4

6.6 THE RATE OF CHANGE OF THE STRESS AT THE SURFACE DURING 50 SECONDS COOLING TIME (GLASS-AIR) RADIATION

In this section, the model is used to examine the effect of the change in glass surface temperature on the rate of change of stress at surface of the glass during cooling between glass and air over a 50 second period. First the surface temperature of a 10 mm thick piece of glass as it cools for 50 seconds in air is found using the relevant modelling parameters given in Section 6.3. This surface temperature is then applied to the mechanical solution by the software, allowing the stress to be plotted over the given time.

Figure 6.8 shows the surface temperature as the glass cools over a period of 50 seconds, the results show that over the initial 10 seconds the glass surface loses heat rapidly falling from 1050 °C to 800 °C (250K). From 10-50 the cooling is more gradual falling a further 300K to 500 °C.

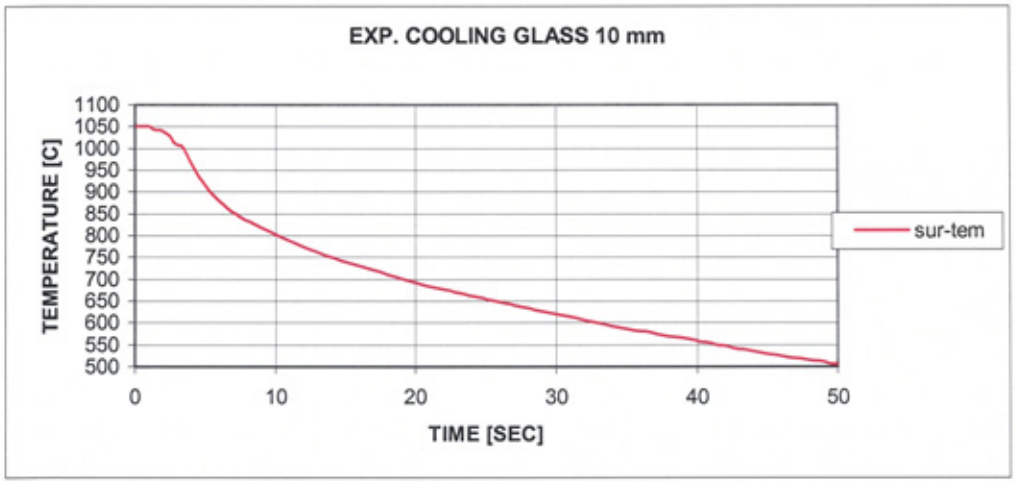

Figure 6.8 Experimental results of surface temperature, of cooling 10 mm thick glass during 50 seconds (Radiation)

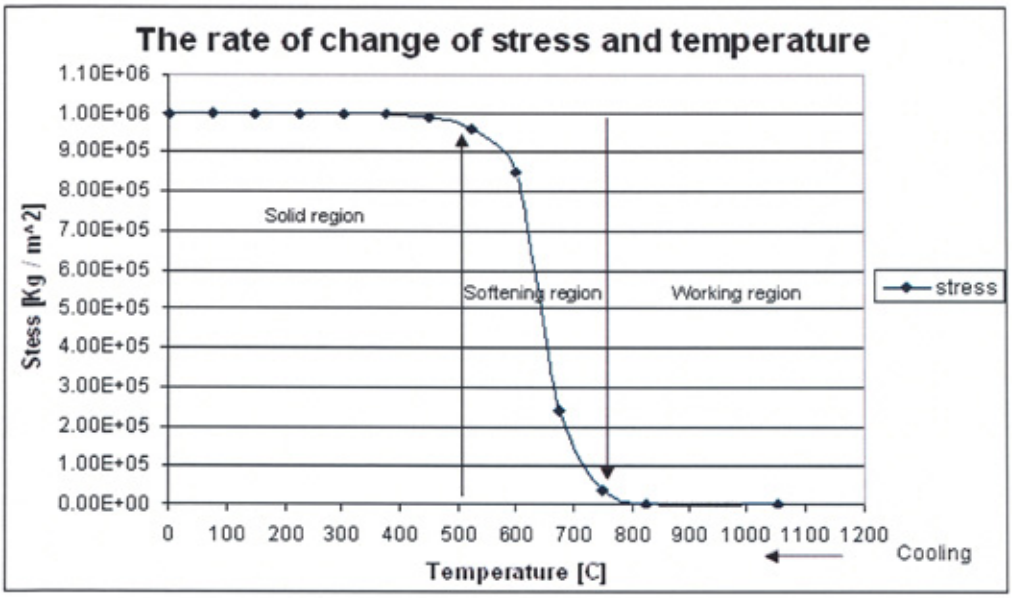

Figure 6.9 Change of stress against temperature (Young's modulus)

Figure 6.9 shows how stress changes with temperature and allows the temperatures plotted in Figure 6.8 to be mapped to an appropriate stress level. The resulting graph of stress against time is shown in Figure 6.10 with a summary of the values provided in Table 6.9.

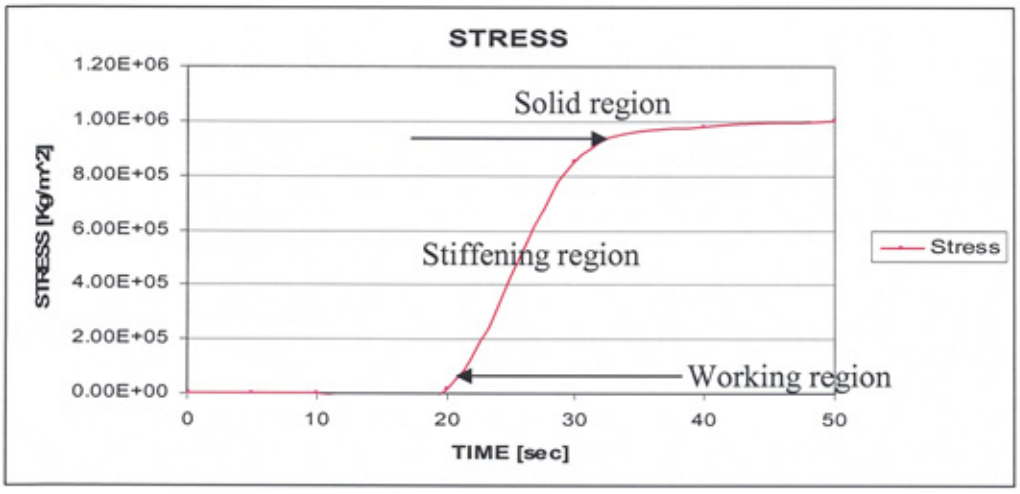

Figure 6.10 Rate of change of stress against 50 seconds time of cooling 10 mm glass thickness (Radiation)

Figure 6.10 shows the surface stress as the glass cools over the 50 second time period. For the first 20 seconds it can be seen that the glass remains in the working region as it

maintains a temperature exceeding 750 °C. From the 20 second barrier the glass passes into the softening region and becomes increasingly viscous. When the glass reaches 500 °C at a time of 30 seconds the glass becomes solid (solid region).

Table 6.9 Variation of surface stress during cooling against temperature

Time (seconds)	0.1	5	10	20	30	40	50
Surface °C	1050	900	800	680	610	550	500
Stress Kg/m^2	0.00	1.00x10	$1.28x10^3$	$1.50x10^4$	$8.50x10^5$	$9.60x10^5$	$1.00x10^6$

Table 6.10 Glass Flux and surface temperature drop

Properties	Heat Transfer Coefficient W/m^2-K	Initial Glass Temp. °C	Initial mould Temp. °C	Contact time sec.	Flux at the surface W/m^2	Glass surface temperature drop °C
Jones and Basnett [12]	1500	1050	490	0.1	2.3×10^6	---
				5.0	2.5×10^5	1050-650
Fellows and Shaw [19]	1600	1077	545	0.1	2.0×10^6	---
				4.0	4.5×10^5	1077-720
Kent [18]	1600	1015	490	0.1	2.38×10^6	---
				0.5	1.60×10^6	1015-760
McGraw [55]	1500	1050	490	0.1	2.30×10^6	---
				5.0	1.35×10^6	1050-650
Modelling Work	1500	1050	490	0.1	2.00×10^6	---
				5.0	4.00×10^5	1050-650

6.7 DISCUSSIONS

In Figures 6.3 and 6.4, where the change in flux through the 10 mm thick glass is shown at specific times up to 5 seconds in the case of heat transfer by both conduction-radiation and conduction only, it can be seen that as the time increases past 0.5 seconds, there is a shift in the location of the maximum flux from the glass surface towards the centre. This shift occurs as the surface temperature approaches that of the mould and with respect to the glass a small depth (0.4-0.5 mm) continues to fall comparatively slowly. This result is also observed in Section 6.5 where the glass is in air and heat transfer is taking place by radiation only.

The investigation showed that by accounting for the internal radiation a small difference in flux is observed only at the surface of the glass. It has also been observed in this investigation by comparison to previously published works (Kent [4]) that when there is a lower initial mould temperature then there is a greater initial flux at the surface of the glass.

The investigation into the surface stress as the glass cools in air shows that it takes up to 20 seconds for the glass to enter its softening region and begin to solidify. It is noticeable that the change in the state of the glass occurs very rapidly. The stress levels cover the entire stiffening region in only 10 seconds, equivalent of the temperature falling from 750 °C to 500 °C.

6.8 SUMMARY

- It seen that the greatest rate of heat loss (flux) by conduction occurs at a depth of 0.4-0.5 mm beneath the glass surface. This is because the temperature of the surface of the glass approaches that of the mould and then continues to fall comparatively slowly to the glass just below the surface. At the centre of the glass, the temperature gradient decreases rapidly; see Section 6.4.
- The glass is able to lose more heat at the surface when internal radiation is taken into account as the radiation is acting as a second heat transport mechanism to the glass surface; see Section 6.4.
- For lower initial mould temperatures higher initial flux values are obtained due to the larger temperature gradient between the glass and the mould; see Section 6.4.
- During the reheat period where heat transfer is by radiation only, the flux profile through the glass is the same as that obtained when the glass is in contact with the mould, however due to the low thermal conductivity of the air the value of flux is around 5 times lower than that observed during contact; see Section 6.5
- Once the temperature of the glass falls below 750 °C the stress increases rapidly and hence also the viscosity. The glass reaches its solid state at around 500 °C taking a time of around 30 seconds when it is cooled from 1050 °C in air; see Section 6.6.

CHAPTER SEVEN – EXPERIMENTAL WORK

7.1 INTRODUCTION

In this chapter experiments used to examine the effect of glass thickness on the heating and cooling of the glass-to-air interface during the forming process are described. The results obtained are compared to results obtained using simulations. The simulation results used for comparison are obtained using the Discrete Ordinates modelling technique as this has been shown to provide results close to those of previous experiments (see Chapter 2).

The equipment used to perform the experiments is described in Section 7.2. The specifications of the furnace including: maximum working temperature, maximum power and electrical supply. The thermocouples used are discussed in Section 7.3, including their working temperature range and their calibration. Two types of thermocouple are compared, namely gas welded and electrically welded. The preparation of the glass sample for the experiment is discussed in Section 7.4, this includes the dimensions of the sample and the manner in which the thermocouples are connected from the glass to the PC.

In section 7.5, the experimental work used to observe the effect of the glass thickness on heating is presented. Three thicknesses of white soda-lime glass 2, 4 and 6 mm are placed in a thermal break allowing the glass to be heated from only one side and the temperature profiles through the glass is observed. By using the thermal break the glass-break interface represents the centre of a piece of glass of double thickness, i.e. a 2 mm sample is considered a 4 mm sample where the bottom of the 2 mm sample represents

the centre and the top of the sample the surface. Comparisons are made between the centre and surface temperatures for each of the thicknesses.

In Section 7.6, experimental work used to observe the effect of slow and fast cooling of glass is presented. The experiment uses a sample thickness of 6 mm placed in a thermal break, thermocouples are located at 2 mm intervals through the glass. To facilitate the slow cooling of the glass the glass sample is heated in the furnace to 700 °C the furnace is then switched off and the sample is allowed to cool within the furnace. To facilitate the fast cooling of the glass, the sample is removed from the furnace once the temperature has been reached. A comparison of the difference between the surface and the bottom of fast and slow cooled glasses is made.

In Section 7.7, experimental work used to observe the effect of the heating and cooling cycle on a 6 mm thick white soda-lime glass sample. The glass is first heated to a pre-selected temperature and then rapidly cooling it to another pre-selected temperature, this cycle is performed repeatedly. To study the temperature profile through the glass as it is heated and cooled the experiment is performed three times with different numbers of thermocouples located at different intervals through the glass.

In Section 7.8 a model of the cooling of 6 mm thick white soda-lime glass mimicking the experiment in Section 7.6 using the DO mathematical formulation is presented for comparison with the experimental results.

7.2 THE FURNACE

The furnace used to perform the experimental work is described in this section. The description includes the furnace dimensions and heating specifications.

7.2.1 FURNACE SPECIFICATIONS

The heating elements used in the furnace are resistance wires fixed on to a refractory muffle. Those resistance wire elements are supported on the sides of the furnace, the door opens vertically to ensure the hot plug is away from the operator at all times. An analogue controller is used to set the temperature and has a range from 20-1500 °C. The furnace is doubly insulated ensuring low outer surface temperature. The dimensions of the furnace are given in Table 7.1 and the heating specifications are given in Table 7.2.

Table 7.1 Furnace dimensions

Dimensions	Height	Depth	With
Chamber size (m)	0.25	0.45	0.23
External size (m)	0.70	0.70	0.60

Table 7.2 Furnace specifications

Description	Value
Maximum temperature	1500 °C
Working temperature	1300 °C
Temperature sensor	Type "N"
Max. power rating	15 (KW)
Electric supply	1Ph 16Amp

7.2.2 FURNACE PERFORMANCE AT STEADY STATE

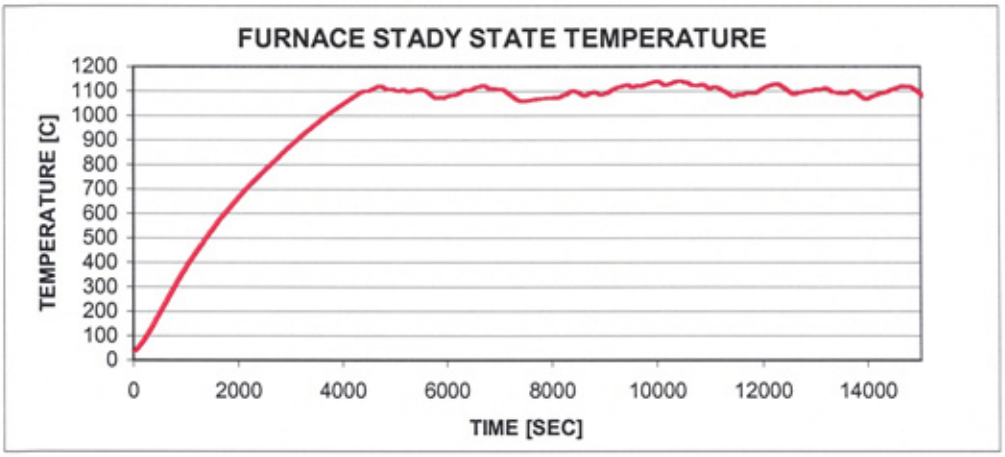

Figure 7.1 Steady state of the furnace form 4300-14500 sec, at maximum temperature of 1100 °C

Figure 7.1 shows the measurement of furnace temperature against time. The furnace temperature is observed over a period of 14500 seconds and varies from room temperature 25 °C as it begins heating and reaches a maximum of around 1150 °C. There is a steady rise over the first 4000 seconds at which point it reaches 1050 °C, beyond this time the furnace temperature fluctuates about the 1100 °C point by as much as ±50 °C.

7.3 THERMOCOUPLE (K) TYPE

The thermocouples used to perform the measurements are discussed in this section. The specifications of the thermocouple are stated and the calibration performed is detailed. Finally, a comparison is made between electrically welded and gas welded thermocouples.

7.3.1 THERMOCOUPLES SPECIFICATIONS

The two legs of the thermocouples are made from the following materials:

+LEG NICKEL-CHROMIUM (Ni-Cr)

-LEG NICKEL-ALUMINIUM (Ni-Al)

Tables 7.3 and 7.4 detail the EMF generated per degree and the working temperatures of the thermocouple.

Table 7.3 Generated EMF change per degree Celsius change

EMF	Temperature
42 μV/C	At 100°C
43 μV/C	At 500°C
39 μV/C	At 1000°C

Table 7.4 Working temperatures

State	Temperature range
Continuous	0 to +1100°C
Short term	-180 to +1350°C

7.3.2 CALIBRATION OF THE THERMOCOUPLES

In comparing the responses of different thermocouples as they are heated a variation in output is observed, this is mainly attributed to the welding joints. Two types of welding joint are commonly used these are gas welded and electrically welded. Gas welding is less accurate than electrical welding and as such the output variation observed between different gas welded thermocouples is greater than that observed for different electrically welded thermocouples.

Figure 7.2 shows the output variation of 4 gas welded thermocouples. It can be seen from the figure that as the temperature increases passed 350 °C then the variation in the thermocouple output temperature increases. The extent of this variation is shown in Table 7.5 where the variation between each pair of gas welded thermocouples is provided.

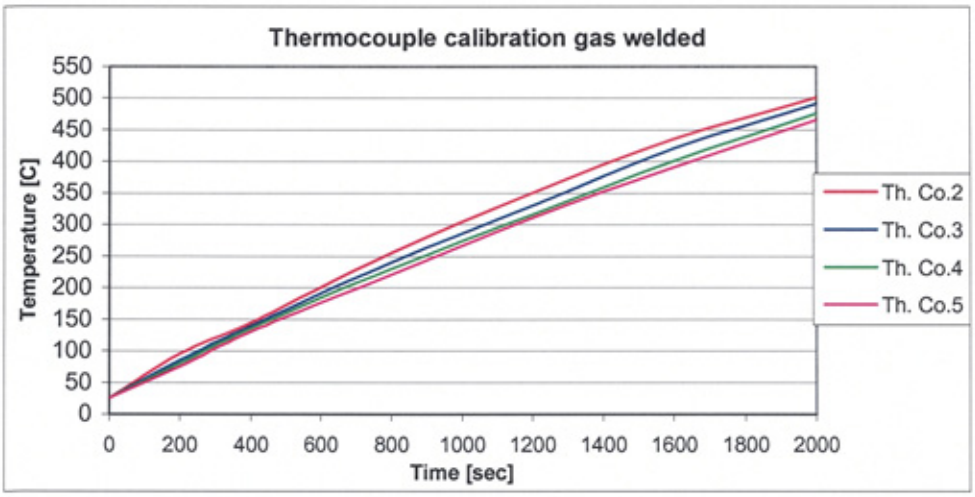

Figure 7.2 Temperature against time of calibrating 4 thermocouples gas welded the recording temperatures difference is high after 400 °C

Table 7.5 Results of temperatures differences of gas welded thermocouples

Time (seconds)	0.0	200	400	800	1200	1600	2000
Th. Co.(2-3)	0	10	5	15	20	15	10
Th. Co.(2-4)	0	15	10	25	35	35	25
Th. Co.(2-5)	0	20	15	35	40	45	35
Th. Co.(3-4)	0	5	5	10	15	20	15
Th. Co.(3-5)	0	10	10	20	20	30	25
Th. Co.(4-5)	0	5	5	10	5	10	10

Clearly for experimental purposes it would be best to use thermocouples with the most similar characteristics, i.e. with the smallest temperature variation, from Table 7.5, it can be surmised that thermocouples that provide the closest results are 3, 4, and 5. The difference in temperature is around 10 °C.

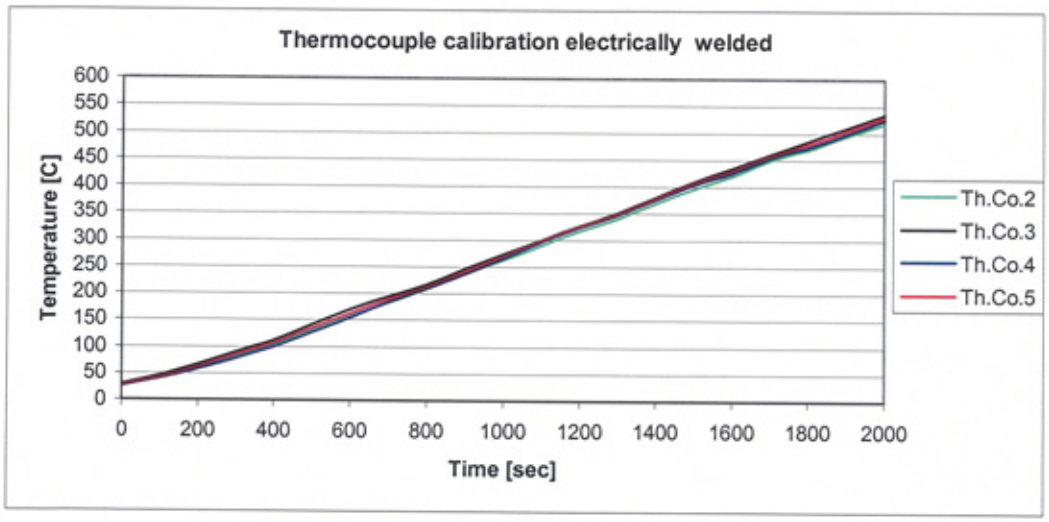

Figure 7.3 Temperature against time of calibrating 4 thermocouples electrically welded the recording temperatures difference is very low

Figure 7.3 shows a comparison of the temperature measured by 4 electrically welded thermocouples. The difference in temperature between each of the thermocouples appears small over the whole range. The temperature difference between each pair of

thermocouples is given in Table 7.6. With the exclusion of thermocouple number 2 the difference in temperature between thermocouples 3, 4 and 5 is a maximum of 3 °C.

Table 7.6 Results of temperatures differences of electrically welded thermocouple

Time (seconds)	0.0	200	400	800	1200	1600	2000
Th. Co.(2-3)	0	2	2	2	2	2	2
Th. Co.(2-4)	0	4	4	4	4	4	4
Th. Co.(2-5)	0	5	5	5	5	5	5
Th. Co.(3-4)	0	2	2	2	2	2	2
Th. Co.(3-5)	0	3	3	3	3	3	3
Th. Co.(4-5)	0	1	1	1	1	1	1

In comparison to the gas welded thermocouples, the electrically welded ones offer far greater repeatability, in terms of attaining the same result for each joint welded.

7.3.3 ERROR OF THERMOCOUPLE READINGS

Performance and specifications

Table 7.7 Analog input section A/D converter type AD 652 V/F converter accuracy and resolution -voltage measurements:

Gain	Range	Accuracy (Worst case)
1	-2.5 to 10V	±.01% of reading ±2.5mV
125	-20 to 80mV	±.01% of reading ± 20μV
166.7	-15 to 60mV	±.01% of reading ± 15μV
400	-6.25 to 25mV	±.02% of reading ± 6.25μV

Table 7.8 Accuracy and resolution of thermocouple measurements

TC Type	Range 0 to 750°C	Accuracy (Worst Case)
J	-200 to 1350°C	±0.5 °C
K	-200 to 1250°C	±1.4 °C
E	-200 to 900°C	±1.1 °C
T	-270 to 350°C	±0.9 °C
R	0 to 1450°C	±2.3 °C
S	0 to 1450°C	±2.3 °C
B	0 to 1700°C	±3.0 °C

7.4 EXPERIMENTAL SYSTEM

In this section the preparation of the glass samples for the experiment is discussed and the manner in which the thermocouples are connected to the PC is also discussed.

7.4.1 GLASS SAMPLE PREPARATION

Figure 7.4 shows the preparation of the glass samples used to perform the experimental work. Glass samples with a surface dimension of 20x20 mm and thicknesses of 2, 4 and 6 mm depths are required. The samples are formed using glass slides of dimensions 20x20x2 mm and they are each placed in a thermal break as shown. The use of a thermal break as such, means that heat can only transfer to and from the glass over the upper 20x20 mm surface area. The thermocouples are fixed in contact with the required

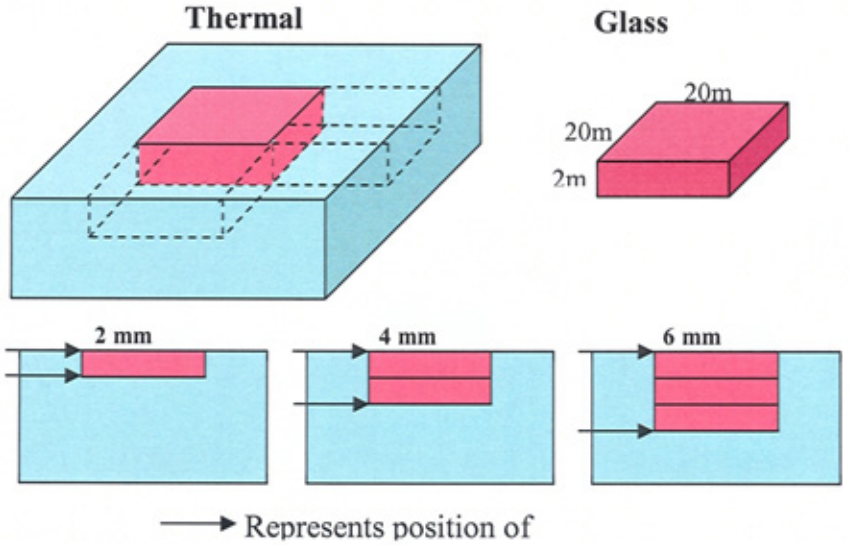

depth within the glass through a small slot cut in the side of the thermal break.

Figure 7.4 Shows glass sample preparation fixing the thermocouples on the surface, middle and bottom of the sample contains six soda lime glass slices, sample dimensions 6 mm height, and 20 x 20 mm area, container of a thermal break

7.4.2 GLASS SAMPLE THERMAL BOARD (PC) CONNECTIONS AND TEMPERATURE RECORDING

The thermocouples are connected to the PC via a PCI-DAS-TC 16-channel thermocouple input board. The board features automatic calibration, cold-junction, and open-channel detection. The analogue input consists of a 16-channel input multiplexer, a CJC input, a programmable-gain amplifier, and a high frequency V/F based A/D converter.

During each scan the A/D converter samples each of the thermocouple inputs, measures the CJC input, auto-calibrates the gain at a Gain = 1 using a reference voltage, and measures the input offset voltage. The CJC and the gain/offset values are stored in onboard RAM and are used by the processor in removing cold junction and in performing the built-in auto calibration. As the thermocouple inputs are scanned, the processor first acquires the raw data. It then calibrates it for the gain/offset error, and linearises it based on lookup tables for each associated thermocouple type.

The processor then converts the data to a temperature by referring to a previously-stored lookup table in ROM. Each thermocouple type has a separate table. The use of lookup tables optimizes linearization by storing many reference points along the thermocouples temperature/voltage curve where the greatest temperature/voltage changes occur. Following linearization, the CPU loads the data in the dual port RAM. When the data is ready to be read, the CPU sends an interrupt to the PC to read the data. [89]. Measurements computing catalogue, more CJC diagrams and specifications are provided in Appendix E.

The experimental system is shown in Figure 7.5 for the case of the measurement of the surface and centre temperature of the 2 mm thick piece of glass. The two thermocouples

are placed at the surface of the glass and at the bottom of the glass and their outputs connected to the terminal board. The terminal board is connected to the PC via a cable. The terminal board converts the signals from the thermocouples that are produced by the heat in the glass, to an equivalent temperature reading. This temperature is then in turn sent to the PC along the serial cable and displayed on the PC monitor. The PC also makes a recording of the values from the thermocouples every second and stores them in a data file.

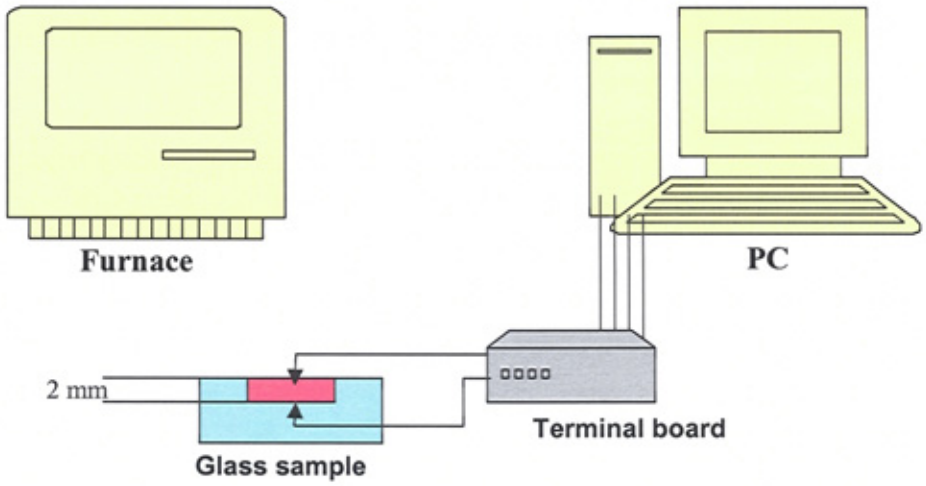

Figure 7.5 shows the connection of the glass sample with the thermocouples, and the terminal board to PC for temperature recording

7.5 THE EFFECT OF THE GLASS THICKNESS ON HEATING TEMPERATURES

In this section the effect of increasing the thickness of white soda-lime glass on the temperature at the surface and bottom of the glass sample as it is heated. Three thicknesses of glass sample are used, 2, 4 and 6 mm, these are placed in a thermal break as shown in Figure 7.4 and the temperature at the surface of the sample and at the bottom of the sample is monitored as the glass is heated.

Each of the glass samples, initially at room temperature (30 °C) is placed in the furnace, which exhibits a uniform controlled temperature of 665 °C. The temperature at the surface and bottom of the glass is monitored via the thermocouples at 1 second intervals until the temperature of the glass reaches 665 °C, the average time it takes for this to happen is 275 seconds. Each of the samples is removed from the furnace at the end of the experiment.

7.5.1 EXP-1 HEATING SODA-LIME GLASS 2 mm

A sample of 2 mm thick white soda lime glass with two thermocouples one fixed on the surface the second fixed at the bottom of the glass, the temperature recorded at the surface and the bottom is plotted in Figure 7.6.

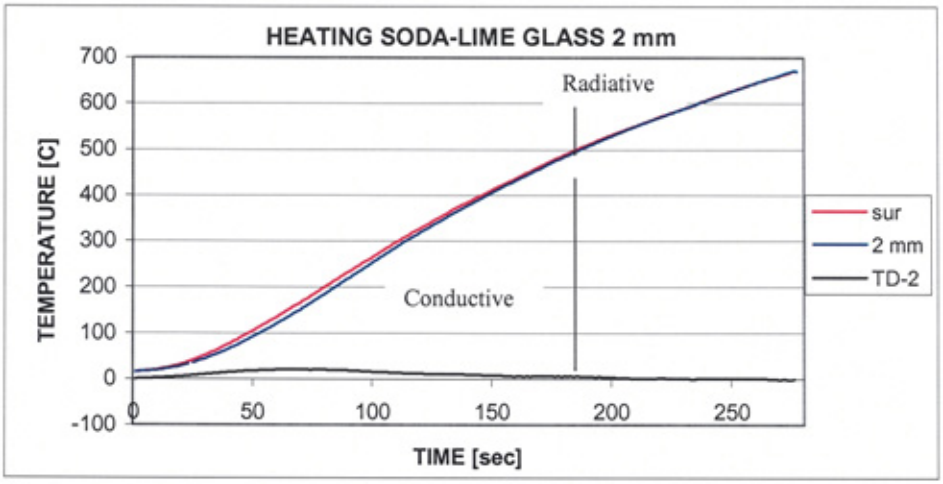

Figure 7.6 Variation of heating temperature with 275 seconds/ of 2 mm glass sample with two thermocouples one fixed on the surface, and the other on the bottom

From Figure 7.6 it can be seen that initially the glass is in a steady state with the surface and bottom temperatures equal. On being placed in the furnace the temperature begins to increase. The surface temperature increases faster than the bottom temperature becoming a maximum difference of 20 °C after 75 seconds, where the surface temperature is 184 °C and the bottom is 164 °C. beyond this maximum divergence, the bottom temperature converges with the surface temperature. At around 500 °C the surface and bottom temperatures are almost equal and the glass begins to radiate. A summary of the results is given in Table 7.9.

Table 7.9 Experimental results of surface and 2mm deep glass temperature variation with 275 seconds heating time

Time (seconds)	25	50	75	100	150	200	275
Surface	40°C	104°C	182°C	263°C	410°C	530°C	665°C
2 mm	35°C	90°C	168°C	252°C	403°C	527°C	664°C
Temp. diff.	7 °C	18°C	20°C	15°C	8 °C	3 °C	1 °C

7.5.2 EXP-2 HEATING SODA-LIME GLASS 4 mm

A sample of 4 mm thick white soda lime glass with two thermocouples one fixed on the surface the second fixed at the bottom of the glass, the temperature recorded at the surface and the bottom is plotted in Figure 7.7.

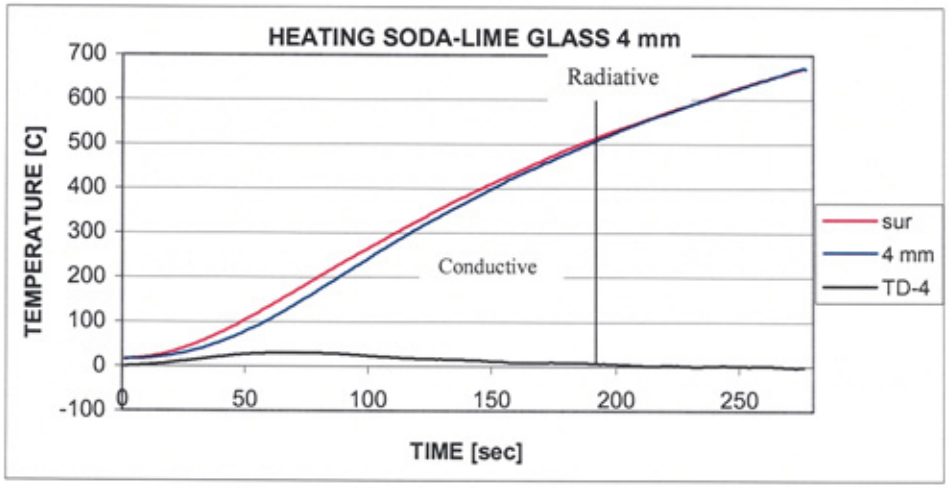

Figure 7.7 Variation of heating temperature with 275 second/ of 4 mm glass sample with two thermocouples one fixed on the surface, and the other on the bottom

From Figure 7.7 it can be seen that initially the glass is in a steady state with the surface and bottom temperatures equal. On being placed in the furnace the temperature begins to increase. The surface temperature increases faster than the bottom temperature becoming a maximum difference of 30 °C after 75 seconds, where the surface temperature is 182 °C and the bottom is 153 °C. beyond this maximum divergence, the bottom temperature converges with the surface temperature. At around 500 °C the surface and bottom temperatures are almost equal and the glass begins to radiate. A summary of the results is given in Table 7.10.

Table 7.10 Experimental results of surface and temperature variation with 275 seconds heating

Time (seconds)	25	50	75	100	150	200	275
Surface	40°C	104°C	182°C	263°C	410°C	530°C	665°C
4 mm	29 °C	77 °C	153°C	240°C	398°C	525°C	663°C
Temp. diff.	11 °C	27 °C	30 °C	23 °C	11 °C	5 °C	2 °C

7.5.3 EXP-3 HEATING SODA-LIME GLASS 6 mm

A sample of 6 mm thick white soda lime glass with two thermocouples one fixed on the surface the second fixed at the bottom of the glass, the temperature recorded at the surface and the bottom is plotted in Figure 7.8.

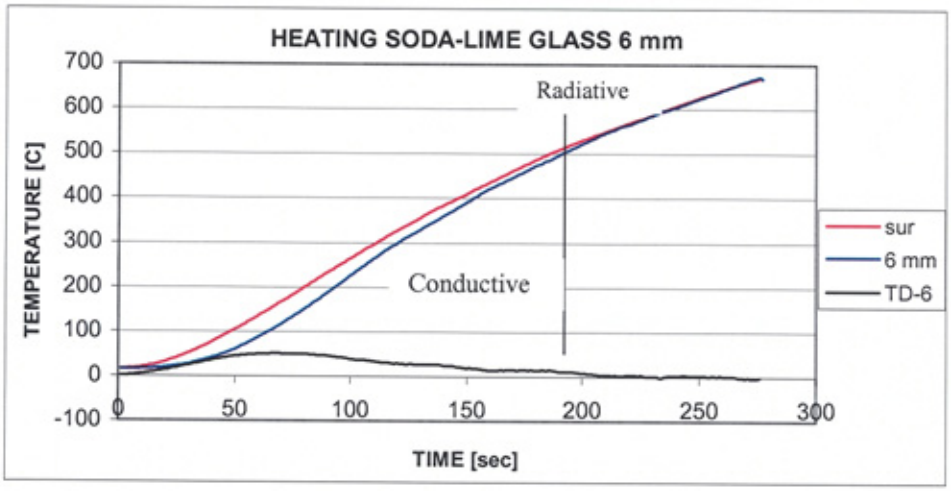

Figure 7.8 Variation of heating temperature with 275 seconds/ of 6 mm glass sample with two thermocouples one fixed on the surface, and the other on the bottom

From Figure 7.7 it can be seen that initially the glass is in a steady state with the surface and bottom temperatures equal. On being placed in the furnace the temperature begins to increase. The surface temperature increases faster than the bottom temperature becoming a maximum difference of 40 °C after 75 seconds, where the surface

temperature is 182 °C and the bottom is 153 °C. beyond this maximum divergence, the bottom temperature converges with the surface temperature. At around 500 °C the surface and bottom temperatures are almost equal and the glass begins to radiate. A summary of the results is given in Table 7.11.

Table 7.11 Experimental results of temperature variation with 275 seconds heating

Time (seconds)	25	50	75	100	150	200	275
Surface	40°C	104°C	182°C	263°C	410°C	530°C	665°C
6 mm	21C	59°C	133°C	225°C	390°C	521°C	662°C
Temp. diff.	19°C	45°C	40°C	38°C	19°C	8°C	3 °C

7.5.4 COMPARING THE SURFACE AND HEART TEMPERATURES OF HEATING GLASS 2, 4, 6 mm THICKNESS

Table 7.15 shows a comparison of the results obtained at the bottom of the glass for each of the three thicknesses. McGraw [2] in the pressing of a parison radiation is seen to have little influence. As the glass thickness is reduced the significance of radiation increases (can be seen on Figure 2.9 and Table 2.12).

Table 7.12 Comparing experimental results of bottom temperature variation of heating glass 2, 4, 6 mm thickness with 275 seconds heating

Time (seconds)	25	50	75	100	150	200	275
2 mm	35°C	90°C	168°C	252°C	403°C	527°C	664°C
3 mm	29°C	77°C	153°C	240°C	398°C	525°C	663°C
6 mm	21°C	59°C	133°C	225°C	390°C	521°C	662°C

Table 7.13 shows a comparison of the results obtained for the temperature differences between the surface and the bottom of each glass sample over the 275 second heating period. It is clear from the table that as the thickness of glass increases then so does the temperature difference between the surface and the bottom of the glass and this

difference increases up to 75 seconds. When the temperature reaches 500 °C, in the time interval from 150 to 200 seconds, the temperature difference decreases rapidly; this is because the glass begins to radiate at 500 °C. This can be seen in results by McGraw [2] Section 2.5.1 in the pressing of a parison radiation is seen to have little influence. As the glass thickness is reduced the significance of radiation increases.

Table 7.13 Comparing Experimental results of temperature difference surface-bottom of heating glass 2, 4, 6 mm thickness with 275 seconds heating

Time (seconds)	25	50	75	100	150	200	275
T.D 2 mm	7 °C	18°C	20°C	15°C	8 °C	3 °C	1 °C
T.D 4 mm	11 °C	27 °C	30 °C	23 °C	11 °C	5 °C	2 °C
T.D 6 mm	19°C	45°C	40°C	38°C	19°C	8°C	3 °C

7.6 THE EFFECT OF THE FAST AND SLOW COOLING ON THE GLASS TEMPERATURE

In this section, experimental work is carried out to investigate the slow and fast cooling of a 6 mm thick sample of white soda-lime glass. Slow cooling is considered the cooling of the sample from a given temperature when the surrounding temperature is non-ambient, i.e. an external heat source is present and hence external emissivity is not equal to 1. To generate this condition the glass sample is heated to a temperature of 656 °C in the furnace and then the power to the furnace turned off and the glass is allowed to cool inside the furnace. Fast cooling is considered the cooling of the glass where no external heat source is present i.e. the surrounding temperature is ambient room temperature and hence external emissivity is equal to 1. To generate this condition the glass is heated to 700 °C in the furnace and then the sample is removed from the furnace and allowed to cool in the ambient room temperature.

In both the slow and fast cooling experiments, the temperatures at the surface and bottom of the glass sample are recorded over a period during 1400 seconds and 80 seconds respectively.

7.6.1 EXP-4 SLOW COOLING SODA-LIME GLASS 6 mm

Figure 7.9 shows the temperature variation at the surface and the bottom of a 6 mm thick piece of soda-lime glass as it is cooled from 656 °C in the furnace once the furnace has been switched off over a period of 1400 seconds, the figure also shows the difference between the two temperatures over the time period. It can be seen that as the glass begins to cool, initially the surface temperature falls more rapidly than the bottom temperature. The temperature difference between the surface and the bottom of the glass reaches its maximum value of 23 °C after 400 seconds. The temperature difference between the surface and bottom decreases with time and reaches its minimum value of 5 °C at the end of the observation period. A summary of the results is provided in Table 7.14.

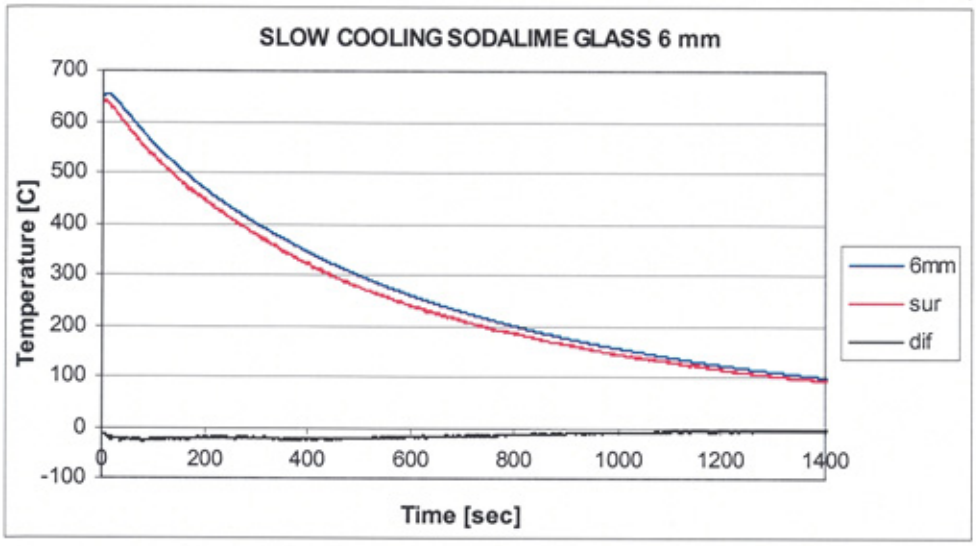

Figure 7.9 Variation of cooling temperature with 1400 seconds of 6 mm glass sample with two thermocouples one fixed on the surface, and the other on the bottom slow cooling

Table 7.14 Experimental results of temperature variation with 1500 seconds slow cooling 6 mm thick glass

Time (seconds)	0.0	200	400	600	800	1000	1400
6 mm. temp	656 °C	466 °C	343 °C	258 °C	198 °C	121 °C	97 °C
Surf. Temp	656 °C	448 °C	320 °C	240 °C	184 °C	114 °C	92 °C
(6mm-surf)Diff.	0.0 °C	22 °C	23 °C	18 °C	14 °C	7 °C	5 °C

7.6.2 EXP-5 FAST COOLING SODA-LIME GLASS 6 mm

Figure 7.10 shows the temperature variation at the surface and the bottom of a 6 mm thick piece of soda-lime glass as it is cooled from 656 °C in air at an ambient temperature of 20 °C over a period of 80 seconds, the figure also shows the difference between the two temperatures over the time period.

It can be seen that when the glass is removed from the furnace and begins to cool, the surface temperature decreases rapidly. Initially the surface temperature falls more rapidly than the bottom temperature, and the difference between the two reaches its maximum value of 120 K after only 10 seconds. The temperature difference between the surface and bottom decreases with time and reaches its minimum value of 10 K at the end of the observation period. The majority of the heat is lost from the glass in the first 20 seconds. A summary of the results is provided in Table 7.15.

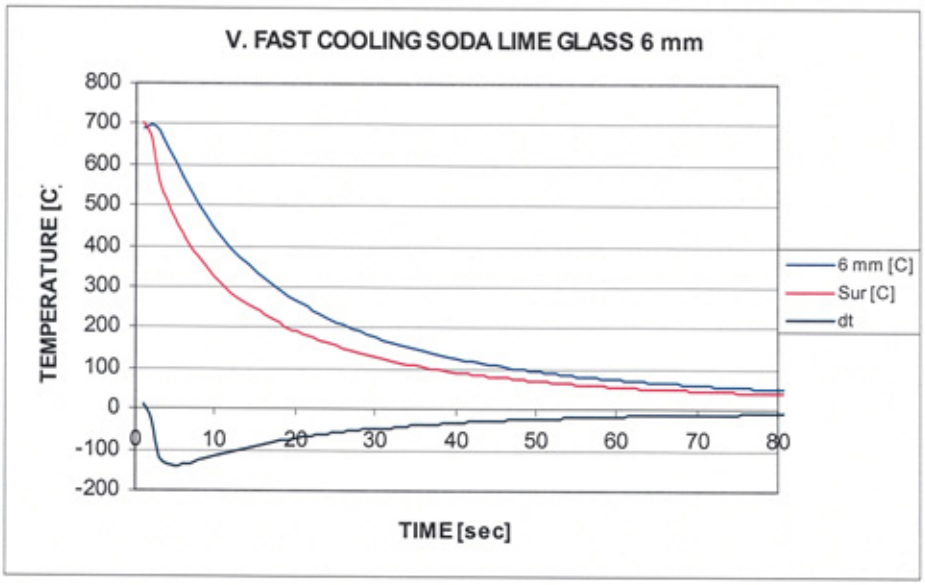

Figure 7.10 Variation of cooling temperature with time of 6 mm glass sample with two thermocouples one fixed on the surface and the bottom fast cooling 80 seconds.

Table 7.15 Experimental results of temperature variation with 80 seconds fast cooling time 6 mm thick glass

Time (seconds)	0.0	10	20	40	60	70	80
6 mm.Temp	700 °C	440 °C	265 °C	130 °C	74 °C	60 °C	50 °C
Surf. Temp.	700 °C	320 °C	190 °C	90 °C	54 °C	45 °C	40 °C
(6mm- surf) Diff.	0.0 °C	120 °C	75 °C	40 °C	20 °C	15 °C	10 °C

7.6.3 COMPARING THE TEMPERATURE DIFFERENC RESULTS BETWEEN THE SURFACE AND THE BOTTOM OF FAST AND SLOW COOLING GLASS

A comparison between the results obtained from the fast and slow cooling glass will now be made. Tables 7.16 and 7.17 show summaries of the temperature differences between the top and bottom of the glass over their particular time periods for slow and fast cooling respectively

Table 7.16 Comparing experimental results of surface-bottom of slow cooling 6 mm thick with 1400 seconds

Time (seconds)	0.0	200	400	600	800	1000	1400
(6mm -surf) Diff.	0.0 °C	22 °C	23 °C	18 °C	14 °C	7 °C	5 °C

Table 7.17 Comparing experimental results of surface-bottom of fast cooling glass 6 mm thick with 80 sec

Time (seconds)	0.0	10	20	40	60	70	80
(6mm- surf) Diff.	0.0 °C	120 °C	75 °C	40 °C	20 °C	15 °C	10 °C

It is clear from the summaries provided that the total temperature loss is far greater in the case of the fast cooling than in the slow cooling. This is expected since in the case of fast cooling, the temperature gradient between the glass and its surroundings is greater than in the slow cooling case where it remains in the furnace after it has been switched off. It is also noticeable that in the heat is lost from the glass much more rapidly in the case of fast cooling.

7.7 CYCLIC HEATING AND COOLING GLASS

In this section experimental work is undertaken to observe the temperature profile through 6 mm thicknesses of white soda-lime glass as it is cycled through a series of heating and cooling. The experiment is carried out 3 times, each time with thermocouples placed at different intervals through the glass. This allows the profile through the glass to be monitored at different depths. In the first experiment, two thermocouples are used one placed on the surface and the second at the bottom of the glass sample. In the second experiment three thermocouples are used, one on the surface one in the centre of the glass at a depth of 3 mm and one at the bottom of the glass. In the final experiment four thermocouples are used, one on the surface, then at depths of 2 mm, 4 mm and on the bottom at 6 mm. In each experiment the glass is first heated to 1100 °C and then cooled in air (ambient air at 10 °C) to 500 °C, it is then placed back in the furnace and reheated to 1100 °C and cooled again to 500 °C, This process of heating and cooling is performed eight times. Both the cooling and heating processes take periods of approximately 50 seconds. It should be noted that when replacing the samples in the furnace, the furnace temperature drops to around 1000 °C due to the door being open and it takes a further 20 seconds to heat back to the desired uniform temperature of 1100 °C.

7.7.1 EXP. 6 CYCLIC HEATING AND COOLING GLASS 6 mm 2-THERMOCOUPLES

Figure 7.11 shows the results obtained by the cyclic of heating and cooling of the white soda-lime glass as described over a period of 800 seconds. The temperature is recorded every 1 second at the surface and bottom of the glass. The Figure also shows the difference between the surface and bottom temperatures.

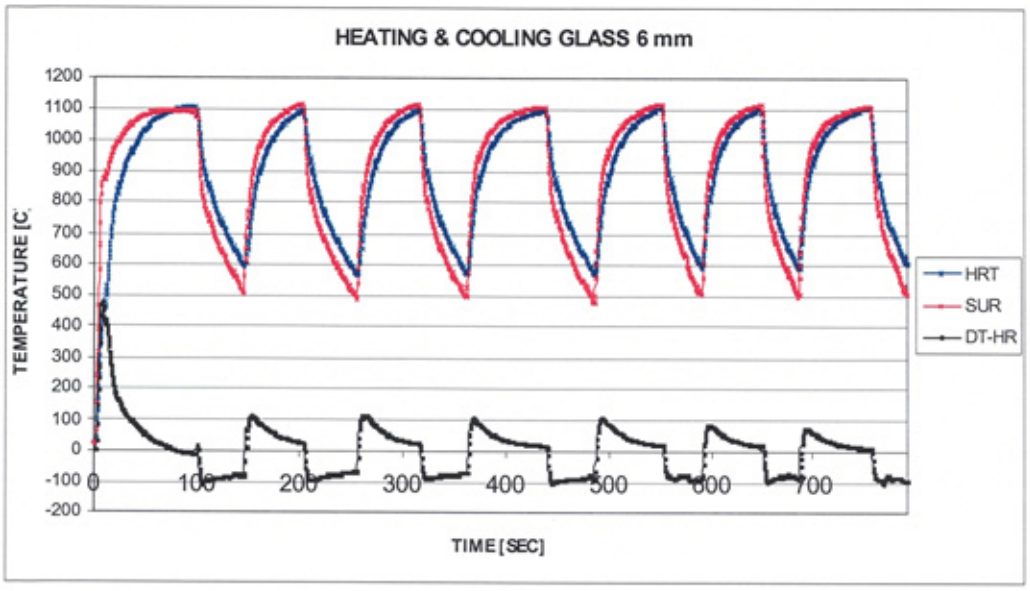

Figure 7.11 Variation of cooling and heating cyclic temperature with 50 seconds red line surface temperature, blue line heart temperature, and black line the difference temperature between the surface and bottom

Figure 7.12 shows an enlarged view of the first 100 seconds of Figure 7.11, this covers the initial heating time of the glass. Figure 7.13 shows one cycle of cooling and then heating, which takes a total of around 100 seconds.

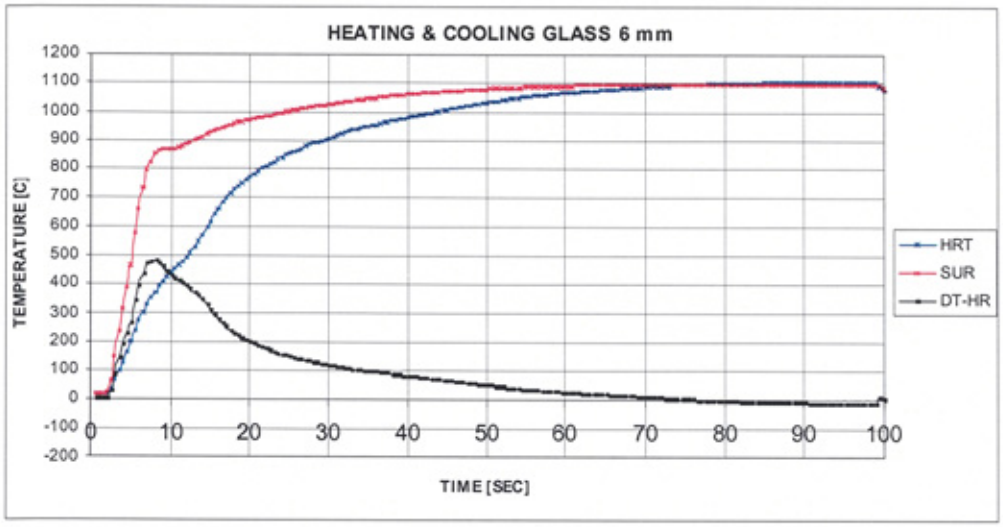

Figure 7.12 Variation of heating temperature with time of 100 seconds, red line surface temperature, blue line heart temperature, black line the difference temperature between the surface and bottom

From Figure 7.12 it is seen that the glass starts at room temperature ≈10 °C and is heated to a temperature of 1100 °C in the furnace. The glass surface temperature increases rapidly from 20-870°C over a period of ≈10 seconds. The rise in temperature then becomes more gradual until it reaches 1100 °C at 100 seconds. The temperature difference between the surface and the core of the glass initially increases rapidly. The temperature difference between the surface and the heart of the glass reaches its maximum value of 480 °C after around 10 seconds. Table 7.18 provides a summary of the results.

Table 7.18 Experimental results of temperature variation with 100 seconds fast heating soda-lime glass 6 mm thickness

Time (seconds)	10	20	30	40	50	70	100
Surf. Temp	870°C	980°C	1020°C	1070°C	1080°C	1095°C	1100°C
6mm.Temp	390°C	780°C	900°C	980°C	1020°C	1080°C	1098°C
Temp. diff.	480 °C	200 °C	120 °C	90 °C	60 °C	15 °C	2 °C

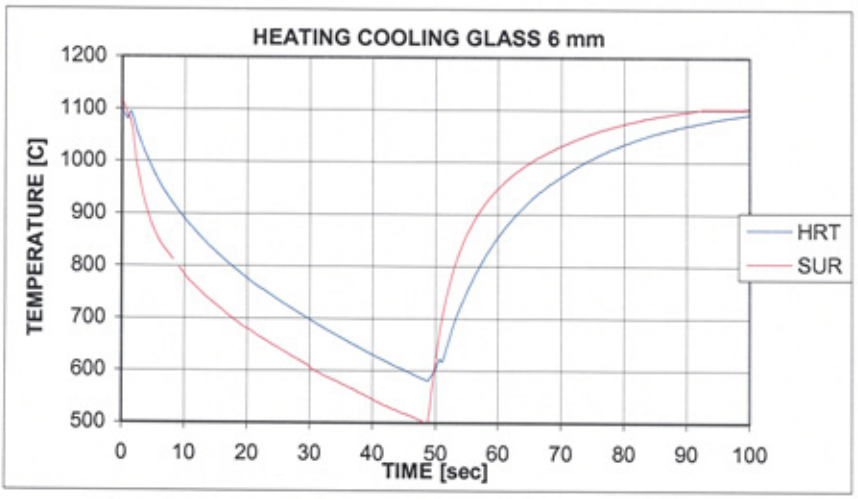

Figure 7.13 Variation of cooling and heating cyclic temperature with 50 seconds red line surface temperature, blue line heart temperature

Figure 7.13 magnifies a cycle of cooling and then heating the glass. The cooling period lasts around 50 seconds and the temperature drops from 1100 °C to 500 °C. The surface temperature falls very fast in the first 10 seconds from 1100-800 °C. The surface temperature falls faster than the heart glass temperature, with a maximum temperature difference between the surface and 6 mm depth of 110 °C. The second part of the cycle represents the heating period, which also last around 50 seconds. The surface of the glass heats faster than the centre with the surface heating from 500-960 °C in the first 10 seconds of heating. The maximum temperature difference between the surface and 6 mm depth during the heating cycle is 90°C; tables 7.19 and 7.20 show a summary of the results in Figure 7.13.

Table 7.19 Experimental results of temperature variation with 50 seconds cooling

Time (seconds)	1	5.0	10	20	30	40	50
6mm.Temp	1090°C	1008°C	910°C	780°C	700°C	630°C	570°C
Surf. Temp.	1100°C	918°C	800°C	680°C	610°C	550°C	500°C
Temp. diff.	10 °C	90 °C	110 °C	100 °C	90 °C	80 °C	70 °C

Table 7.20 Experimental results of temperature variation with 50 seconds heating

Time (seconds)	50	60	70	80	90	100
Surf. Temp.	500°C	960°C	1040°C	1080°C	1100°C	1100°C
6mm.Temp.	570°C	870°C	980°C	1040°C	1075°C	1095°C
Temp. diff.	70°C	90°C	60°C	40°C	25°C	5°C

7.7.2 EXP.7 CYCLIC HEATING AND COOLING GLASS 6 mm 3-THERMOCOUPLES

Figure 7.14 shows the results obtained by the cyclic of heating and cooling of the white soda-lime glass as described over a period of 800 seconds. The temperature is recorded every 1 second at the surface the centre and the bottom of the 6 mm thick glass. The Figure also shows the difference between the surface and bottom and surface and centre temperatures.

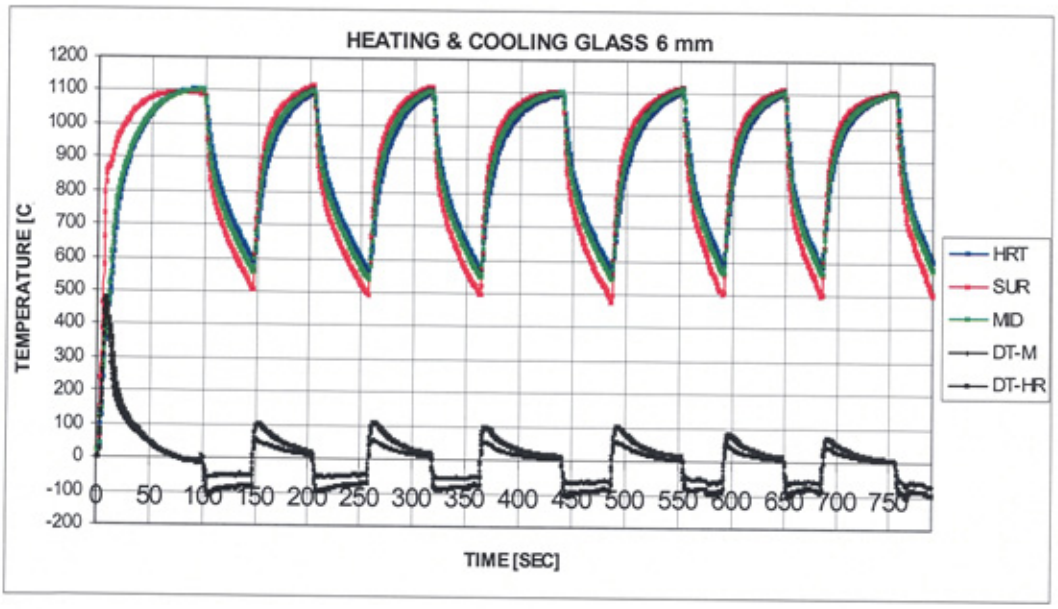

Figure 7.14 Variation of cooling and heating cyclic temperature with 50 seconds red line surface temperature, blue line heart temperature, black line the difference temperature between the surface and bottom

Figure 7.15 shows an enlarged view of the first 100 seconds of Figure 7.14, this covers the initial heating time of the glass. Figure 7.16 shows one cycle of cooling and then heating, which takes a total of around 100 seconds.

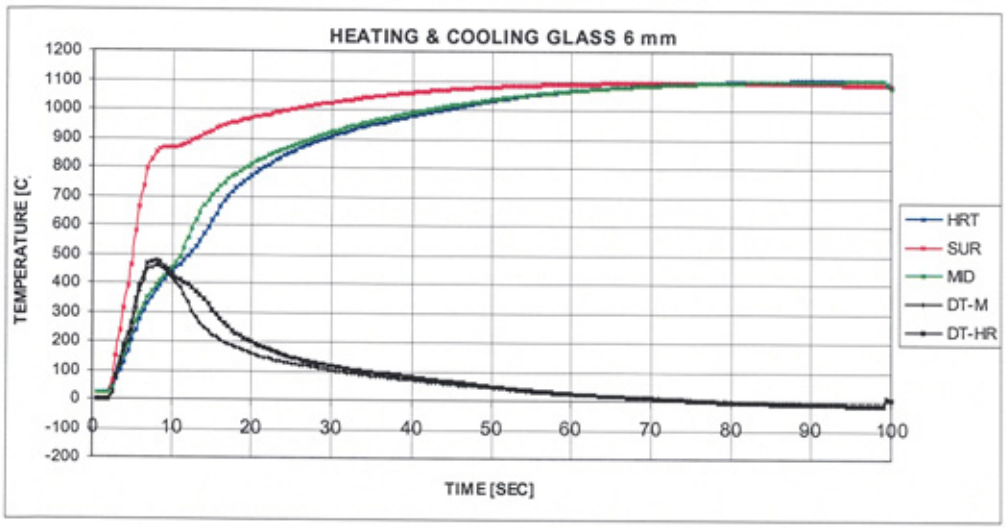

Figure 7.15 Variation of heating temperature with 90 seconds, red line surface temperature, blue line heart temperature, black line the difference temperature between the surface and bottom

From Figure 7.15 it is seen that the glass starts at room temperature ≈20 °C and is heated to a temperature of 1100 °C in the furnace. The glass surface temperature increases rapidly from 20-870°C over a period of ≈10 seconds. The rise in temperature then becomes more gradual until it reaches 1100 °C at 100 seconds. The temperature difference between the surface and the core of the glass initially increases rapidly. The temperature difference between the surface and the heart of the glass reaches its maximum value of 480 °C after around 10 seconds. The temperature at the middle of the glass (3 mm depth) has the same behaviour as that at the bottom of the glass. Table 7.21 provides a summary of the results.

Table 7.21 Experimental results of temperature variation with 100 seconds fast heating

Time (seconds)	10	20	30	40	50	70	100
Surf. Temp.	870°C	980°C	1020°C	1070°C	1080°C	1095°C	1100°C
3mm.Temp	450°C	810°C	920°C	990°C	1030°C	1090°C	1100°C
6mm.Temp	390°C	780°C	900°C	980°C	1020°C	1080°C	1098°C
Temp. diff.	480 °C	200 °C	120 °C	90 °C	60 °C	15 °C	2 °C

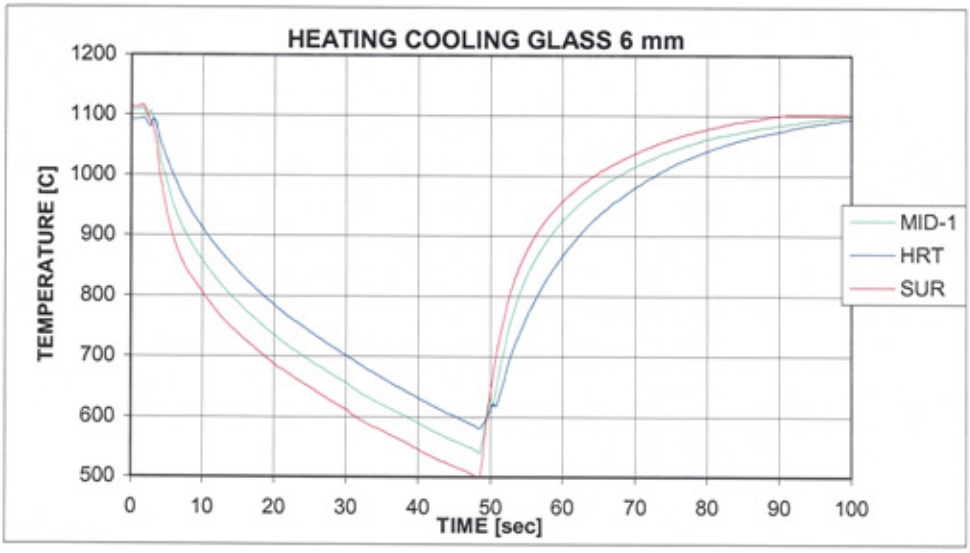

Figure 7.16 Variation of cooling and heating cyclic temperature with 50 seconds red line surface temperature, blue line heart temperature, and green line mid temperature

Figure 7.16 magnifies a cycle of cooling and then heating the glass. The cooling period lasts around 50 seconds and the temperature drops from 1100 °C to 500 °C. The surface temperature falls very fast in the first 10 seconds from 1100-800 °C. The surface temperature falls faster than the heart glass temperature, with a maximum temperature difference between the surface and 6 mm depth of 110 °C. This matches the behaviour observed in the first experiment of Section 7.7.1 (and can be seen by Rawson [11] Chapter 2 Table 2.9), the surface temperature reaches 940 °C, after 3.0. This work the

surface temperature reaches 920 °C, after 5.0. Table 7.22 shows a summary of the cooling cycle results.

Table 7.22 Experimental results of temperature variation with 50 seconds cooling

Time (seconds)	1	5.0	10	20	30	40	50
6mm.Temp.	1090°C	1008°C	910°C	780°C	700°C	630°C	570°C
3mm.Temp.	1100°C	980 °C	870°C	740°C	650°C	580°C	540°C
Surf. Temp.	1100°C	920°C	800°C	680°C	610°C	550°C	500°C
Temp. diff.	10 °C	90 °C	110 °C	100 °C	90 °C	80 °C	70 °C

The second part of the cycle represents the heating period, which also last around 50 seconds. The surface of the glass heats faster than the centre with the surface heating from 500-960 °C in the first 10 seconds of heating. The maximum temperature difference between the surface and 6 mm depth during the heating cycle is 90°C. The centre and bottom temperatures of the 6 mm thick glass show the same behaviour. Table 7.22 shows a summary of the heating cycle results.

Table 7.23 Experimental results of temperature variation with 50 seconds heating

Time (seconds)	50	60	70	80	90	100
Surf. Temp.	500°C	960°C	1040°C	1080°C	1100°C	1100°C
3mm.Temp.	540°C	930°C	1020°C	1075°C	1080°C	1095°C
6mm.Temp.	570°C	870°C	980°C	1040°C	1075°C	1090°C
Temp. diff.	70°C	90°C	60°C	40°C	25°C	10°C

7.7.3 EXP. 8 CYCLIC HEATING AND COOLING GLASS 6 mm 4-THERMOCOUPLES

Figure 7.14 shows the results obtained by the cyclic of heating and cooling of the white soda-lime glass as described over a period of 550 seconds. The temperature is recorded every 1 second at the surface and then depths of 2 and 4 mm and then on the bottom of the 6 mm thick glass. The Figure also shows the difference between the surface and bottom and surface and centre temperatures.

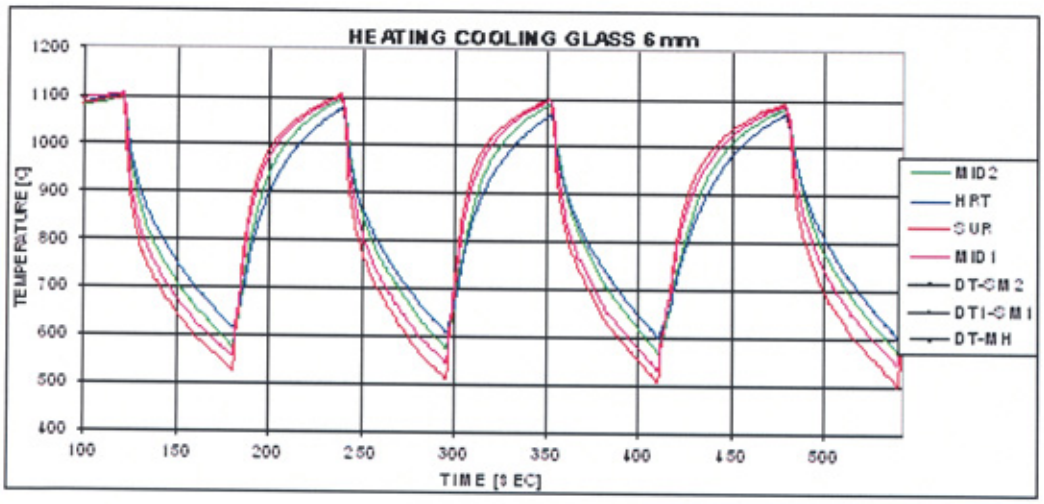

Figure 7.17 Variation of cooling and heating cyclic temperature with 50 seconds red line surface temperature, blue line heart temperature, and black line the difference temperature between the surface and bottom

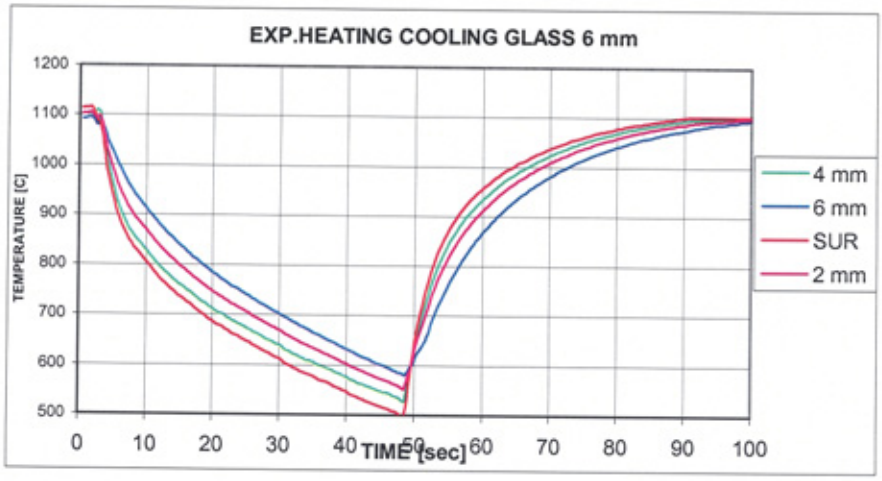

Figure 7.18 Variation of cooling and heating cyclic temperature with 50 seconds red line surface temperature, blue line heart temperature

Figure 7.18 magnifies a cycle of cooling and then heating the glass. The cooling period lasts around 50 seconds and the temperature drops from 1100 °C to 500 °C. The surface temperature falls very fast in the first 10 seconds from 1100-800 °C. The surface temperature falls faster than the heart glass temperature, with a maximum temperature difference between the surface and 6 mm depth of 110 °C. This matches the behaviour observed in the first experiment of Section 7.7.1 and can be seen by Rawson [11] Chapter 2 Table 2.9, the surface temperature reaches 940 °C, after 3.0. This work the surface temperature reaches 920 °C, after 5.0. Table 7.26 shows a summary of the cooling cycle results.

The second part of the cycle represents the heating period, which also last around 50 seconds. The surface of the glass heats faster than the centre with the surface heating from 500-960 °C in the first 10 seconds of heating. The maximum temperature difference between the surface and 6 mm depth during the heating cycle is 90°C. Table 7.25 shows a summary of the heating cycle results.

Table 7.24 Experimental results of temperature variation with 50 seconds cooling

Time (seconds)	1	5.0	10	20	30	40	50
6mm.Temp	1090°C	1008°C	910°C	780°C	700°C	630°C	570°C
4 mm Temp.	1100°C	990°C	870°C	750°C	670°C	600°C	555°C
2 mm Temp.	1100°C	940°C	820°C	710°C	630°C	570°C	530°C
Surf. Temp.	1100°C	918°C	800°C	680°C	610°C	550°C	500°C
Temp. diff.	10°C	90°C	110°C	100°C	90°C	80°C	70°C

Table 7.25 Experimental results of temperature variation with 50 seconds heating

Time (seconds)	50	60	70	80	90	100
Surf. Temp.	500°C	960°C	1040°C	1080°C	1100°C	1100°C
2 mm Temp.	530°C	940°C	1020°C	1070°C	1090°C	1098°C
4 mm Temp.	555°C	910°C	1010°C	1060°C	1085°C	1096°C
6mm.Temp	570°C	870°C	980°C	1040°C	1075°C	1095°C
Temp. diff.	70°C	90°C	60°C	40°C	25°C	5°C

7.8 DO- MODELLING PROPERTIES OF COOLING GLASS

In this section the CO modelling methodology, as discussed in Chapter 4, is used to model the cooling of a 6 mm thick white soda-lime glass in ambient air over a period of 50 seconds. The temperature profile through the glass is obtained on the surface of the glass and at depths of 2, 4, and 6 mm. The modelling parameters required are given in Tables 7.26 and 7.27 below.

Table 7.26 Bands of wavelengths and absorption coefficients, used by Jones and Basnett [12], for white glass Table 2.22

Bands	Absorption coefficient (α)	Wavelength (μ)
Band-1	23 m^{-1}	(0.8--2.25) μ
Band-2	45 m^{-1}	(2.25--2.75) μ
Band-3	100 m^{-1}	(2.75--4.3) μ

Table 7.27 Initial glass and air temperatures and the properties of glass and air as used by Jones and Basnett [12], Rawson [27], McGraw [3], in (radiation case) Tables 2.22 and 2.24

Property	Units	Glass (fluid)	Air (fluid)
Density	Kg/m^3	2500	0.0242
C_p (Specific heat)	J/kg-k	1350	1000
Thermal conductivity	W/m-k	1.45	1.225
Heat transfer coefficient	W/m^2-k	-	10
Absorption coefficient white (G)	m^{-1}	23, 45, 100	-
Refractive index	-	0.5	-
Centre temperature	°C	1100	20
Thickness	mm	10	10
Time	Second	50	50

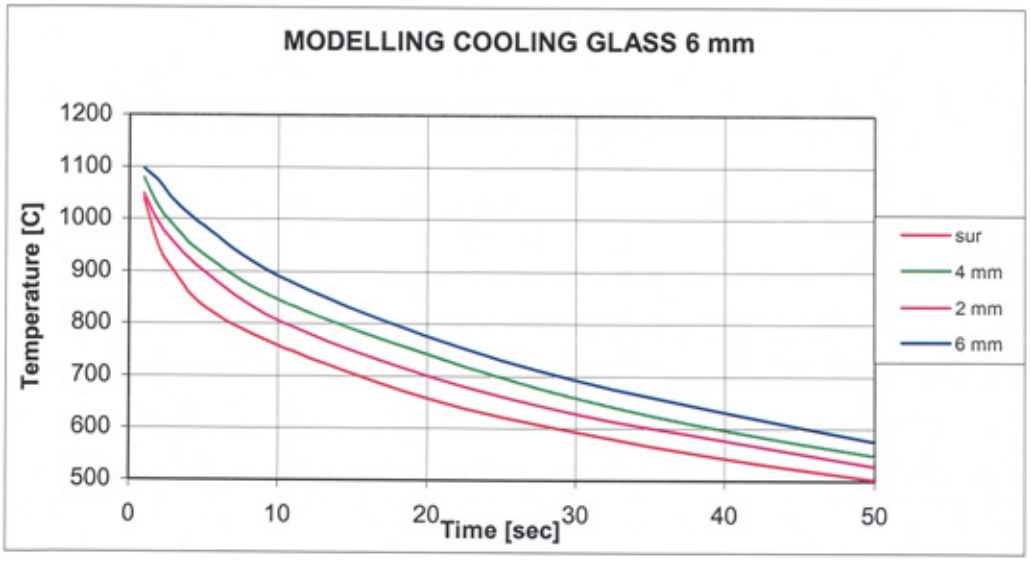

Figure 7.19 Variation of cooling temperature with time of 50 seconds, red line surface temperature, purple line 2 mm deep temperature, green line 4 mm deep, blue line 6 mm deep

Figure 7.19 shows the results obtained from the simulation using the DO modelling methodology. The figure shows that the modelling predicts in the first 10 seconds the

surface temperature will drop from 1100 °C to 760 °C and then the temperatures at 2, 4 and 6 mm drop to 800 °C, 845 °C and 890 °C respectively. By 50 seconds, they have each dropped to 500, 530, 545, and 570 °C; these results are summarised in Table 7.28.

Table 7.28 Temperature modelling results of variation with 50 seconds cooling

Time (seconds)	1	5.0	10	20	30	40	50
6mm.Temp	1100°C	990°C	890°C	770°C	700°C	630°C	570°C
4 mm Temp.	1090°C	980°C	845°C	740°C	650°C	590°C	545°C
2 mm Temp.	1070°C	975°C	800°C	695°C	620°C	575°C	530°C
Surf. Temp.	1050°C	865°C	760°C	660°C	600°C	550°C	500°C
Temp. diff.	50°C	125°C	135°C	110°C	100°C	80°C	70°C

Comparing the experimental and modelling results shown in Figures 7.18 and 7.19 and in Tables 7.24 and 7.28, it can be seen that the shapes of the profiles are the same. In both experimental and modelling cases the surface temperature decreases most quickly and so on through the glass with the 6 mm depth losing heat the slowest. The difference in temperatures through the profile of the glass decreases with time. From the tables of results shows after 30 seconds of cooling time until the end of 50 seconds the results between the experimental and the modelling are almost identical

7.9 DISCUSSIONS

In Sections 7.2 and 7.3 two thermocouple types were investigated, gas welded and electrically welded, to find which offered the most consistent results in terms of both the repeatability and variation between them. It was found that the electrically welded thermocouples were the best with a variation between them of 1-2 K.

In the investigation of the heating of different thicknesses of glass the difference between the surface and bottom temperatures was observed. It was seen that the maximum difference in the two temperatures was reached after 75 seconds in all three cases (2, 4 and 6 mm), however the level of the temperature difference also increases with thickness. At 500 °C the temperature difference between the core and surface for all three thicknesses of glass becomes very small and approximately very similar. This is because the glass begins to radiate at 500 °C is presented in Section 7.5.1-7.5.3

In this investigation of cooling, the glass was heated to 656 °C and then the furnace was turned off and the sample allowed to cool slowly in the furnace (for 4 hours). At the beginning of the cooling period the glass surface temperature falls faster than the bottom temperature, the difference becomes a maximum of 23 °C after 400 seconds, as shown in Table 7.14. As the time increases the bottom of the glass loses heat more rapidly, which makes the temperature difference smaller. In the fast cooling case, where the glass sample is removed from the furnace at 700 °C, the temperature difference between the surface and the bottom of the glass is very large at the beginning of cooling comparing to the slow cooling (takes only 50 seconds), as shown in Figure 7.10 and Table 7.15. Most of the heat energy of the glass is lost in a time period of 10 seconds. Fast cooling the glass loses energy in a time faster than the slow cooling, because the

glass is able to lose heat to its surroundings faster as there is a larger temperature gradient.

Figure 7.11 shows cyclic of heating and cooling of the surface and bottom of soda lime glass of 6 mm thickness, the measurement of temperature against time, over a period of 800 seconds. The glass is heated suddenly to a temperature of 1100 °C, as shown in figure 7.12. The temperature increases rapidly from 20-870 °C over a period of ≈10 seconds. As the time increases the temperature increases until it reaches 1100 °C in a period time of 100 seconds, the temperature difference between the hot surface and the core of the glass increases rapidly as the glass is placed in the 1100 °C furnace. As shown in Table 7.18 the temperature differences between the surface and the heart of the glass reaches its maximum value of 480 °C after 10 seconds and the minimum temperature difference value of 2 °C at 100 seconds as presented in Section 7.7.1.

Figure 7.13 shows two consecutive cycles of cooling and then heating the glass each part taking a period of 50 seconds. The temperature drop is from 1100 to 500 °C, the drop is very fast from 1100-800 °C in the first 10 seconds and the surface temperature cools faster than the bottom glass temperature. The second cycle represents the heating; the surface of the glass heats faster than the bottom of the glass as presented in Section 7.7.1

Using a third thermocouple to monitor the temperature at a depth of 3 mm during the cyclic of heating and cooling the same results between the surface and bottom glass were obtained as in the previous experiment, and the centre temperature followed that of the bottom temperature.

When four thermocouples are used as in Figure 7.17, which shows the cyclic of cooling and heating soda lime glass with a thickness of 6 mm. Measurement of temperature

against time, over a period of 550 seconds. Once again the same results are obtained for surface and bottom temperatures as those observed in the other two experiments with two and three thermocouples. The thermocouples at 2 and 4 mm depths show that the temperature varies with the same shape profile as that at the bottom of the glass.

The results obtained from modelling showed the same profile shapes as those obtained from the experimental work. However in comparing the relative temperatures between the two it was seen that, over the initial cooling period the model offers lower values than the experimental readings, but as the cooling time increases the temperatures become the same, as presented in Section 7.8.1

7.10 SUMMARY

- Electrically welded thermocouples provide a more consistent and repeatable measurement than gas welded thermocouples, due to the nature of the welding process and possible oxidation of the metals.
- As the glass thickness increases the time taken for the glass to heat increases. Most of the heat energy is gained during the first 30 seconds regardless of thickness.
- The rate of change of the temperature difference between the surface and the bottom of the glass becomes smaller at 500 °C, where the glass starts to radiate internally.
- As the thickness of the glass increases the time it takes for the glass to cool also increases. When the rate of cooling is high, the maximum temperature difference is larger. In the fast cooling most of the heat lose from the glass occurs at the first few seconds.
- The temperature difference through a piece of glass as it is heated or cools increases positively or negatively accordingly.
- The DO model is able to provide results close to those obtained experimentally however it was found to overestimate the initial cooling of the glass predicting smaller temperatures. However as time increases the models results become more reliable.

CHAPTER EIGHT – EXPERIMENTAL WORK WHITE AND GREEN GLASS

8.1 INTRODUCTION

In this chapter practical work is undertaken to further investigate the effect of absorption coefficient on the cooling of glass. The modelling investigation performed in Chapter 2 showed that as the absorption coefficient increases then the rate at which the glass is able to attain or lose heat also increases.

Prior to the discussion of the experimental work some information is provided regarding the absorption coefficient of glass, including what causes different absorption coefficient and how it is defined.

The experimental procedures used in the investigation are described in Section 8.3 along with the techniques used to form and prepare the glass samples. The techniques used to characterise the surfaces are also introduced. The equipment used, consists of a furnace (Appendix E), the dimensions and specifications of which were previously presented in Sections 7.2.1 and 7.2.2. The thermocouples used are the same as those used in Chapter 7, (electrically welded).

The experiment observes the heating and cooling of white and green glass samples. The samples are heated in a furnace from a room temperature of 20 °C to 1050 °C, and then cooled to 500 °C in air and then heated again in the furnace to 1050 °C. The cyclic of heating and cooling is repeated for a time of 550 seconds. The results obtained are discussed in Sections 8.4 and 8.5.

Modelling of the experimental work is carried out using the DO formulation and the results obtained are presented and compared with the experimental results in Sections 8.6 8.7 and 8.8.

Further discussions are provided in Section 8.9 and a summary of the findings of the chapter is offered in Section 8.10.

8.2 ABSORPTION COEFFICIENT OF WHITE AND GREEN GLASS

The absorption coefficient of glass has been studied by several investigators including Endrys, Geotti and Luka, [22] Kruszewski [15]. The absorption coefficients of glass in the wavelength region of its transparency are influenced by two main factors. The first one is the content of transition metal oxides, which are present in glass either as batch impurities (usually Fe_2O_3) or as colouring agents (Fe_2O_3, Cr_2O_3, MnO_2, CoO, NiO etc.). Such oxides give rise to absorption peaks in the visible and near infrared region of the spectrum (0.4 to 2.6 μ m), coloured with Cr_2O_3 and Fe_2O_3 in different ratios. The absorption in the visible and near infrared region (0.4 to 2.5 μ m) for white glass is very small, due to the very low Fe_2O_3 content. Also, the content and state of oxidation have a decisive influence on the transparency as well as on the k (thermal conductivity) value of glass especially at high temperatures as noted by Grove and Jellyman, [32] Franz, [33] Blazek, Endrys and et al.

The wavelength and temperature dependence of the absorption coefficients considering the glass compositions are given in Figure 8.1, the glasses measured may be divided into three different groups. The first includes white as indicated in Figure 8.1, the second half-white, the third includes green indicated in Figure 8.2 Hagy [23].

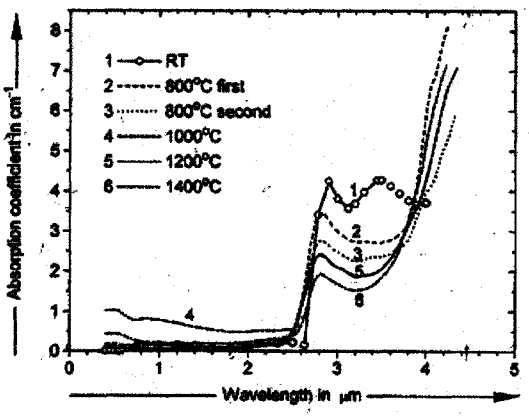

Figure 8.1 the absorption coefficients and wavelengths white soda lime glass Hagy [23]

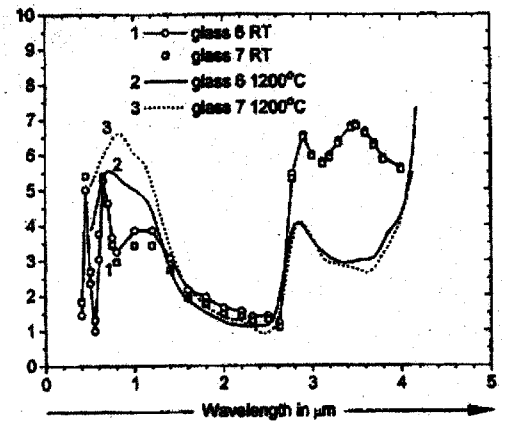

Figure 8.2 the absorption coefficients and wavelengths green soda lime glass Hagy [23]

The thermal properties of the glass used in this modelling are as those used in previous studies by Jones and Basnett [1], Rawson [11], and McGraw [6], consider a Specific heat of 1350 J/kg-K, thermal conductivity of 1.45 W/m-K and density of 2500 Kg/m^3. The air properties from the previous study by Rawson [11], and McGraw [6], in open blank (reheat), consider the air properties; such as air density of 0.024 Kg/m^3, specific heat of 1000 J/kg-K, thermal conductivity of 1.20 W/m-K and a heat transfer coefficient of 10 W/m^2-K between the air at an ambient temperature of 20 °C and the surface of the hot glass of 1050 °C.

8.3 PREPARING GLASS SAMPLES

In this section the experimental set-up is explained. Two types of glass samples white and green glass with the same dimensions as shown in figure 8.3 below are prepared. The investigation examines the rate of heating and cooling and the effect of the absorption coefficient on the glass surface temperature.

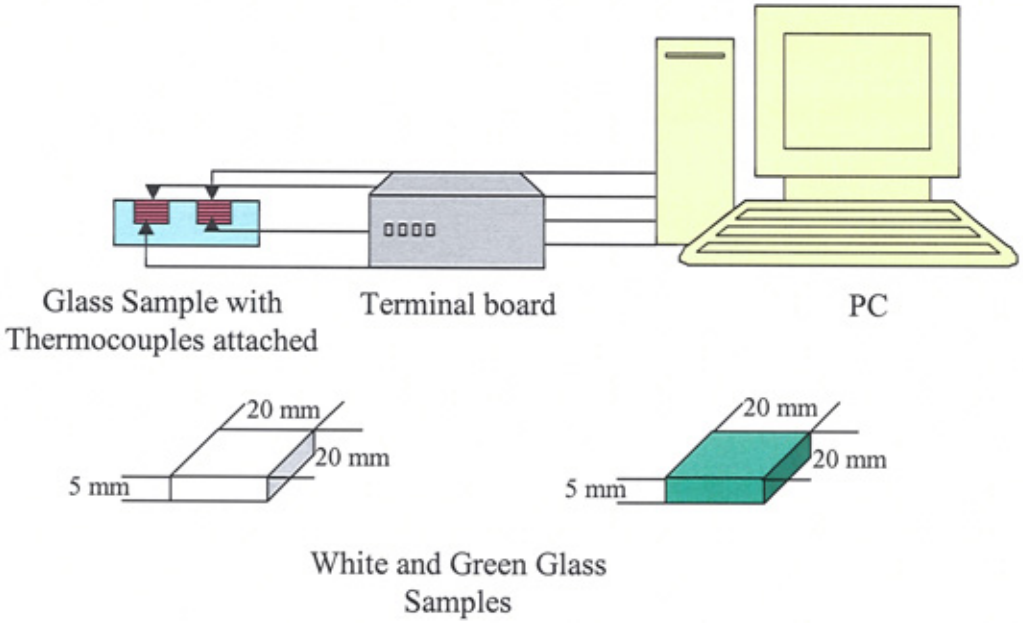

Figure 8.3 shows the connection of the glass sample with the thermocouples, and the terminal board, to PC for temperature recording

The present experimental system involves taking a sample of glass 5 mm thick and mounting two thermocouples one on the surface and one at a depth of 5 mm (the bottom of the glass), for both white and green samples. The outputs of the thermocouples were connected to the terminal board and then the terminal board connected to the PC. The sample of glass is taken from room temperature (20 °C) and introduced to the furnace, which exhibits a uniform controlled temperature of 1050 °C. The glass is then cooled to 500 °C in air and then replaced in the furnace and reheated to 1050 °C. The cyclic is repeated for 550 seconds.

8.4 EXPERIMENT CYCLIC HEATING AND COOLING WHITE AND GREEN GLASS

The results obtained for the cyclic of heating and cooling of both the white and green glass as described in Section 8.3 are shown in Figures 8.4 and 8.5.

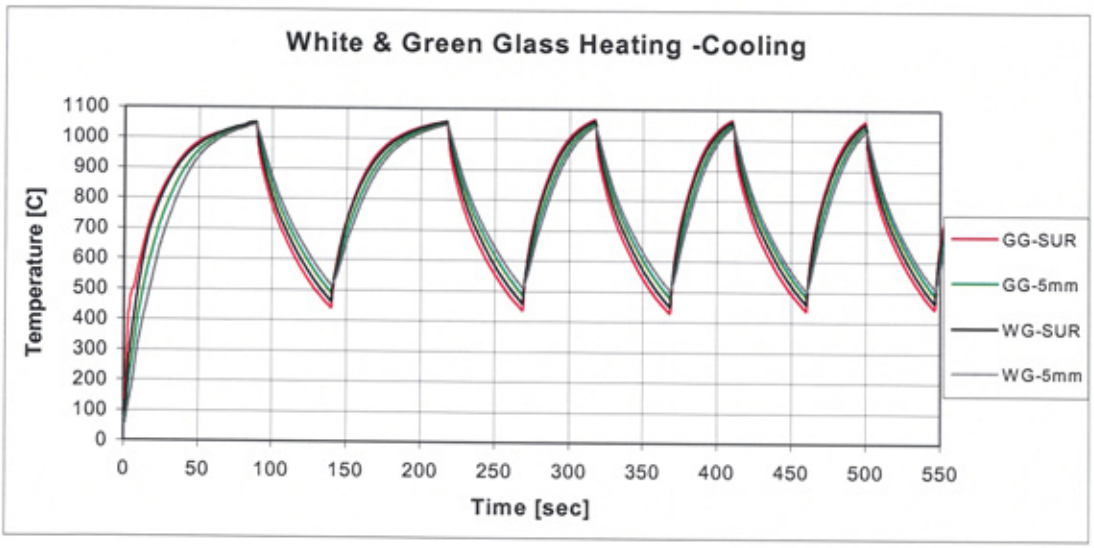

Figure 8.4 Variation of heating and cooling cyclic temperatures red line surface temperature, green line bottom temperature, of green glass, black line bottom temperature, grey line surface temperature, of white glass

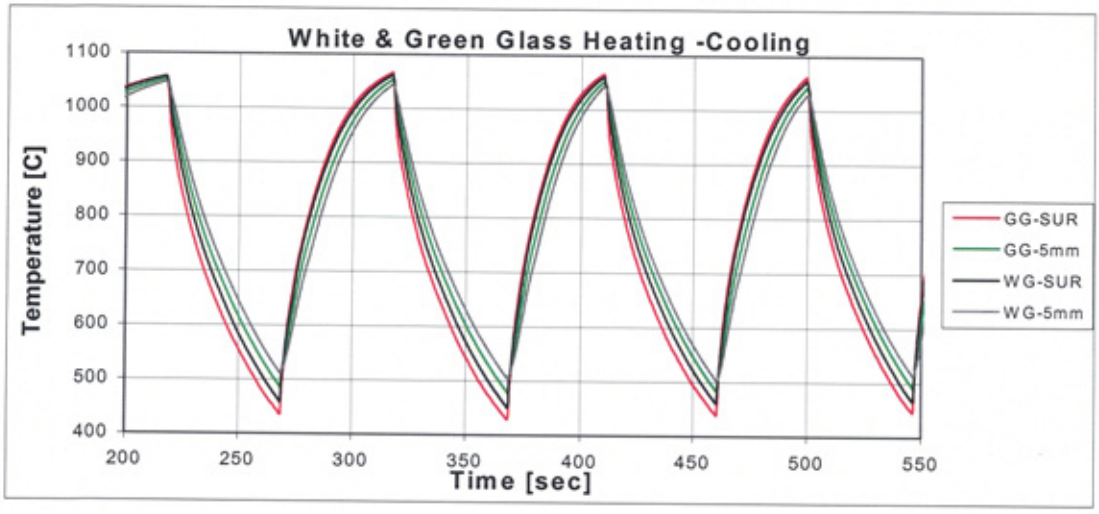

Figure 8.5 Variation of heating and cooling red line surface temperature, green bottom temperature, of green glass, black line surface temperature, and grey bottom temperature, of white glass

Figures 8.4 and 8.5 show cyclic of heating and cooling of both white and green soda-lime glass of 5 mm thickness. From the figures it can be seen that the temperature range varies between 20 and 1050 °C. From Figure 8.5 it can be seen that the green glass heats faster than the white glass at both its surface and its bottom. In both cases the surface temperature rises faster than the bottom temperature.

One of the cycles of cooling and then heating for the white glass is shown enlarged in Figure 8.6. Both the surface and bottom temperature variations with time are shown.

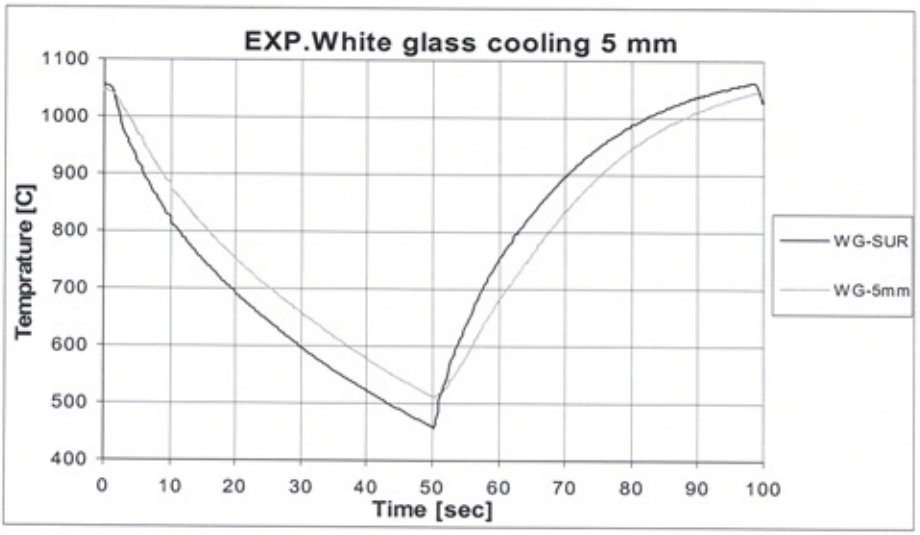

Figure 8.6 Variation of cooling and heating black line surface temperature, grey line 5 mm temperature, of White glass

The figure shows that in the first 10 seconds of cooling time the surface temperature of the white glass drops rapidly from 1050 to 820 °C. As shown in table 8.1 as the time increases from 10 to 50 seconds, the surface temperature of the white glass decreases from 820 to 460°C. The surface temperature decreases faster than the temperature at a depth of 5 mm. This is because it is exposed to the ambient air of 20 °C, while the bottom temperature cools more slowly relative to the surface. McGraw [6].

The second part of the cycle represents the heating, which takes a period of around 50 seconds. In the first 10 seconds of heating, the surface temperature of the white glass heats from 460 °C to 750 °C, as shown in table 8.2. As the time increases from 10 to 50 seconds, the surface temperature of the white glass increases from 750 to 1045°C. The surface temperature in the heating cycle has a higher temperature than the bottom temperature, because the surface exposed to the high furnace temperature relative to the bottom. McGraw [6].

One of the cycles of cooling and then heating for the green glass is shown enlarged in Figure 8.7. Both the surface and bottom temperature variations with time are shown.

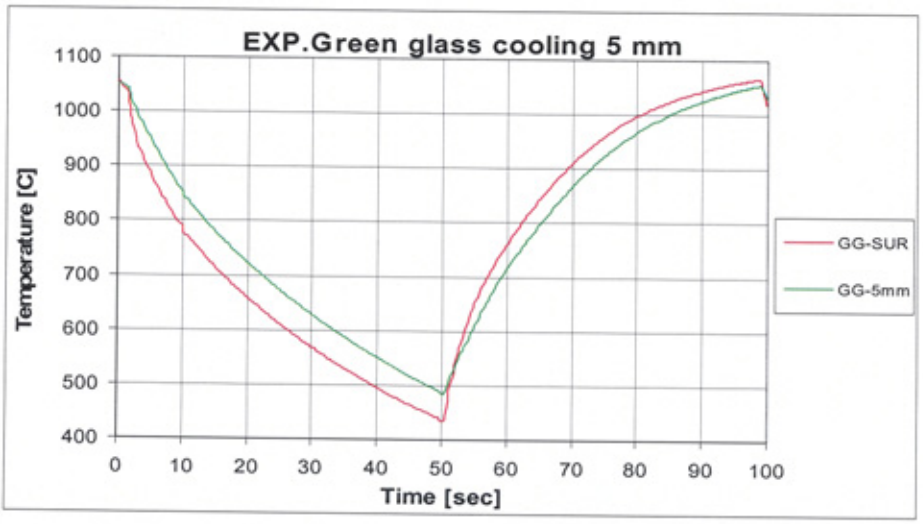

Figure 8.7 Variation of cooling and heating red line surface temperature, green line heart temperature, of green glass

The figure shows that in the first 10 seconds of cooling time the surface temperature of the green glass drops rapidly from 1050 to 780 °C. As shown in table 8.1 as the time increases from 10 to 50 seconds, the surface temperature of the green glass decreases from 780 to 445 °C. The surface temperature decreases faster than the temperature at a depth of 5 mm. This is because it is exposed to the ambient air of 20 °C, while the

bottom temperature cools more slowly relative to the surface. It should also be noted that the surface temperature of the green glass falls faster than that of the white glass. (See section 2.3.1 ad 2.3.1 for further discussion of cooling white and opaque glass) also discussed by Kruszewski [15]

The second part of the cycle represents the heating, which takes a period of around 50 seconds. In the first 10 seconds of heating, the surface temperature of the green glass heats from 445 °C to 765 °C, as shown in Table 8.2. This is a greater increase than the white glass for the same time period. As the time increases from 10 to 50 seconds, the surface temperature of the green glass increases from 765 °C to 1045 °C. The green glass heats faster than the white glass in each of the time intervals given in Table 8.2. The surface temperature in the heating cycle has a higher temperature than the bottom temperature, because the surface exposed to the high furnace temperature relative to the bottom. (See section 2.3.1 ad 2.3.1 for further discussion of cooling white and opaque glass by Jones and Basnett [1]) also discussed by Kruszewski [15].

Table 8.1 Summary of the above discussed of experimental cooling of white and green glass

Time (seconds)	0.0	5	10	20	30	40	50
White glass 5mm.temp (°C)	1050	970	875	750	660	580	510
White glass surf. temp (°C)	1050	920	820	690	600	520	455
Green glass 5mm.temp (°C)	1050	950	850	745	645	560	480
Green glass surf. temp (°C)	1050	890	780	660	570	495	445
W. surf-G. Surf Temp. diff (K)	0	30	40	30	30	25	10

Table 8.2 Summary of the above discussed of experimental heating of white and green glass

Time (seconds)	0.0	10	20	30	40	50
White glass 5mm.temp(°C)	510	680	835	945	1010	1050
White glass surf. temp (°C)	460	750	895	985	1035	1045
Green glass 5mm.temp (°C)	580	720	865	965	1025	1050
Green glass surf. temp (°C)	445	765	910	995	1045	1045
G. surf-W. surf Temp. diff (°C)	15	15	15	10	10	0

8.5 MODELLING DISCRETE ORDINATES (DO)

The modelling performed in this investigation concerns only the cooling of the two types of glass. A full description of the modelling process was made in Section 3.6. The modelling and material parameters used modelling with the DO formulation in this investigation are given in Tables 8.3, 8.4 and 8.5.

Table 8.3 Bands of wavelengths and absorption coefficients, as used by Jones and Basnett [1], for white glass Table 2.22

Bands	**Absorption coefficient (α)**	**Wavelength (μ)**
Band-1	23 m^{-1}	(0.8--2.25) μ
Band-2	45 m^{-1}	(2.25--2.75) μ
Band-3	100 m^{-1}	(2.75--4.3) μ

Table 8.4 Green glass absorption coefficient (α) 3 Bands by Henery and Hagy [23]

Bands	Absorption coefficient (α)	Wavelength (μ)
Band-1	200 m^{-1}	(0.8--2.25) μ
Band-2	100 m^{-1}	(2.25--2.75) μ
Band-3	300 m^{-1}	(2.75--4.3) μ

Table 8.5 Initial glass and air temperatures and the properties of glass and air is as used by Jones and Basnett [1], Rawson [11], McGraw [6], Table 2.22 in (radiation) case Table 2.24

Property	Units	Glass (fluid)	Air (fluid)
Density	Kg/m^3	2500	0.0242
C_p (Specific heat)	J/Kg K	1350	1000
Thermal conductivity	W/m K	1.45	1.225
Heat transfer coefficient	W/m^2 K	1500	10
Absorption coefficient white G.	m^{-1}	23, 45, 100	-
Absorption coefficient green G.	m^{-1}	200, 100, 300	-
Refractive index	-	0.5	-
Centre temperature	°C	1050	20
Thickness	mm	10	10
Time	Seconds	50	50

The modelling considers the cooling of the white and green glass from 1050 °C in air over a period of 50 seconds as in the experimental case. The only difference in the two models is in the definition of the absorption coefficient of the glass. The results obtained for the two types of glass are shown in Figures 8.8 and 8.9.

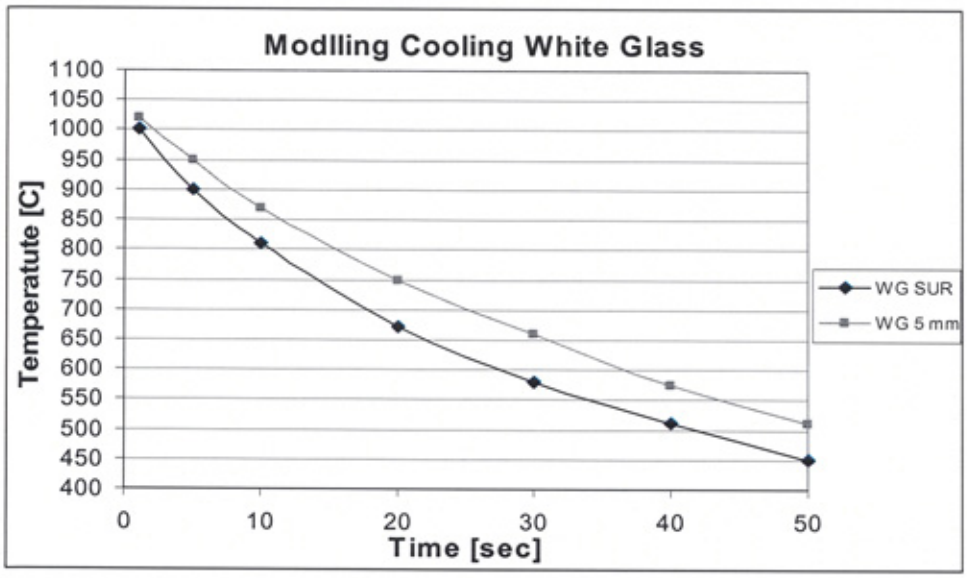

Figure 8.8 Modelling of cooling whit glass time of 50 seconds black line surface temperature, grey line 5 mm deep temperature

Figure 8.8 shows the modelling results obtained for the white glass. The surface and bottom temperatures of the glass are plotted over the 50-second time period as the glass cools. The surface temperature of the white glass decreases from 1050 to 450 °C, and the bottom from 1050 to 510 °C, the results are shown in table 8.6

Table 8.6 Modelling results cooling process white glass $\alpha = 23, 45, 100\ m^{-1}$

Time (seconds)	0.0	5	10	20	30	40	50
White glass 5mm. temp (°C)	1050	950	870	750	660	580	510
White glass surf. temp (°C)	1050	900	815	670	595	520	450

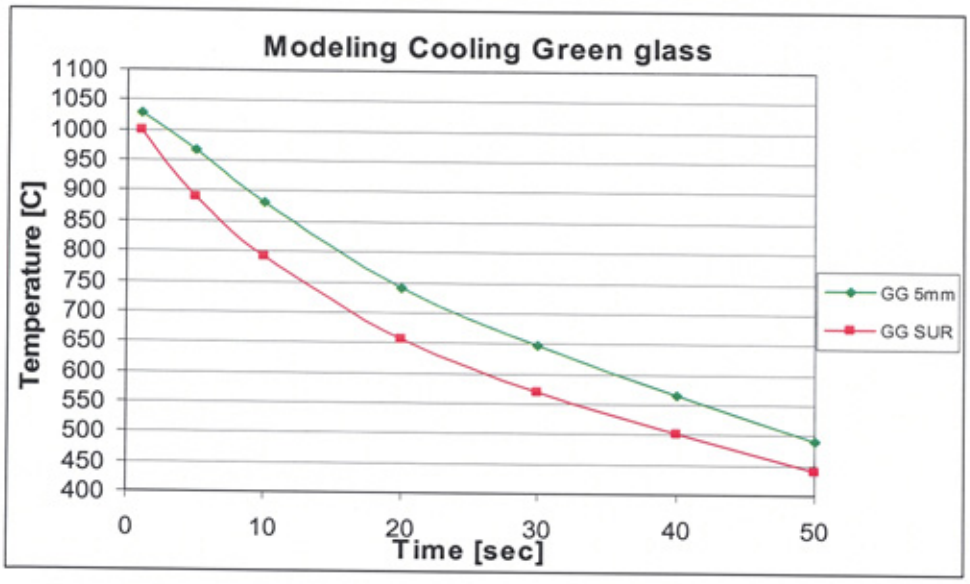

Figure 8.9 Modelling of cooling green glass time of 50 seconds red line surface temperature, green line 5 mm deep

Figure 8.9 shows the modelling results obtained for the green glass. The surface and bottom temperatures of the glass are plotted over the 50-second time period as the glass cools. The surface temperature of the white glass decreases from 1050 to 440 °C, and the bottom from 1050 to 480 °C, the results are shown in table 8.7

Table 8.7 Modelling results cooling process green glass $\alpha = 200, 100, 300\ m^{-1}$

Time (seconds)	0	5	10	20	30	40	50
Green glass 5mm. temp (°C)	1050	966	880	740	645	560	480
Green glass Surface temp. (°C)	1050	890	790	655	569	500	440

8.6 COMPARISON OF EXPERIMENTAL AND MODELLING RESULTS FOR THE COOLING OF WHITE AND GREEN GLASS

Tables 8.8 and 8.9 show comparisons of the results obtained from the experimental work and the modelling work for the white and green glasses respectively.

Table 8.8 Comparison of experimental and modelling results for 5 mm thick white Soda-lime glass cooled in air for 50 seconds

Time (seconds)	0.0	5	10	20	30	40	50
Experimental Sur. temp (°C)	1050	920	820	690	600	520	455
Experimental 5mm.temp (°C)	1050	970	875	750	660	580	510
Modelling sur. temp (°C)	1050	900	815	680	595	520	450
Modelling 5mm. temp (°C)	1050	950	870	750	660	580	510

Table 8.9 Comparison of experimental and modelling results for 5 mm thick green Soda-lime glass cooled in air for 50 seconds

Time (seconds)	0.0	5	10	20	30	40	50
Experimental Sur. temp (°C)	1050	890	780	660	570	495	445
Experimental 5mm.temp (°C)	1050	950	850	745	645	560	480
Modelling sur. temp (°C)	1050	890	790	655	569	500	440
Modelling 5mm. temp (°C)	1050	966	880	740	645	560	480

In comparing the results given in Tables 8.8 and 8.9, the temperatures recorded for the green glass show more rapid cooling than those for the white glass. This is due to the higher absorption coefficient value (See section 2.3.1 and 2.3.1 for further discussion of cooling white and opaque glass by Jones and Basnett [1]) also discussed by Kruszewski [15].

8.7 DISCUSSIONS

Figures 8.4 and 8.5 show the experimental results obtained for the cyclic of heating and cooling of samples of white and green glass both with the same dimensions 20x20 mm area and 5 mm height. Measurements of temperature were made at 1 second intervals over a 550 second time period at the surface and base of the glass. The glass starts at room temperature (20 °C) and is heated suddenly to a temperature of 1050 °C, as shown in Figure 8.2 The temperature increases rapidly from 20-1050°C over a period of ≈90 seconds. In the cooling period of ≈50 seconds the surface temperature drops from 1050 °C to 440 °C for green glass, and from 1050 °C to 460 °C for\white glass. It is seen that the green glass has a higher drop in the temperature than the white glass. This is because of its higher absorption coefficient value of $\alpha = 200, 100, 300\ m^{-1}$ compared to the white glass where $\alpha = 23, 45, 100\ m^{-1}$.

Figures 8.6 and 8.7 magnify a cycles of cooling and heating for both white and green glass respectively. The glass is cooled by removing it from the furnace to a room temperature of 20 °C. Over the first 10 seconds the surface temperature of green glass drops from 1050 °C to 780 °C, as shown in Table 8.1 and of the white glass from 1050-820 °C, as shown in Table 8.2. The surface temperature of the green glass cooled faster than the surface temperature of the white glass. As the time increases from 10 to 50 seconds, the surface temperature of the green glass decreases from 780 °C to 445 °C and of the white glass from 820 °C to 460°C. The green glass loses heat faster than the white glass over the time period when comparing both the surface and bottom temperatures. In a previous study by Rawson [27] (Chapter 2 Table 2.9), the surface

temperature falls to 940 °C from 1050 °C in a 3.0 second period. This work supports this figure, from Table 8.8 the temperature here falls to 920 °C in 5 seconds.

The seconds cycle represents the heating over 50 seconds. The surface temperature of the green glass heats faster than that of the white glass in the first 10 seconds. As shown in Table 8.2. As the time intervals increases from 10 to 50 seconds, the surface temperature of the green glass increases from 765 °C to 1045 °C and of the white glass from 750 °C to 1045 °C. Throughout the heating time the surface temperature of the green glass increases faster than that of the white glass. This follows for the bottom temperature, which also increases faster for the green glass as seen in Table 8.2.

The results obtained by the modelling show similar profiles to those obtained in the experimental work, this can be seen in Tables 8.8 and 8.9. In each case the modelling results show the glass losing heat faster than the experimental results. However as time increases the modelling results and experimental results become closer. This initial difference in results may be due to the time taken to remove the glass from the furnace to the ambient air temperature, which happens instantaneously in the software. The modelling results support the experimental results showing that the green glass loses heat faster than the white glass and hence gives substance to the conclusion that as the absorption coefficient increases then so does the ability of the glass to gain or lose heat energy.

8.8 SUMMARY

A summary of the findings made in this chapter is given below:

- As glass is heated and cooled the surface of the glass gains and loses heat energy faster than the bottom of the glass.
- During the initial stages of cooling, or heating, a large temperature difference develops between the surface and the bulk as heat is emitted or absorbed more rapidly than it is redistributed within the body of the glass.
- The absorption coefficient of the glass has a large influence on the ability of the glass to gain or lose heat energy. As the absorption coefficient of the glass increases so does its ability to gain or lose heat energy.
- DO modelling is able to predict the results obtained by experimental work and is able to offer support to the conclusions drawn from the experimental results.

CHAPTER NINE–CONCLUSION AND FURTHER WORK

9.1 CONCLUSIONS

The aim of this chapter is to amalgamate all of the important findings of this research work, detailing what has been gained as a result of the work and showing how the objectives initially identified have been addressed. A discussion of the direction in which this work can be taken forward and where the findings may be applied in other areas is also presented.

By modelling the work presented in previous literature, this work confirms that as the absorption coefficient of the glass increases then the rate at which the glass is able to gain or lose heat also increases. Two glasses with different absorption coefficients in the third wave band were modelled; these were white and opaque glass. White glass has an absorption coefficient of 110 m^{-1} and opaque glass an absorption coefficient of 300 m^{-1} in their third wave bands. In their first two wavebands the glasses have identical coefficients of 23 m^{-1} and 45 m^{-1} respectively. In the model the temperature change at the surface and centre of the glass was observed over a 5 second period as the glass cools in contact with the mould. Heat transfer was by conduction-radiation and for a 10 mm thick glass sample the centre temperatures fell by 30 K and 15 K for opaque and white glass respectively. This modelling work was presented in Chapters 2 and 5 and confirmed by experimental work in Chapter 8 which used white and green glass to provide different absorption coefficients. The study also showed that as glass thickness

reduces the significance of internal radiation increases. This is because the radiative effect is able to transfer heat from the centre of the glass to the surface more efficiently at high temperatures.

The investigation of the reheat process showed that after being removed from the mould, the glass surface undergoes a period of reheat. It was seen that after 2 seconds, the surface heated by 215 K when considering heat transfer by radiation only. If radiation together with conduction is considered the surface reheat after 2 seconds is 200 K, 15 K less than the radiation only case due to the differing temperature distributions.

Changes in the initial mould temperature have been confirmed to affect the rate of heat loss from the surface of the glass. As the mould temperature decreases more heat is removed from the glass at a higher rate. It was shown that for a contact time of 4 seconds a mould with initial temperature 42 °C reduces the surface temperature of a 10 mm glass sample at an initial temperature of 1050 °C by 430 K, however increasing the mould temperature to 545 °C the glass surface temperature drop is only 330 K; the maximum heat flux observed in each case was 2.5×10^6 W/m^2 and 1.3×10^6 W/m^2. This work was presented in section 2.6.1.

In Chapter 4, the ability of the RO, DTRM, P-1 and DO heat transfer formulations to predict the heat loss over 50 seconds from a 6 mm thick glass sample under radiative conditions was examined. The results were compared with experimental results obtained for a glass sample under the same conditions as used in the models. From the results it was clear that the RO and DTRM formulations were not able to accurately predict the heat transfer. The P-1 and DO models provide much better approximations of the heat transfer offering a far higher degree of accuracy. The DO formulation gives the best solution to the problem and subsequent modelling was performed using it. Viskanta and Song [31] and Cheong Moon and Song [30] reported similar results.

The refractive index has a significant influence on the rate at which heat is lost from the surface and centre of the glass during cooling regardless of the heat transfer mechanism. As the refractive index increases from 0.5 to 1.0 then the rate at which the glass loses heat increases. This result can be found in Chapter 5.

The heat transfer coefficient has a significant effect on the rate at which the surface temperature falls during cooling. The effect of increasing the heat transfer coefficient is greater at the surface of the glass than at the centre, though at both locations an increase in the loss is observed. The modelling results obtained were comparable to those presented in previous work; see Chapter 5.

Variation of the external emissivity in the model is seen to have little effect on the rate of cooling at the centre of the glass under heat transfer via conduction-radiation or radiation only. However, the rate of cooling at the surface is increased in the radiation only case as the external emissivity increases. By changing the external emissivity from

0.8 to 1.0 a 5% change in the surface temperature drop is observed. By using a value of 0.9 results obtained are comparable to those presented in previously published works; see Chapter 5.

Variation of the specific heat (Cp) in the modelling work is seen to have a significant effect on both the centre and surface temperatures in both cases of heat transfer (conduction-radiation and radiation only). As the specific heat increases then the drop in centre and the surface temperature observed decreases. The temperature dependent curve gives comparable results over a working range of temperatures 1000-1500 °C is presented in Chapter 5.

As the thermal conductivity increases more thermal energy transfers from the centre of the glass to the surface, this results in an increase in surface temperature drop in the case of conduction-radiation. The loss of heat from the centre is less in the radiation only case due to the relatively low heat transfer coefficient of the air in comparison to the mould/plunger.

When the glass melt is brought into contact with the mould tool, the initial rise in flux has been reported to be very rapid. At the centre of the glass, the temperature gradient decreases rapidly with distance. The glass loses heat more rapidly at the surface by conduction this rate increases slightly when internal radiation is considered. Similar results were presented by Jones and Basnett [1] in their modelling of the pressing process; see Chapter 6.

As the initial mould temperature decreases then the initial flux is observed to increase, this links to the previous conclusion regarding the increased heat loss from the surface due to the decreased initial mould temperature. The heat flux decreases as the contact time increases and the difference between the flux observed for each initial mould temperature becomes less prominent. This is compatible with the results were observed by Roger Kent [4] and Fellows and Shaw. [1].

The maximum flux obtained from the modelling work was 5 times greater in the case of conduction-radiation than in the case of radiation only. Even though the air temperature is less than that of the mould and so has a greater thermal gradient, because the air has a much lower effective conductivity the flux is lower.

The rate of change of stress of the glass as it is cooled over a 50 second period was shown in Figure 6.12. The figure shows that the glass enters the softening/stiffening region at a temperature of 750 °C and takes only 10 seconds to cool from here passed the 500 °C point into the solid region, the rate of stiffening during this time period is very high.

Glass thickness has been shown to have a significant influence on the rate of heating of the centre of the glass. As the thickness increases then so does the time for the central temperature to reach that of the surface. As a glass sample is heated to a constant temperature the surface of the glass heats faster than the centre until the glass begins to radiate, at this point the centre temperature heats faster until it reaches the same

temperature as the glass surface, the time taken for this to occur increases with glass thickness.

In the cooling experiments as in the heating experiments the thickness of the glass has a large influence on the rate of cooling, as the thickness of the glass decreases the rate of cooling increases, and most of the heat lose from the glass occurs at the first 10 sec. Again, the surface loses heat faster than the centre initially and then as the heat radiated from the centre to the surface of the glass increases the centre temperature approaches that of the surface. These results can be seen in Chapters 2 and 7. The effect of the glass thickness on the heat transfer radiation is that as the thickness of the glass reduces then the significance of radiation increases and more heat energy is lost.

Experimental work on the cycling of heating and cooling while observing the temperature profile of the glass at different depths showed that the temperature gradient though the glass, from the surface to the centre, increases positively with heating and negatively with cooling. The average times taken for the heating (from 500 °C to 1100 °C) and cooling (from 1100 °C to 500 °C) parts of the cycle both are 50 seconds. The results obtained by modelling for the cooling of glass over a 50 second period followed the same general trend as those achieved in the experimental work and the difference between the two decreases as time increases. At 35 seconds the modelled and experimental results show a negligible difference in temperature at the surface, however the differences between results from different depths into the glass are greater. See Chapter 7

Figures 8.6 and 8.7 show the cooling and heating of samples of white and green glass respectively. The green glass has a higher absorption coefficient and so as shown in work of Chapter 2, the surface temperature of the green glass cooled and heated faster than that of the white glass. The modelling work of this experiment predicted lower absolute temperature results than obtained experimentally however the relative differences between the white and green glass were the same. As time increases the temperature difference between the experimental results and modelled results becomes smaller, until at 20 seconds the difference is negligible at the surface. However, as depth increases the temperature difference between the two also increases.

The work presented in this thesis has been aimed at clarifying some of the underlying issues regarding the effects of glass thermal and mechanical properties during the pressing and reheat stages of manufacture. Modelling and experimental work has been used to confirm the theory and provide some examination of working ranges for glass properties, which has culminated in the production of a detailed insight of the effects of property variation.

9.2 FURTHER WORK

So far this work has developed an understanding of the nature of heat transfer within and at the surface layer of a hot glass body.

From the understanding obtained of the use of modelling tools it is suggested that topics for future study should include:

- An investigation of the distribution of temperature within glass layers during dynamic contact with mould tooling as occurs in commercial forming processes.
- This would be further extended to consider the nature of the deformation due to gravity during the reheat stage of the process.
- To develop this understanding to include the modification to the chemical composition of surface layers due to tool contact and the resultant change in the temperature/viscosity relationship.
- Further investigation of the heat transfer through other glass colours including chemical and colloidal colours. This will involve further examination of the response of the models to more complex absorption spectra and also a body with a dispersed second phase absorbing, re-emitting and scattering component.
- Further experimental work should consider the nature of the interface between the tools and the glass to investigate the magnitude of the contact time (loss of surface contact) presumed in the literature to take place during pressing.
- In the longer term this enhanced knowledge may be developed into software tool for commercial glassware productions.

10-REFERENCES

[1] S.P Jones and P. Basnett: "A theoretical investigation of heat transfer processes in the glass forming" *Journal of the Glass Tech. Jun.* 18(1969)

[2] D. A. McGraw: *J. Amer. Ceramic. Soc.* 44, 353 (1961)

[3] C. J. Fellows, and F. Shaw: "A laboratory investigation of glass to mould heat transfer during pressing" *Glass Technology* 19 1 pp 4-9 (1978)

[4] R. Kent: "Mould temperature and heat flux measurements and the control of heat transfer during the production of glass containers" *IEEE Transactions on Industry* app. vol.12, No.4, July/august (1976)

[5] R. Gardon: "The emissivity of transparent materials", *J. Am. Soc.*39 no. 8, P.278-287 (1956)

[6] D.A. McGraw: "Transfer of heat in Glass during Forming," ibid.44 7 353-363 (1961)

[7] W. Trier: "Temperature Distribution and heat flow in Glass in blank Moulds of container Machines" *Journal of American Ceramic Society* Vol. 44, no.7. July, PP. 339-345 (1961)

[8] R. Gardon: *International Congress of Glass*, PP. 85-95 (1968).
Society of Glass Technology, Sheffield England (1969)

[9] S. P. Jones: *British Glass Industry Research Association*, res. Rep. No. 33, (1968)

[10] W. Trier: "Temperature measurement in glass Moulds" *Glastech. Ber.* 28 9(1952)

[11] H. Rawson: "Radiative heat transfer in glass manufacture-one –and two-dimensional problems" *Glasstech. Ber.*66 No.4 (1993)

[12] R. Gardon: "A review of radiant heat transfer in glass" *Journal of American Ceramic Soc.* Vol.44 no. 7July (1961)

[13] C.L. Babcock. and McGraw D.A: pp.164-76 *in proceeding of IV th Inernational Glass Congress*. Imprimerie Chaix. Paris, (1957)

[14] T.K.G. Howse, R. Kent, H. Rawson: "The determination of glass-mould heat fluxes from mould temperature measurements" *Glass Technology* 12 4 pp84-93 (1971)

[15] S. Kruszewski: "Total heat-transmission coefficient of amber and green glass in temperatures of melting range" *Journal of American Ceramic Society* vol. 44, no.7 (1961)

[16] R. L. Curran and Ihab H. Farag: "Modelling radiation pyrometery of glass during container forming process" *Glastech Ber* 61 No.12 (1988)

[18] T. J. Naughton and D.A. McGraw: in *Advances in Glass Technology* Pp. 603-18 Part 1, Compiled by *The American Ceramic Soc.* Plenum Press, New York, (1962)

[19] G. S. Fulcher: *Journal. Am. Ceram. Soc.*, 8: 339 (1925)

[20] T. Lakatos, L. G. Johansson and B simmingskold: "The effect of some glass components on the viscosity of glass" 27: 2 (1972)

[21] H. R. Lillie: P*roc. 3d Intern. Congr. Glass, Rome* p.318, pub (1954)

[22], F. Geotti, and L. De Riu: "Study of the high temperature Spectral behaviour of container glass" *Glastech Ber Glass Sc.Tech* 70 No.6 (1997)

[23] E. Hagy, Willis H. Barney, John S. McCartny, Charles J.Parker and William A. Plummer: "The hand book of glass manufacture" Vol.II 3rd ed. *Ashlee Publishing New Yourk* 1984

[24] S. P. Jones: *Appl. Phys.* 40, 2418 pp. 195-96 in Ref.5 (1969)

[25] D. E. Sharp and L. B. Ginther: *Journal. Am. Ceram. Soc.* 34: 260 (1951)

[26] R. B. Sosman.: "The Properties of Silica," *ASC, Chemical Catalog Company, Inc.*, Mon. 37 New York, (1927).

[27] C. W. Parmelee and A. E. Badger: *Univ. Ill. Eng. Expt. Sta. Bull.* 271, (1934)

[28] C Kittle ; Phys. Rev., 75: 972 (1949)

[29] H. Wakatsuki, Motoichi Iga and Isao Satoh:" Numerical simulation of deformation and residual stress for press-formed glass*" Extended Abstracts, Edinburgh, Scotland,* Volume 2,1-6 July (2001)

[30] K. B. Cheong, K. M. Moon and T.H. Song: "Treatment of radiative transfer in glass melts: validity of Rosseland and P-1 approximation" *Physics and Chem. of Glasses* Vol. 40 No. 1 Feb. (1999)

[31] R. Viskanta and T.H Song on: "The diffusion approximation for radiation transfer in glass" *Glastech Ber* 58 (4), 80-6 (1985)

[32] F. J Grove; Jellyman, P. E.: The infrared transmission of glass in the range room temperature to 1400 °C. *J. Soc. Glass Tech*, 39 (1955) p. T3-TI5

[33] H Franz.: "Infrared absorption of molten soda-lime-silica glasses containing transition metal oxides". *International Congress on Glass Versailles* Paris: lnst Verre, Vol. 1 p. 243-260 (1971)

[34] J. Endrys, A. Blazek and Ederova: "Experimental determination of the effective thermal conductivity of glass by steady state method" *J. Glastech Ber.* 66 No 6/7GI (1993)

[35] H Scholze : Der Einbau des Wassers in Gliisern. T. 1. Der Einflu B desim: *Glas Gelbsten Wassers* auf das Ultrarot Spektrum und die quantitative no. 3, p. 81-88; no. 4, p. 142-152; no. 8, p. 314-320. (1959)

[36] F. Deidewig and Geoff Parkinson: "Transient temperature behaviour in blank and blow moulds during normal container production on IS-machines" (2002)

[37] I Deidewig, Frank Pro.: "How to effect the temperature distribution in blank and blow moulds-Comparison between FEM calculations measurement results" *Int. Congress Glass* Vol. 2 Edinburgh, Scotland, 1-6 July (2001)

[38] F. Lentes N. Siedow: "Three-Dimensional Radiative heat transfer in glass cooling Process". *Berichte, Kaiserslautern*, Nr.4, ITWM (1998)

[39] R. Bauer G. Peters, H. Muysenger, and F. Simons: "Advanced Control of Glass Tanks by use of simulation models" *Proc Forth Int. Conf.* "Advance in Fusion, and processing of glass". Wuzburg P. 31-8 (1995)

[40] H.P. Liu and J.R.Howell: Scale modelling of radiation in enclosures with absorbing / emitting and isotrpically media *J. Heat transfer*, Vol. 109, no. 2,pp. 470-477(1987)

[41] U. Fortheringham and F.Thomas: "Active thermal conductivity of hot glass" *Glastech Ber Glass Sc.Tech.* 67 No.12 (1994)

[42] R. Viskanta: "Review of three-dimensional mathematical modelling of glass melting". *J. Non-Crystal. Solids*, pp. 177, 347-62 (1994)

[43] M. G. Carvalho, and M. Nogueira: "Modelling of glass melting industrial progress" *J. De Physique* IV, 3, 1357-66 (1993)

[44] I. H. Farag and R. L. Curran: "Application of Radiation pyrometry of glass plates non-uniform temperature distribution", *Glastech. Ber.* 56K. Bd. 1 P.319-324 (1983)

[45] M. Sikri and Simmons: "Simplified mathematical model simulating heat transfer in glass-forming moulds" *Journal of American Ceramic Soc.* Vol.57 No.8 Aug. (1974)

[46] R. Kent: "Mould temperature and heat flux measurements and control of heat transfer during the production of glass containers" *IEEE Transactions on Industry Applications* Vol. IA-12 4 pp.432-439 (1967)
[47] S. Chandrasekhar: "Radiative Transfer". *Dover Publications*, Inc. Toronto, (1960)

[48] J. Beattie, E. Coen.: "Spectral emission radiation by glass" Br. J. *Apple Phys* 11 no. 4, p. 151-157 (1960)

[49] H. Charnock, F. J. Grove and J.R. Beattie: "Determination of spectral transmission of glass in the temperature 20-1400 °C, *Am. Ceramic Soc.* Philadelphia PA, (USA) (1960)

[50] H. H. Holscher, J.C. Coleman and C.C. Cookein: V th *International Glass Congress*, Muenchen, pp.11/1-17 1959 *Glastech Ber.* 32K, (1959)

[51] C. Guillermo, Lopez A. and Loredo J.: "Temperature measurements on mould cavity" *Personal Communication* January (2002)

[52] V. A Khonik., Ohta M. and Kitagawa K.: "Heating rate depends of the shear viscosity of a finite glass alloy" *Scripta Materialia* 45 1393-1400 (2001)

[53] M. Hyre and Yves Rubin : "Modelling the glass container forming process" *Proc. Iint. Cong Glass*. Volume 2 Extended Abstracts, Edinburgh, Scotland, 1-6 July (2001)

[54] P. Moreau, C. Marechal and D. Lochegnies: "Optimum parison shape for glass blowing" *Proc. Int. Congers Glass*, volume 2 extended abstracts, Edinburgh, Scotland, 1-6 July (2001)

[55] F. Deidewig: "How to effect the temperature distribution in blank and blow moulds-comparison between FEM calculations and measurement results *Proc. Int. Congers Glass,* Volume 2 extended abstracts, Edinburgh, Scotland, 1-6 July (2001)

[65] M. Mori, Hirrosh Wakatsuki and Motoichi Iga: "Numerical simulation of glass flow during pressing" *Int. Congress of Glass* Vol. 2 Scotland, 1-6 July (2001)

[75] G. Keijts, K. van der Werff: "Heat transfer in glass container production during the final blow" *Glass Technology*, 42 (3), 104-8 (2001)

[58] B.J. Van Der Linden, K. Laevsky, R. M. Mattheij: "Radiative heat transfer in a press-and-blow forming process" *Glass in the New Millennium* Amsterdam ICG June (2000)

[59] R. Siegel :"Transient effect of radiative transfer in semitransparent materials" *International Journal of Engineering Science* 36 pp.1701-1739 (1998)

[60] J. F. Clouet: "The Rosseland approximation for radiative transfer problems in heterogeneous media". *J. Quant. Spectrosc. Radiate. Transfer* Vol. 58 No, 1. Pp. 33-43, (1997)

[61] R. Penlington, M. Sawar and A.W. Armitage: "A Review of narrow neck press and tool technology" University of Northumbria at Newcastle *Fundamentals of Glass Science and Technology* (1997)

[62] R. Viskanta: "Heat transfer by conduction and radiation in absorbing and scattering materials" *J. heat transfer*, Vol. 87, no. 1, pp. 143-150, (1965)

[63] B. O. Ugustsson: "Changes in glass surface structure from plunger contact" *Glasteknisk Ttidskrift*, Sweden No. 3 Vol. 51, (1996)

[64] D. Lochegnies, C. Thibaud and J. Oudin: "Centrifugal casting of glass plates: a finite-element analysis of process parameter influence" *Glastech Ber Glass Sc. tech.* 68 No.1 (1995)

[65] D. Loyd and M. Froier: "Heat transfer analysis of structures containing phase-change material" C*ommunications in Applied Numerical Methods*, Vol. 4 607-615 (1988)

[66] S. Rattana, Th. Lornage, J.M. Bergheau, and A. Miton: "Numerical simulation of glass forming process" *BSN Emballage, Centre de Research,* Givors France (1985)
[67] S. K. Pchelyakov and Yu A. Guloan: "Heat transfer at the glass-mould interface" *State Scientific-Research Institute of Glass* No. 9, pp. 14-15, September, (1985)

[68] D.M. Shetterly, N.T. Huff: "Glass to metal heat flow during glass container forming". *Journal of non- Crystalline Solids* 38 and pp.873-878 (1980)

[69] D.M. Shetterly, N.T. Huff, and L.C Hibbits: "Mould surface temperature during glass container forming *Journal of non-crystalline Solids* 38 and 39 pp.867-872 (1980)

[70] T. Capurso and J. Petopoulos: "Heat transfer through glass and mould during the glass forming process" *Glass International* Sep. (1979)

[71] J. Manthuruthil, T. R. Sikri and G.A. Simmons: "Simplified mathematical model Simulating heat transfer in glass forming models" *Journal of American Ceramic Soc.* Vol.57 no.8 March 21, (1974)

[72] M. Kunugi and Hisayoshi Murakami: "Temperature distribution and heat transfer in container glass during forming operations" *Kyoto-University, Japan* Vol. Xxxii Pt. 4 Oct (1971)

[73] R. C. Steere: "Glass surface reheat in press-ware forming" *Journal of Applied Physics* 40 p3884 3885 (1969)

[74] R. Van Laethem, L. Leger, M. Boffe, and E. Plumat: "Temperature measurement of the glass by radiation analysis" *Journal of American Ceramic Soc.* Vol.44 No.7 July (1961)

[75] H. Charnock: "Experimental and theoretical radiation conductivity predicted by steady state theory" *Journal of American Ceramic Soc.* Vol.44 No.7July (1961)

[76] W. D. Kingery: "Heat-Conductivity Process in glass "*Journal of American Ceramic Soc.* Vol.44 no.8 July (1961)

[77] F. J. Grove. "Spectral transmission of glass at high temperatures and its Application to heat transfer" *Journal of American Ceramic Soc.* Vol.44 no.7July (1961)

[78] W. Giegerich: "Relations between heat loss of glass, forming times and bottle production in blowing machines" *Journal of American Ceramic society* Vol. 44, no. 7 July (1961)

[79] J. Boow and W.E.S. Turner: "The viscosity and working properties of glass rate of cooling and setting of colourless and coloured glass" *Journal of the Society of Glass Tech.* 27 1 pp94-112 (1943)

[80] R viskanta.: "Radiation transfer and interaction of convection with radiation heat transfer" *Advances in heat transfer* Vol. 3, pp. 175-251, (1966)

[81 B. S. Kellett: *Journal. Soc. Glass Tech.* 37: 268 (1953)

[82] H. R Lillie: *Journal. Am. Ceramic. Soc.*, 16: 619 (1933)

[83] R.Viskanta: "Heat transfer in glass. In: Heat Transfer", *Denver 1985. Symp. Ser.* 81 no. 245, p. 63-69 (1985)

[84] J. Boow :"The viscosity and working characteristics of glass rate of cooling and viscosity of glass during manipulation by automatic machine" *Journal of Glass Tech.* Vol. Xxix No. 134 Aug. (1945)

[85] J. Boow and W.E.S. Turner: "The viscosity and working properties of glass part and setting of Colourless and coloured glasses" *Journal of the Glass Tech.* Jun.18 (1941)

[86] R.Gardon: *American, Ceramic. Soc.* 41, 200

[87] W. Geffcken: "The transmission of heat in glass at high temperature" *Deutsche Glastechnische, Gesellschaft.* IV

[88] U. Fotheringham: "The active thermal conductivity of hot glass: Verification of the concept"

[89] Measurements computing catalogue "TC ltd. Temperature sensing, measurement and control" new copy (2003)

11-APPENDIX (A) MODELS

A.1- INTRODUCTION TO RADIATIVE HEAT TRANSFER

FLUENT provides five radiation models, which allow radiative heat transfer to be considered with or without a participating medium:

Discrete transfer radiation model (DTRM) P-1 radiation model, Rosseland radiation model, discrete ordinates (DO) radiation model

Heating or cooling of surfaces due to radiation and/or heat sources or sinks due to radiation within the fluid phase can also be included in the models.

A.1.1 Radiative Transfer Equation

The radiative transfer equation (RTE) for an absorbing, emitting, and scattering medium at position $\vec{r}$ in the direction $\vec{s}$ is

$$\frac{dI(\vec{r},\vec{s})}{ds} + (a+\sigma_s)I(\vec{r},\vec{s}) = an^2\frac{\sigma T^4}{\pi} + \frac{\sigma_s}{4\pi}\int_0^{4\pi} I(\vec{r},\vec{s}\,')\,\Phi(\vec{s}\cdot\vec{s}\,')\,d\Omega' \quad \text{(A-1)}$$

Where

$\vec{r}$	Position vector
$\vec{s}$	Direction vector
$\vec{s}'$	Scattering direction vector
s	Path length
a	Absorption coefficient
n	Refractive index
σ_s	Scattering coefficient
σ	Stefan-Boltzmann constant ($5.672 * 10^{-8}$ W/m^2-K^4)
I	Radiation intensity, which depends on(r) position And direction (**s**)
T	Local temperature
Φ	Phase function
Ω'	Solid angle

The refractive index n is important when is considering radiation in semi-transparent media. Figure A-1 illustrates the process of radiative heat transfer.

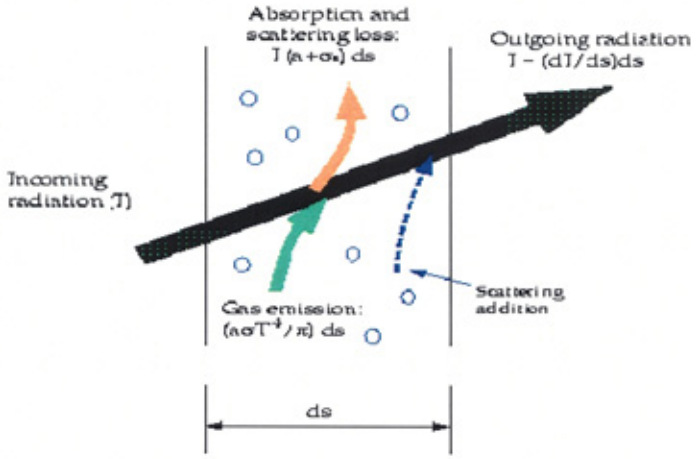

Figure A-1: Radiative heat transfer

A.1.2 - Applications of Radiative Heat Transfer

Typical applications well suited for simulation using radiative heat transfer include the following:

- Surface-to-surface radiant heating or cooling
- Coupled radiation, convection, and/or conduction heat transfer
- Radiation through windows in HVAC applications, and cabin heat transfer analysis in automotive applications
- Radiation in glass processing, glass fibre drawing, and ceramic processing

Radiative heat transfer should be included in your simulation when the radiant heat flux, $Q_{rad} = \sigma(T_{max}^4 - T_{min}^4)$, is large compared to the heat transfer rate due to convection or conduction. Typically this will occur at high temperatures where the fourth-order dependence of the radiative heat flux on temperature implies that radiation will dominate.

APPENDEX (B) PROPERTIES

B.1 VISCOSITY

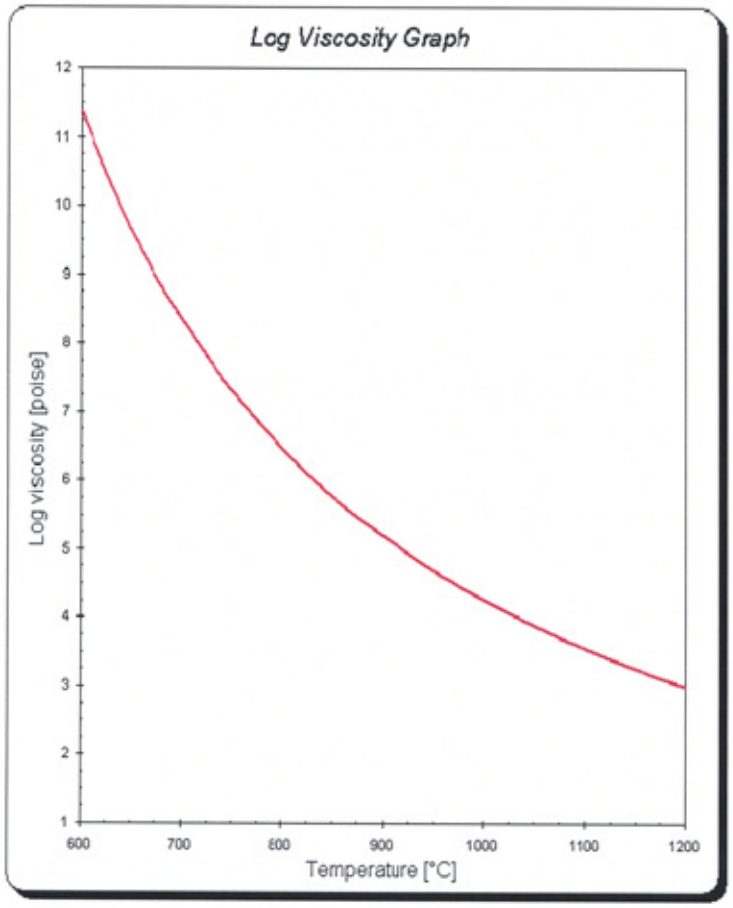

Figure B-1

B.2 DENSITY

The density of glass is dependent upon its thermal history. If studies are made by quenching a glass from a temperature at which it was in equilibrium a density characteristic of such a temperature will be found. This temperature has been termed the "fictive temperature". Glasses cooled a various rates from well above the annealing

point will differ in density with the more rapidly cooled glasses having a higher "Fictive temperature" and a lower density

B.3 HEAT CAPACITY AND SPECIFIC HEAT

No.	SiO_2	B_2O_3	Na_2O	K_2O	CaO	MgO	PbO	Al_2O_3	Fe_2O_3	Mean Specific Heat 40–[illegible]°C	40–[illegible]°C
1	74.3	...	16.7	0.04	4.7	3.2	...	0.33	0.07	0.260	0.292
2	71.9	...	17.6		5.0	3.6	...	1.21	0.07	0.266	0.290
3	73.3	...	15.3		5.3	3.9	...	0.48		0.260	0.285
4	75.0	...	15.8		4.8	3.3	...	1.13		0.265	0.289
5	71.8	...	14.3	...	12.9	0.1	...	0.54	0.12	0.274	0.289
6	74.8	...	16.5		2.6	1.8	...	4.36		0.279	0.291
7	61.9	...	8.3	6.2	tr.	tr.	22.2	1.00	0.15	0.211	0.224
8	80.6	12.6	4.2	0.15	...	tr.	...	1.92	0.08	0.271	0.287
9	67.5	...	8.8	3.3	10.6	...	0.1	6.01	0.08	...	0.289

Table B3-1

B4 ELASTIC PROPERTIES

Elastic Constants for Glasses and Glass-Ceramics

Code	Type	E psi x 10^{-6}	G psi x 10^{-6}	μ
7940	Fused Silica	10.4	4.5	0.16
7900	96% Silica	10.0	4.2	0.19
7740	Borosilicate, Low Exp.	9.1	3.8	0.20
7070	Borosilicate, Low Loss	7.4	3.0	0.22
1723	Aluminosilicate	12.5	5.1	0.24
0080	Soda-lime	10.2	4.2	0.22
9606	Glass-Ceramic	17.2	6.9	0.25
9608	Glass-Ceramic	12.5	5.0	0.25

Courtesy Corning Glass Works

Table B4-1

Figure B4-1. Shows the effect of temperature on measured strength for several glasses the initial reduction in strength with increasing temperature is characteristic of most glasses but some glasses with higher silica content showed a continual increase in strength above room temperature. These glasses also show an increasing modulus with

temperature as indicated in Figure B4-1. Phillips in an interesting review article emphasized the relationship between Young's Modulus and observed practical strength but pointed out that this could result from the effects of flaw producing mechanisms as well as an inherent strength. Shand found the correlation somewhat vague though the glass with high lead content was indeed weakest and the alumino-silicate glass strongest. For practical engineering purposes all other glasses must be consider equal in strength.

In annealed glass the discussion above is due to the significant effect of residual stress present in surface layers as a contribution to the resultant tensile stress value. Extreme high strength can be attained through conduction of defect severity by forming conditions, surface layer removal or modification HF etch procedures. The ineffective practical procedure used to improve the capability of glass to withstand load produced tensile stress is to deliberately introduce a controlled surface compressing. This pre-stress can be introduced by their tempering, chemical treatment or by the use of fused surface layers having a lower coefficient of expansion. While glass articles treated in this way fail at approximately the same tensile stress, such tensions do not develop until the initial compression has been exceeded by the externally created stress. The effect on measured strength is apparent in Figure B5-1. Surface compressed glasses also show more resistance to flaw production by abrasion and exhibit a much reduced relative static fatigue effect.

Another recent approach to increasing the usable strength has been through the introduction of glass-ceramics (ceramics crystallized from glass). While the maximum attainable strength is lower than that observed for conventional glass, abraded strength values are higher. This seems to be related to the flaw production and growth

mechanisms. Commercial materials generally show short term strength values of 10,000 to 25,000 pounds per square inch.

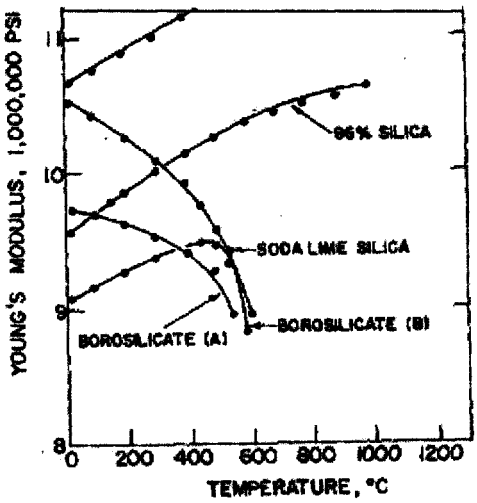

Figure B4-1.

B.5 THERMAL CONDUCTIVITY

The thermal conductivity of' a glass is the rate of heat flow per unit area under the existence of a temperature gradient in the glass. The recommended SI Units are Watts/cm K and the imperial unit is Btu, conversion factors are given in Table B5-1. It is notable that in the English system the temperature gradient can be expressed as °F/ft or °F/in. A related property the thermal diffusivity is of importance under transient or non steady state conditions. It is simply the ratio of the thermal conductivity to the volume specific heat K C_v and is expressed in cm^2/sec. For most glasses it is somewhat greater than twice the magnitude of the thermal conductivity.

Conversion Factors for Thermal Conductivity

	$\frac{W}{cm\ K}$	$\frac{cal\ cm}{cm^2 s\ deg\ C}$	$\frac{Btu\ ft}{ft^2\ h\ deg\ F}$	$\frac{Btu\ in}{ft^2\ h\ deg\ F}$
$1\ \frac{W}{cm\ K}$	1	0.2388	57.78	693.3
$1\ \frac{cal\ cm}{cm^2 s\ deg\ C}$	4.1868	1	241.9	2903
$1\ \frac{Btu\ ft}{ft^2 h\ deg\ F}$	1.731×10^{-2}	4.134×10^{-3}	1	12
$1\ \frac{Btu\ in}{ft^2 h\ deg\ F}$	1.442×10^{-3}	3.445×10^{-4}	8.333×10^{-2}	1

Table B5-1

It is not realistic to take the measured thermal conductivity and use it to calculate temperature distributions for larger specimens and different conditions. In diathermies materials such as glass, two mechanisms of radiant transfer are involved. One is direct radiant exchange through the entire thickness which can easily be predicted from knowledge of the absorption coefficients of the glass. The other involves emission and reabsorption of radiation within the material which can be termed "internal Radiative transfer." This is more difficult to compute. It is the combination of these two Radiative mechanisms superposed on the conduction that describes the "apparent thermal conductivity." For thin specimens only the direct radiation and true conduction are important. In glass tanks and large cast discs such as for telescope mirrors, internal Radiative transfer dominates the heat transfer. Rather than rely on experimental measurements to determine the relative importance, it is easier to compute the rates of heat flow from the temperature, specimen size and optical constants of the glass.

APPENDEX (C) LITRITURE

C-1 [1] Jones and P. Basnett "A theoretical investigation of heat transfer processes in the glass forming" *Journal of the Glass Tech. Jun.* 18(1969)

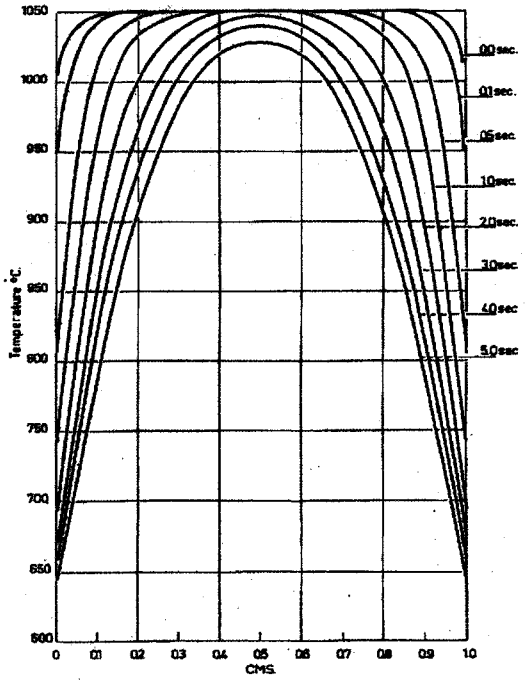

Figure (C-1) Temperature distribution in pressing at various times surface and centre (White glass)

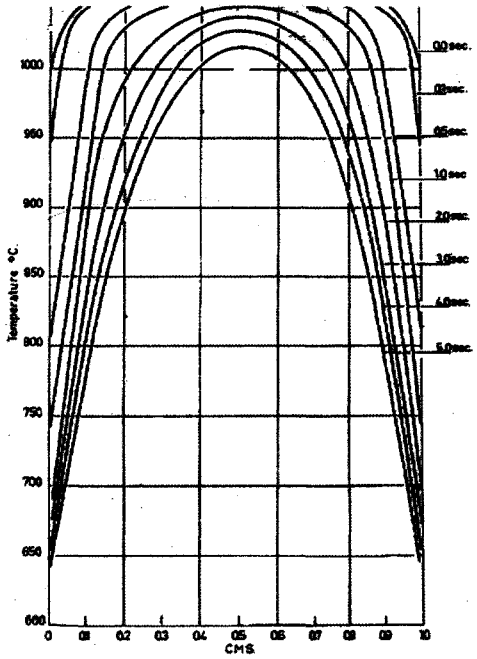

Figure (C-2) Temperature distribution in pressing at various times surface and centre (Opaque glass)

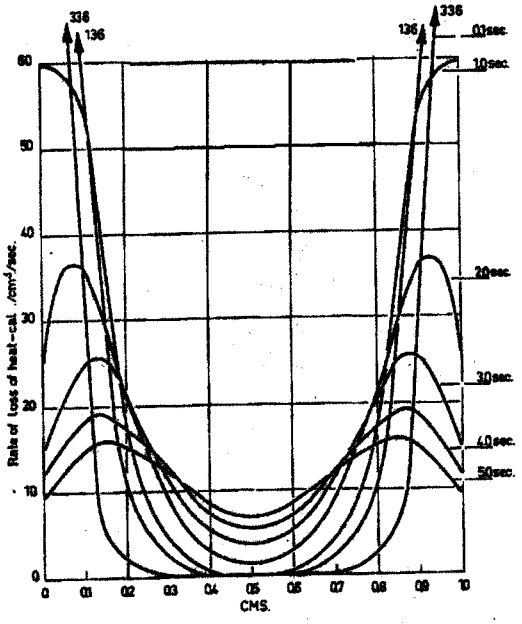

Figure (C-4) Temperature distribution in pressing at various times, surface conduction

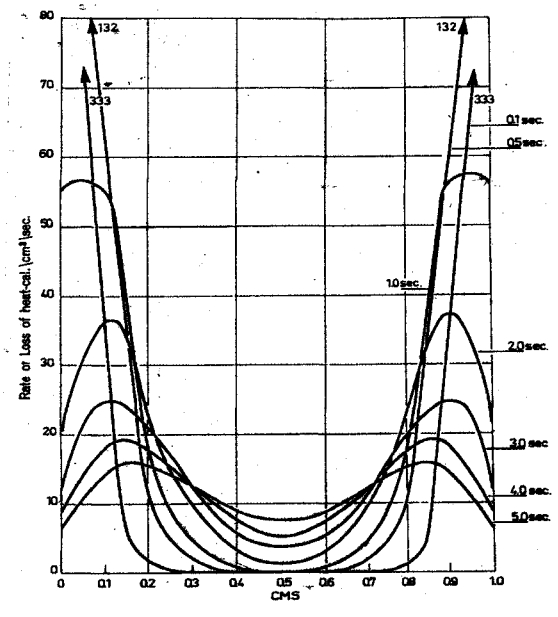

Figure (C-3) Temperature distribution in pressing at various times surface conduction and radiation

C-2 [11] H. Rawson "Radiative heat transfer in glass manufacture-one-and two-dimensional problems" *Glasstech Ber.*66 No.4 (1993)

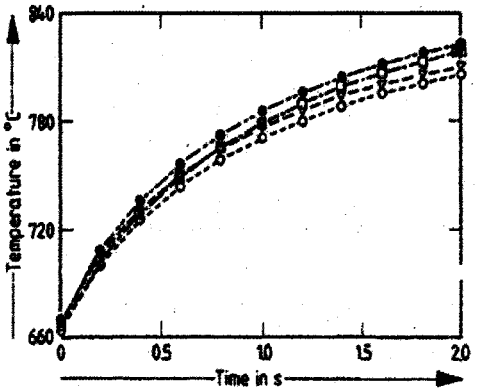

Figur C-5 urface reheat of two glasses during the first 2 s after release from the mould. □: float glass, condition "L"; ○: float glass, condition "H"; ▽: amber glass, condition "L"; ●: amber glass, condition "H".

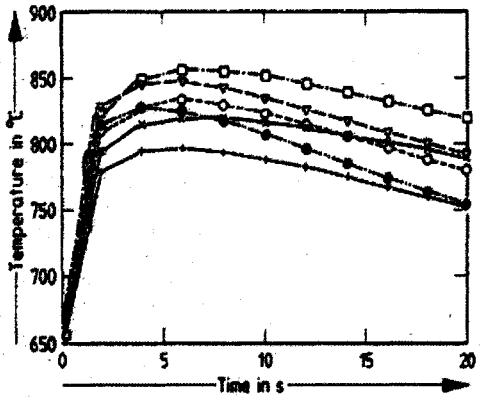

Fig.C-6. Surface reheat of two glasses during the first 20 s after release from the mould. □: float glass, condition "L"; ○: float glass, condition "H"; ▽: amber glass, condition "L"; ●: amber glass, condition "H"; ×: opaque glass, condition "L"; +: opaque glass, condition "H".

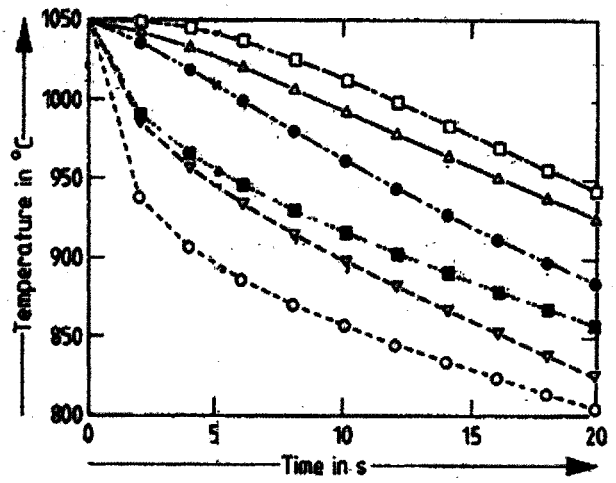

Fig.C-7 **Cooling curves at the centre and surface of 10 mm thick slabs of three different types of glass. ●: float glass, centre; ■: float glass, surface; △: amber glass, centre; ▽: amber glass, surface; □: opaque glass, centre; ○: opaque glass, surface.**

C-3 [3] C. J. Fellows, and F. Shaw "A laboratory investigation of glass to mould heat transfer during pressing" *Glass Technology* 19 1 pp 4-9 (1978)

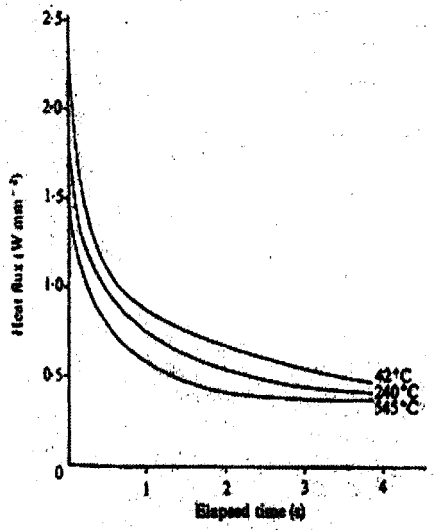

Fig.C-10 *Effect of initial mould temperature on heat flux*

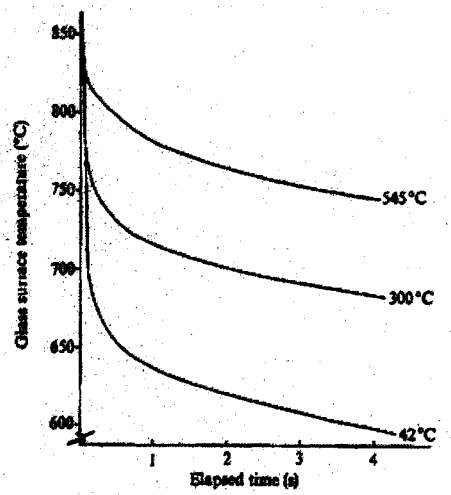

Fig.C-9 *Effect of initial mould temperature on glass surface temperature*

C-4 [4] R. Kent "Mould temperature and heat flux measurements and the control of heat transfer during the production of glass containers" *IEEE transactions on industry* app. vol.12, No.4, July/august (1976)

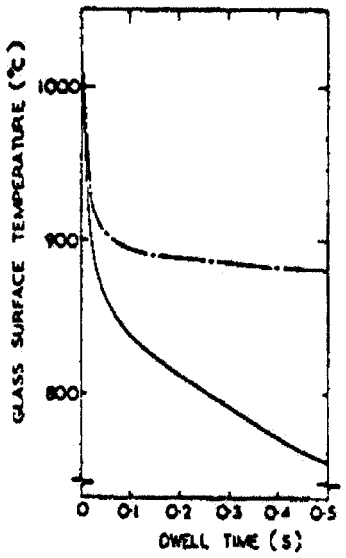

figure C-12 Variation of glass surface temperature with time calculated from heat flux variations given in Fig. 5. Solid line is when initial surface temperature of plunger was 490°C. Dashes are when initial surface temperature of plunger was 560°C.

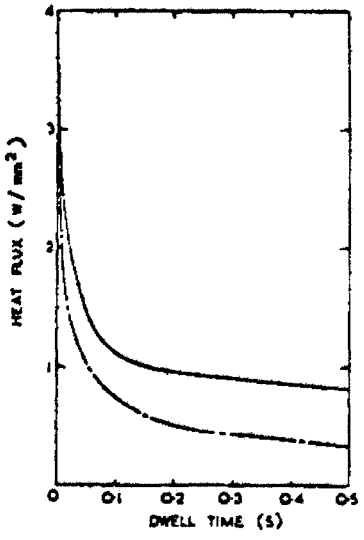

figureC-1 Variation of heat flux with time into plunger of automatic press. Initial surface temperature of glass was 1015°C. Solid line is when initial surface temperature of plunger was 490°C, and velocity of plunger at glass-plunger contact was 231 mm/s. Dashes are when initial surface temperature of plunger was 560°C, and velocity of plunger at glass-plunger contact was 198 mm/s.

The heat from a glass melt during container production is extracted by the cooler mould via a mixture of conduction (which is the predominant mode below 200°C) and radiation (which becomes increasingly predominant above 200°C) W. Giegerich [78]. Heat flow between the glass melt and the metal mould during the formation of containers is therefore complicated.

However, it is also well known that container glass has a relatively low effective thermal conductivity i.e. when compared to a metal such as the mould, Jones [1]. The surface of the glass therefore will be rapidly cooled by the mould surface (i.e. faster than heat can be transferred from the bulk of the glass to reheat the surface). This phenomenon will dramatically reduce the effective temperature difference between the glass and moulding surface, which drives heat flow, and will effectively limit the temperature rise on the surface of the mould after the initial contact.

Previous work has shown that the glass contact surface temperature inside glass making moulds cycles on contact with the glass melt during forming W. Trier [7] and H. Holscher [50] et al. The temperature fluctuations have been found to be most evident on the contact surface of the mould and decline towards the outer surface. The measurements have shown that the temperature cycles in blank moulds between 420 and 500°C whilst in blow moulds.

This work confirms that the 80°C temperature rise found on contact of the plunger with the glass melt during forming is typical of that found in practice during the formation of glass containers.

Corresponding work has also been carried out to investigate how the temperature of the glass melt is affected when brought into contact with a relatively cool blank mould during the formation of glass containers W. Trier [10] to calculate the temperature

distribution curves. However, this method could not be used to determine the actual temperature distribution at the glass-to-mould interface. It is between 450 and 500°C. Figure 108 shows how the temperature at the glass contact surface of a blank mould varies with time during the manufacture of colourless glass containers.

C-4 Heat Transfer

Heat transfer is the limiting factor in commercial glassware production speeds as the amount of heat being transferred from the glass to the mould determines how long the glass needs to spend at each stage during production.

High heat transfer coefficients are thought to indicate good thermal contact at the glass-to-mould interface indicating that perfect contact between the glass and the mould would assist in the most rapid heat transfer and therefore increase potential production speeds.

Heat transfer at the glass-mould interface occurs on contact of the glass melt with the mould, the melt contracts as it cools, whilst the mould expands as it is heated which both aid the prevention of sticking. It has been reported that the thermal contact at the glass melt-to-mould interface reduces as the melt cools, due to the differences in expansion between the glass and mould Fellows and Shaw [3]. Theoretical investigations of how heat transfers between the glass and mould during container production have shown there to be more than one mechanism in operation. The heat transfer was determined by examining the glass-to-mould separation distance during the forming and dwell times.

Many parameters have been found to affect the heat transfer characteristics between the glass and mould during manufacture. When the glass is brought into contact with the

mould, the initial rise in temperature has been reported to be very rapid, at several hundreds of degrees per second, and is dependent upon the initial mould temperature. On analysing the heat transfer at the interface, Howse, R. Kent, H. Rawson [14] found that the heat transfer coefficient (i.e. the heat flux per degree of temperature difference between the two surfaces) is time dependent. The rise in mould temperature at the contact surface has also been found to depend on parameters such as the melt temperature, time of pressing and duration between pressing cycles Motoichi and Wakatsuki and Mineo [39]. The initial temperature of the mould has been shown to affect the surface temperature of the parison formed with the total heat removed decreasing with increasing mould temperature, Roger Kent [4] and Fellows and Shaw [3]. Reasons for this discrepancy may be due to other differences in the processing parameters used as the former work was carried out in a laboratory, whilst the latter work was carried out on an industrial scale with additional parameters involved such as the use of mould properties etc.

Table 1: Chemical composition (in wt% and concentration of water in ppm, respectively) of the investigated glasses

	sample number and color									
	1 white	2 half-white	3 green UV[1]	4 green UV[1]	5 green	6 green	7 green	8 green	9 green UV[1]	10 amber
SiO_2	72.3	70.4	71.5	71.2	71.4	71.4	71.2	71.1	70.8	71.9
Al_2O_3	2	3	2.2	2.2	2.2	2.2	2.2	2.4	2.5	2.6
Na_2O	12.3	13.8	13.3	13.3	13	13.1	13.2	13.1	12.9	12.8
K_2O	0.6	1.2	0.9	0.9	0.9	0.9	0.9	0.9	0.9	1.1
CaO	9.8	10.4	9.9	9.8	9.8	9.7	9.8	9.7	9.8	10.1
MgO	2.8	0.8	1.9	1.9	1.8	1.8	1.8	2.2	2.3	0.8
SO_3	0.18	0.24	0.03	0.02	0.04	0.04	0.06	0.01	0.04	0.07
Fe_2O_3	0.03	0.16	0.31	0.31	0.32	0.34	0.34	0.28	0.64	0.3
FeO	0.01	0.04	0.22	0.21	0.12	0.1	0.09	0.11	0.41	0.23
Cr_2O_3	–	–	0.15	0.15	0.25	0.26	0.26	0.13	0.07	0.02
$c\ H_2O$ in ppm	300	340	400	400	400	410	410	370	350	330

Table [1] Yellow-green glass with an enhanced absorption in the UV part of the spectrum.

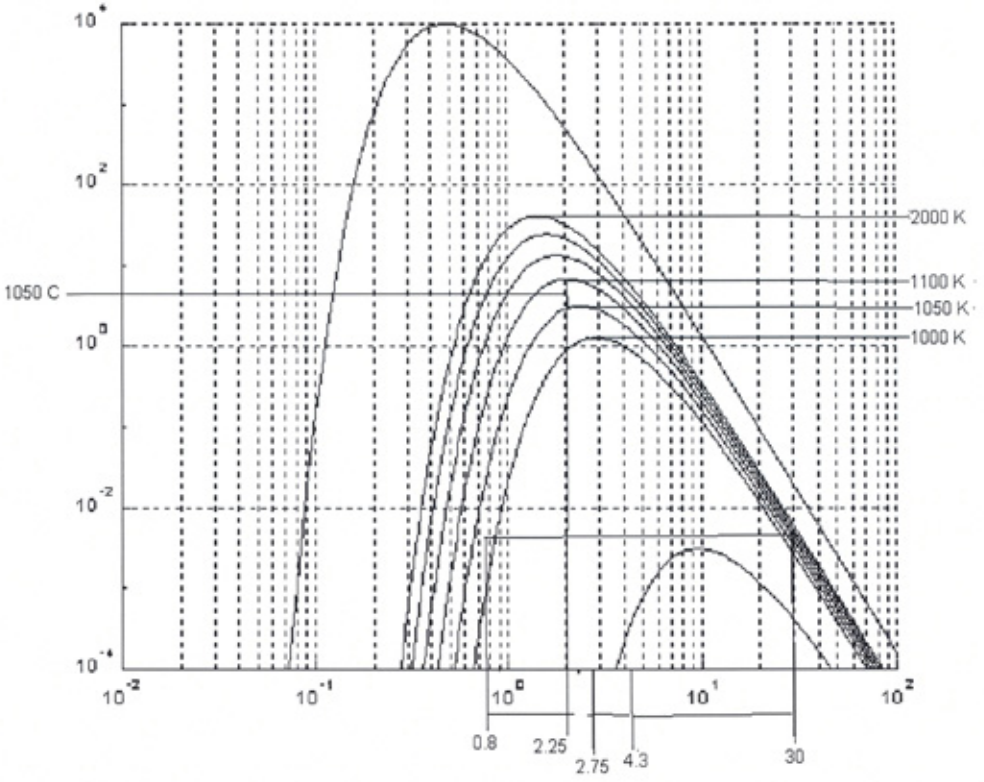

Figure C5-5: shows the three wave bands of absorption coefficients of white soda-lime glass at maximum temperature of 1100 C° Table below shows the values of each band.

Bands	Absorption coefficient (α)	Wave length (μ)
Band-1	23 m^{-1}	0.8--2.25
Band-2	45 m^{-1}	2.25--2.75
Band-3	100 m^{-1}	2.75--4.3

C-6 Refractive Index

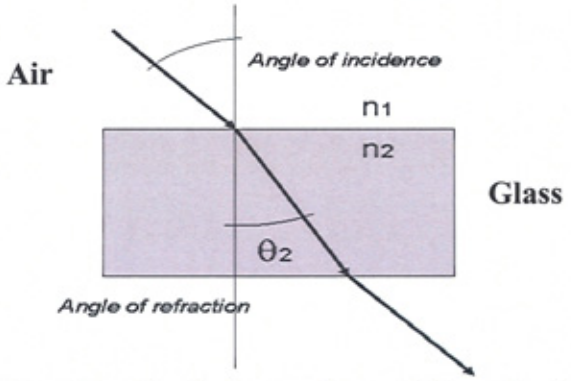

Figure C6-1: Shows the refractive Index n where (θ_1), angle of incidence and (θ_2), angle of refraction

C-5 [22] J Endrys, F. Geotti, and Luka De Riu "Study of the high temperature spectral behaviour of container glass" *Glastech Ber Glass Sc. Tech* 70 No.6 (1997)

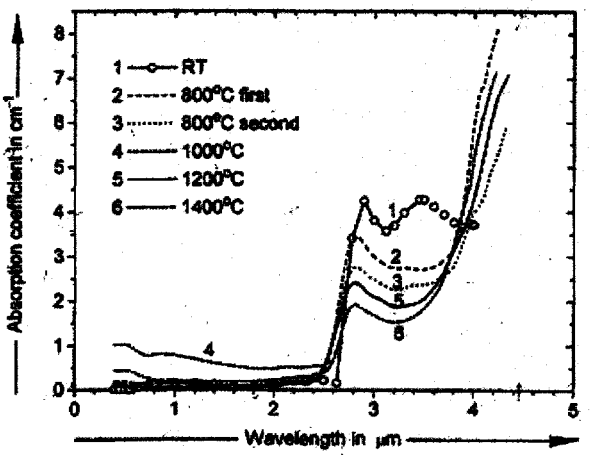

Fig. C 5-1 Wavelength dependence of the absorption coefficients at different temperatures for white glass no. 1.

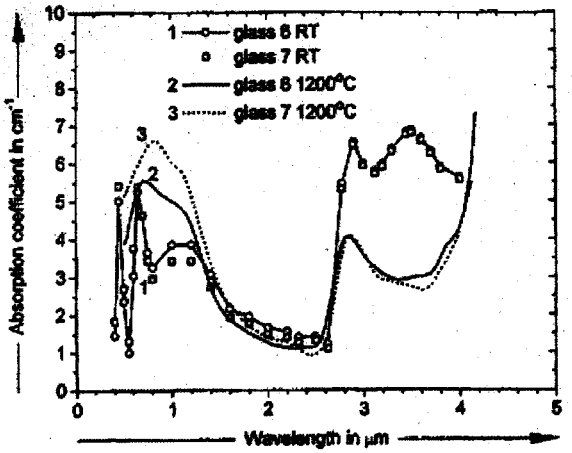

Fig. C 5-2 Comparison of wavelength dependence for green glasses with very close compositions (no. 6 and 7).

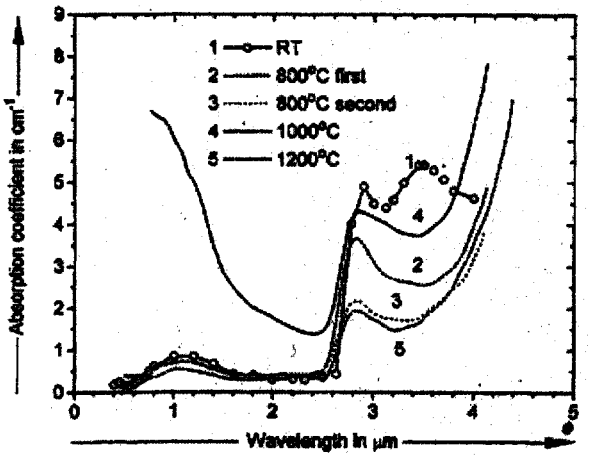

Fig. C 5-4 Wavelength dependence of the absorption coefficients at different temperatures for half-white glass no. 2.

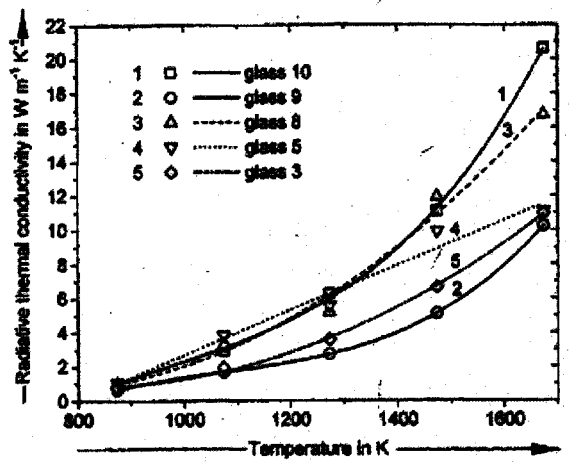

Fig. C 5-3 Temperature dependence of radiative thermal conductivities for glasses no. 3, 5 and 8 to 10.

APPENDEX (D) MODULE

METHOD AND DESCRIPTION (FLUENT)

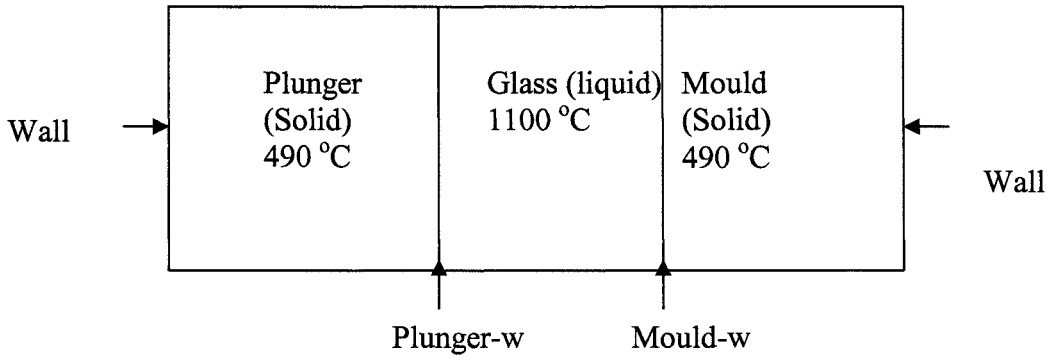

Figure D-1

D.1 MATERIAL PROPERTIES

Property	**Units**	**Glass (fluid)**	**Mould and Plunger steel (solid)**
Density	Kg/m^3	2500	8000
C_p (Specific Heat)	J/Kg K	1350	500
Thermal Conductivity	W/m K	1.45	200
Viscosity	Kg/m s	10	-
Temperature	°C	1100	490
Heat transfer coefficient	$W/m^2 K$	-	1500
Absorption coefficient	m^{-1}	23, 45, 100	-
Refractive Index	-	0.5	-
Thickness	mm	10	20
Time	Second	5	5

METHOD AND DESCRIPTION (ELFEN)

ELFEN Version 3.0.3 BUILD 26

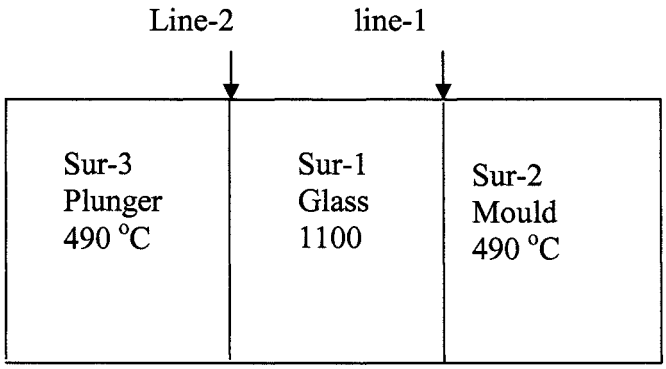

Figure D-1

D.4 MATERIAL PROPERTIES

D.4.1Thermal

Thermal properties	Glass- (solid)	Plunger- Steel (solid)	Mould- Steel (solid)
Thermal Conductivity	1.45	200	200
Specific heat	1350	500	500
Density	2500	8000	8000

D.4.2 Mechanical

Mechanical properties	**units**	**Glass**	**Mould and plunger steel (solid)**
Young's modules(E)	Pascal (N/m^2)	7.8×10^8	1.85×10^6
Poisons ratio(μ)	----	0.45	0.36
Expansion coefficient	m/m/°C	1.35×10^{-5}	1.35×10^{-3}
Shear modules(G)	Pascal (N/m^2)	3.98×10^6	4.7×10^{10}
Density	2500	8000	8000

APPENDEX (E) MODULE

16 Differential thermocouple input channels plus one CJC channel.

- Four programmable gain ranges
- Resolution to 0.03°C depends on conversion rate.
- Reads thermocouple types J, K, E, T, R, S, B.
- Conversion to degrees C or degrees F.
- Gain and Offset automatically calibrated on each scan.
- Cold Junction Compensation done on each scan.
- Overall Conversion rate 4.6 to 22.2 ms
- Provides 500 VDC isolation
- Fully Plug-and-Play

16-Channel 6 thermocouple input board with automatic calibration, cold-junction compensation and open-channel detection [89] Measurements computing catalogue

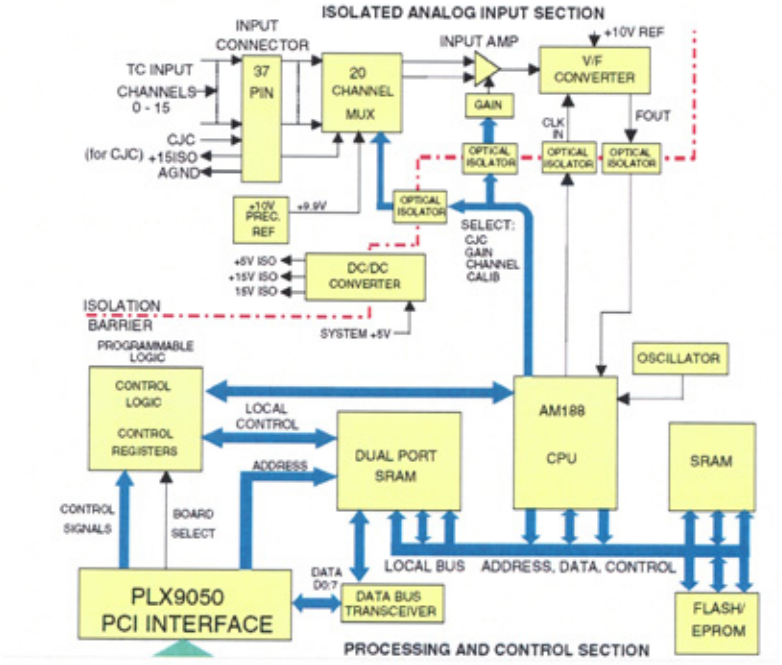

PCI-DAS-TC Block Diagram

Photograph of Hot Glass Sample